DETRITAL ZIRCON GEOCHRONOLOGY OF UPPER MISSISSIPPIAN TO LOWER PENNSYLVANIAN STRATA OF THE ARDMORE BASIN, OKLAHOMA

by

FABIÁN HILARIO PEÑA

Bachelor of Science, 2018
The University of Texas at San Antonio
San Antonio, Texas

Submitted to the Graduate Faculty
of the College of Science and Engineering
Texas Christian University
in partial fulfillment of the requirements
for the degree of

Master of Science

May 2023

DETRITAL ZIRCON GEOCHRONOLOGY OF UPPER MISSISSIPPIAN TO LOWER PENNSYLVANIAN STRATA OF THE ARDMORE BASIN, OKLAHOMA

by

Fabián Hilario Peña

Thesis Approved:

Major Professor

For the College of Science and Engineering

ACKNOWLEDGMENTS

I would like to express my sincere gratitude to everyone who contributed to the completion of this project. First and foremost, I thank my research advisor, Dr. Xiangyang Xie, for accepting me as a student, presenting the idea for this project, guiding me through the process, and pushing me to complete it. I am also grateful to my thesis committee, Dr. Hanson and Dr. Pelch, for their valuable contributions to this writing as well as their support throughout my graduate school experience. Of course, none of this would be possible without the unwavering support of my loving parents, Rosa Marina and Efrén.

Additionally, I would like to acknowledge the generous contributions of the organizations that supported my research and educational expenses through scholarships and grants, including the American Association of Petroleum Geologists, Society of Independent Professional Earth Scientists, South Texas Geological Society, TCU College of Science and Engineering and Department of Geological Sciences.

I am grateful for the friendships I have made during my time at TCU, especially those in the graduate geology program. I also thank my brothers, Darío and Efrén, as well as my lifelong friends for their love and encouragement. Lastly, I would like to thank the Texas Christian University community for providing a nurturing and beautiful environment where I met many great people, made valuable memories, and learned so much. I could not have completed this project or my degree alone. Thank you all. Go Frogs!

Table of Contents

LIST OF FIGURES

LIST OF TABLES

1. INTRODUCTION

Rifting of the supercontinent Rodinia formed a broad passive margin along eastern and southern Laurentia during the Neoproterozoic-Cambrian (Miall and Blakey, 2019). Following the breakup of the supercontinent, from the Ordovician through Early Mississippian, southern Laurentia developed a thick sedimentary succession of mostly shallow-water carbonates (Miall, 2019). The Laurentian passive margin experienced large-scale changes in topography and sedimentation starting in the Late Mississippian with the start of convergence of Laurentia and Gondwana, which formed the Appalachian-Ouachita orogen along the eastern and southern margins (Figure 1) (Lawton et al., 2021; Thomas, 2006). As the continental suture advanced from east to west in the Pennsylvanian, far-field effects of convergence occurred in the continental interior and resulted in uplifting of the basement-cored Ancestral Rocky Mountains (Figure 1) (Leary et al., 2020; Waite et al., 2020).

The onset of the continent-wide orogenic system produced major changes in sediment-dispersal systems (Chapman and Laskowski, 2019; Xie and Manger, 2022). Throughout the Devonian and into Early Mississippian time, sedimentary deposition in southern Laurentia was dominated by a stable carbonate platform (Johnson et al., 1989). Sedimentary conditions transitioned to predominantly siliciclastic deposition during the Late Mississippian start of the Absaroka sequence (Sloss, 1963). Over the last two decades detrital zircon geochronology studies have analyzed sedimentary deposits across the region to better understand sediment dispersal during the collisional orogeny.

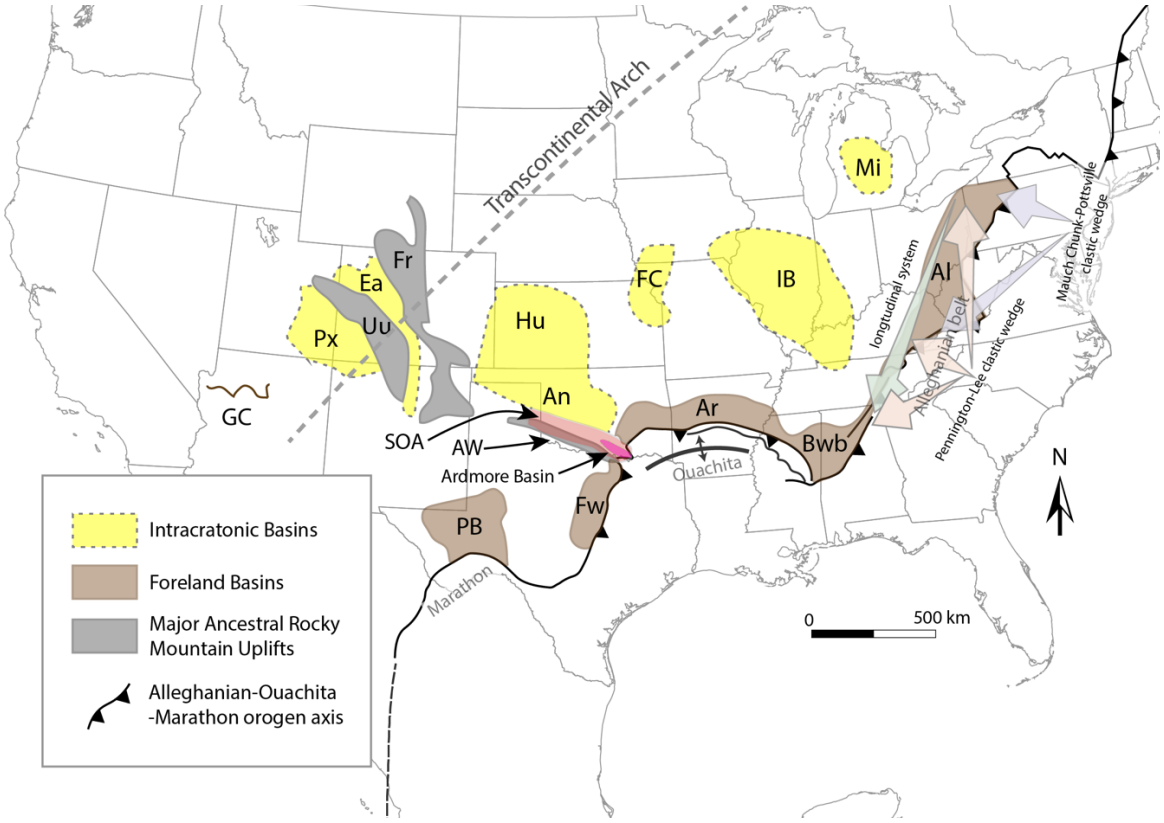

Figure 1: Major sedimentary basins along the Laurentian margin and major Ancestral Rocky Mountain uplifts adapted from Lawton et al. (2021) and Leary et al. (2020). Sedimentary wedge deposits in the Appalachian foreland after Thomas et al. (2017). Al: Appalachian Basin; An: Anadarko Basin; Ar: Arkoma Basin; AW: Amarillo-Wichita uplifts; Bwb: Black Warrior Basin; Ea: Eagle Basin; FC: Forest City Basin; FR: Front Range; FW: Fort Worth Basin; GC: Grand Canyon; Hu: Hugoton Embayment; IB: Illinois Basin; Mi: Michigan Basin; PB: Permian Basin; Px: Paradox Basin; SOA: Southern Oklahoma Aulacogen; Uu: Uncompahgre Uplift.

Appearance of detrital zircon grains from the Appalachian orogen in Upper Mississippian siliciclastic deposits of the Grand Canyon revealed a transcontinental sediment transport system carrying detritus into the western part of the continent (Gehrels et al., 2011). Several prior studies agree that the Appalachian orogen was a dominant sediment supplier throughout Laurentia in the Late Mississippian (Chapman and Laskowski, 2019; Xie and Manger, 2022). However, questions about the spatial and temporal limits of sedimentary control from the active tectonic system, and the role of recycling of pre-existing sedimentary

strata, such as the southern reach of Appalachian sediment, and the opposing influence from the developing Ouachita orogen and the Ancestral Rocky Mountains, remain under debate.

The Ardmore Basin of south-central Oklahoma (Figures 1 and 2) is a relatively small basin adjacent to the Ouachita orogen. The southeastern end of the basin meets frontal thrusts of the Ouachita orogen which are now covered by Cretaceous strata (Johnson et al., 1989; Meek, 1983). The Ardmore Basin sits north of the Fort Worth Basin and west of the Arkoma Basin. Previous provenance studies show that Late Mississippian-Pennsylvanian sedimentation in the Fort Worth Basin and the Arkoma Basin is mainly controlled by recycling of detritus from sedimentary strata of the cratonic interior and active orogenic belts to the east and south (Alsalem et al. 2017; McGuire, 2017; Sharrah, 2005), but many details are disputed. Provenance study of the Ardmore Basin provides an excellent opportunity to further investigate the complex sediment delivery systems during the onset of continent-wide orogenesis.

In the current study, I used U-Pb detrital zircon geochronology to document provenance of Upper Mississippian-Lower Pennsylvanian sandstones of the Ardmore Basin. Nine samples were collected and analyzed and yielded a total of 1135 concordant detrital zircon U-Pb ages. Newly obtained data herein and results from previous studies have been integrated to interpret the provenance of sediment and associated sediment dispersal patterns in the Ardmore Basin and surrounding area.

2. TECTONIC HISTORY AND GEOLOGICAL BACKGROUND

2.1. Regional tectonics

Passive margin conditions in eastern Laurentia, following the early Paleozoic rifting of Rodinia, were interrupted by the Middle Ordovician Taconic orogeny, which involved the collision of 470-450 Ma magmatic arcs against the Laurentian margin in the present-day central to northern Appalachian region. The hinterland of the Taconic orogen reveals significant magmatic activity, deformation, and metamorphism at ~465 Ma, and the oldest accreted terrane is a ~530 Ma allochthon (Drake et al., 1989; Park et al., 2010). The Acadian orogeny (~400-350 Ma) followed in the Early Devonian to Early Mississippian, as the Avalonia microcontinent collided in the northern Appalachian region and the Carolina terrane collided in the southern and central Appalachian region. The youngest tectonic event in the Appalachians is the Alleghanian orogeny which started in the Late Mississippian, lasted through the middle Permian, and resulted from the collision and eventual amalgamation of Laurentia and Gondwana (Becker et al., 2005; Thomas et al., 2017).

The collision progressed from east to west along the southern Laurentian margin, ending passive margin conditions there and resulting in the Ouachita orogen (Becker et al., 2005; Lawton et al., 2021; Thomas et al., 2017). The geometry of the extensive collisional zone has a distinct shape (Figure 1) established during rifting of Rodinia (Thomas, 1977). The Ouachita orogen, which is now largely overlain by younger rocks, forms a curved salient in Texas, Oklahoma, and Arkansas, with arms trending east and southwest (Figures 1 and 2). Mapping of cross-cutting relationships reveals that eastern areas of the Ouachita belt formed prior to the southern Alleghanian belt (Viele and Thomas, 1989). One frontal section of the

Ouachita fold and thrust belt in Oklahoma and Arkansas includes the Mississippian-Pennsylvanian deep-water strata known as the Ouachita facies, which is up to 16 km thick and is thrust onto folded basement rock of the Benton Uplift (Morris, 1989; Thomas et al., 2010). South of the Benton Uplift oceanic or transitional crust lies beneath buried metasedimentary rocks that onlap onto a fragment of continental crust farther south known as the Sabine Terrane (Mickus and Keller, 1992; Thomas et al., 2010).

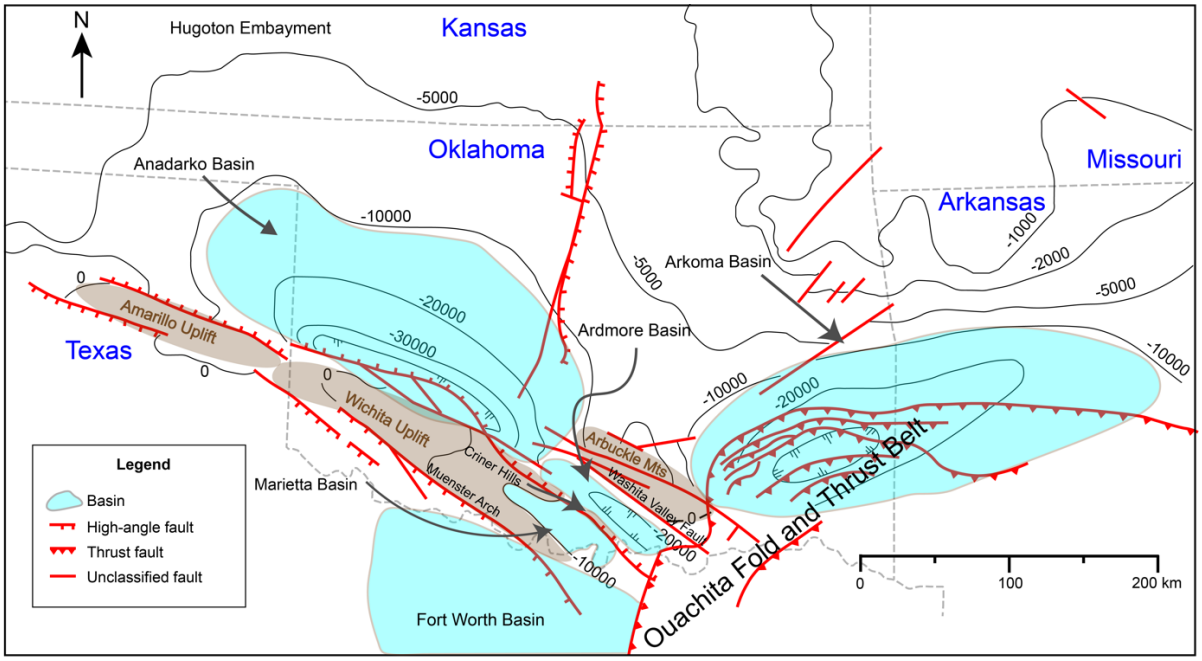

Figure 2: Structural map of the midcontinent, after Rascoe and Adler (1983) and Wang and Bidgoli (2019). Contours are in feet.

2.2. Geologic History of the Southern Oklahoma Aulacogen and the Ardmore Basin

Intraplate magmatism occurred in eastern and southern Laurentia during and prior to the rifting of Rodinia in the Neoproterozoic-Cambrian. One prominent example lies in southern Oklahoma and part of the eastern Texas panhandle where a northwest-southeast-

trending rift zone exists (Hanson et al., 2013). In that region of the southern midcontinent, the Wichita Igneous Province (WIP) contains a bimodal igneous assemblage of late Ediacaran-Cambrian age emplaced during extensional or transtensional tectonism within the Southern Oklahoma Aulacogen (SOA) before the opening of the southern Iapetus Ocean in the Cambrian (Wall et al., 2020).

The SOA covers an area of approximately 480 km by 80 km (Figure 1). It is known as the deepest sedimentary trough in North America with as much as 12,200 m of Paleozoic sediment. The SOA experienced three major development stages (rifting, subsidence and deformation) during the Paleozoic (Ham et al., 1964). The rifting stage, connected to the breakup of Rodinia, involved the development of marginal extensional faults associated with intrusive and extrusive igneous activity during the latest Neoproterozoic through early Cambrian (Ham et al., 1964; Wall et al., 2020). The subsidence stage followed in the late Cambrian through Middle Mississippian and involved thermal subsidence and deposition of a thick succession of mostly carbonates during a regional marine transgression (Ham et al., 1964; Hanson et al., 2013). Subsidence ended with the start of deformation in the Late Mississippian. The deformational stage of the SOA involved the division of the trough into separate elongated basins and uplifts and ended in the Early Permian. The resulting structures include the Ardmore, Marietta and Anadarko Basins and the Arbuckle and Wichita Uplifts (Figure 2) (Ham et al., 1964; Johnson et al., 1989).

The first phase of the deformation stage of the SOA occurred in the Late Mississippian-Early Pennsylvanian and was related to strike-slip motions attributed to far-field influences of the developing Ouachita orogen. This phase involved the structural inversion of the core of the SOA, forming the large-scale Anadarko Basin, the Wichita Uplift

and its smaller eastern extension, the Criner Hills, the topographic barrier between the Ardmore Basin and the Marietta Basin (Figure 2) (Granath, 1989; Perry, 1989). During the Middle Pennsylvanian, the second stage of deformation in the SOA further intensified structural inversion through transpressional faulting, and deformation progressed further west into the SOA (Granath, 1989). Deformation of the SOA resulted in the Ardmore Basin being bounded by several structural features. To the northwest, the Ardmore Basin is bordered by a major fault separating it from the Anadarko Basin with up to several hundred meters of vertical displacement, with the Ardmore Basin sitting on the upthrown block (Hemish and Andrews, 2001). The northern boundary of the Ardmore Basin is the reactivated Washita Valley Fault (Figure 2), which formed during the rifting stage and separated the cratonic basement to the north from Cambrian igneous rocks within the SOA (Johnson et al., 1989).

Cambrian through Upper Pennsylvanian strata of the Ardmore Basin are approximately 9,100 m thick, with over half (5,500 m) being Mississippian and Pennsylvanian in age (Johnson et al., 1989). The oldest sedimentary unit deposited unconformably on the igneous rocks of the SOA is the basal Cambrian Reagan Sandstone which is seen throughout the SOA and records a period of widespread erosion after the igneous activity (Ham et al., 1964). Shallow marine carbonate deposition followed the initial clastic deposition and continued into the Middle Ordovician. The Upper Cambrian-Ordovician succession of mostly carbonates (up to 2.2 km thick) is consistent with post-rift thermal subsidence (Thomas and Astini, 1999). Upper Ordovician-Mississippian heterolithic sediment was deposited over the carbonate succession as the continental shelf stabilized (Johnson et al., 1989).

Following the mostly carbonate deposition of the early to middle Paleozoic, the Ardmore Basin experienced an influx of clastic sediments beginning in the Upper Mississippian-Lower Pennsylvanian (Figure 3). Lithofacies of the formation consist of marine to delta-front shales and some sandstones showing a shallowing upward trend. Meek (1983) described the Chesterian (Upper Mississippian) Goddard Shale Formation (Figure 3) as the first indicator of deformation in the SOA due to its greater thickness relative to coeval sediments to the north. The Goddard Formation is ~600-750 m thick and consists predominantly of shales and some sandstones with an unclear source direction (Hemish and Andrews, 2001).

Conformably deposited over the Goddard Formation, the Springer Formation ranges in thickness from 430 to 975 m. Subsurface data indicate that sandstones of the formation narrow towards the southeast, implying a primary source of sediment from the northwest, which is consistent with paleocurrent data (Meek, 1983; Tomlinson and McBee, 1959). Sandstone layers are thickest (~30 m) in the northern part of the basin and less thick (~12 m) in central and southern parts (Johnson et al., 1989). The Springer Formation is composed of the following three shale and three sandstone members: 1) the basal Rod Club Sandstone, 2) the Overbrook Sandstone, 3) the Lake Ardmore Sandstone, and their associated overlying shales (Figure 3) (Meek, 1983; Johnson et al., 1989). The Mississippian-Pennsylvanian (Chesterian-Morrowan) boundary is found within the Lake Ardmore Sandstone where a lentil of skeletal packstone known as the Target Limestone (Figure 3) is considered to represent the start of the Pennsylvanian (Meek, 1983; Straka, 1972). The unnamed shale overlying the Lake Ardmore Sandstone marks the uppermost unit of the Springer Formation just below the base the Golf Course Formation (Figure 3) (Meek, 1983).

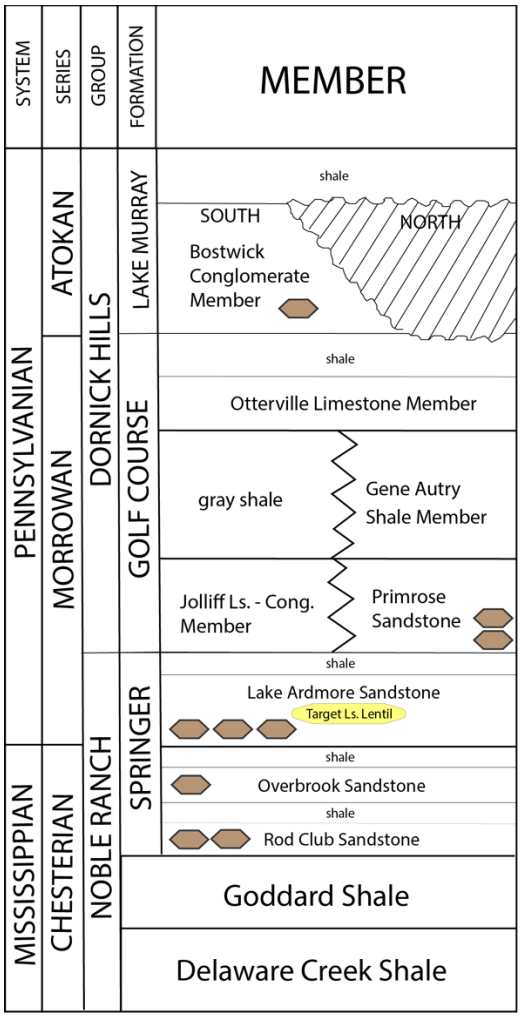

Figure 3: Stratigraphic column of the Ardmore Basin, after Tomlinson and McBee (1959) and Johnson et al. (1989). Brown polygons represent the units that were sampled for detrital zircon analyses. Ls = limestone; Ss = sandstone.

The Morrowan Golf Course Formation has two basal units depending on the area within the basin, the Primrose Sandstone Member and the Jolliff Member, also referred to as the Jolliff Limestone Conglomerate Member (Figure 3) (Hemish and Andrews, 2001; Meek, 1983). Conglomerates of the Jolliff Member are found in the southern part of the basin and likely accumulated as alluvial outwash fans or as submarine fans from the active Criner Hills uplift (Maley, 1986). The northern part of the basin was simultaneously being supplied by a system to the north-northwest during the deposition of the Primrose Sandstone (Johnson et

al., 1989). Sedimentation continued with deep water shales, referred to as the Gene Autry Shale Member in the part of the basin overlying the Primrose Sandstone and unnamed above the Jolliff Limestone Conglomerate Member. This was followed by deposition of the Otterville Limestone in shallower water and a shale overlying that unit represents the final unit with the Golf Course Formation (Johnson et al., 1989; Maley, 1986).

Deformation of the Wichita-Criner uplifts intensified in the Atokan with continued uplift and deposition of the Bostwick Conglomerate Member of the Lake Murray Formation along the northeast margin of the Criner Hills. Dominant lithologies of the Bostwick include limestone and chert conglomerates with irregularly interbedded shales. The limestone cobbles are largest and most abundant at exposures in the southern part of the Ardmore Basin, indicating that the greatest uplift on the Criner Hills axis was south of the present-day Criner Hills (Figure 4). It has been suggested that these limestone cobbles were not carried far from their sources because the cobbles do not extend to the northeast of the Ardmore Basin, although there is also speculation that the unit may have been partially or fully eroded in northern areas (Johnson et al., 1989).

2.3. Previous regional provenance studies

The flexural response of the rigid continental lithosphere during Alleghenian orogenesis resulted in varying topography along the adjacent foreland including overfilled and underfilled areas along the basin, and development of drainage systems within the foreland and extending out into the interior of Laurentia (Lawton et al., 2021). The Mauch Chunk-Pottsville clastic wedge comprises a large portion of the Upper Mississippian strata of the central Appalachian foreland with two extensive fluvial systems which dispersed west-

northwest, and southwest into the continental interior (Figure 1) (Thomas et al., 2017). The other two major sedimentary systems originating in the Appalachian orogen, the Pennington-Lee clastic wedge and a longitudinal transport system (Figure 1), started during the Early Pennsylvanian (Thomas et al., 2004, 2017).

The discovery of Appalachian sediment in Upper Mississippian strata of the Grand Canyon, which revealed the possibility of a transcontinental transport system (Gehrels et al., 2011), has been followed by several studies over the last decade aiming to understand the large-scale transport system and its spatial and temporal reaches. Upper Mississippian strata throughout the midcontinent record detrital zircon signatures characteristic of the Appalachian orogen. Such areas include the Forest City Basin, Hugoton Embayment, and Arkoma Basin and Arkoma shelf (Figure 1) (Kissock et al., 2017; Wang and Bidgoli, 2019; Xie et al., 2016; Xie and Manger, 2022).

However, detrital zircon U-Pb geochronology studies on older sedimentary rocks of the eastern midcontinent have shown that sediments of Appalachian origin started being distributed in more orogen-proximal areas as early as the Devonian. Sedimentary influence from the first event of the three-part orogenic series, the Taconic orogeny, is recorded in the Devonian deposits of the Appalachian Basin (Park et al., 2010). Further evidence of Appalachian sediment dispersal prior to the collision of Laurentia and Gondwana is recorded in Lower Mississippian strata of the Michigan Basin and Middle Mississippian strata of the Illinois Basin (Thomas et al., 2020a). In short, sedimentary influence from the multi-stage Appalachian orogen occurred in a diachronous fashion, from east to west. As a result, the recycling of the older Appalachian-derived deposits must be considered in source-to-sink reconstructions of the Late Mississippian-Pennsylvanian, as the uplifting and erosion of these

strata from the eastern midcontinent was likely, especially in sandstones with high textural and compositional maturities (Kissock et al., 2017; Xie and Manger, 2022).

Xie and Manger (2022) proposed that carbonate sedimentation in the early Paleozoic southern midcontinent transitioned to a collection of intertwined sediment delivery systems including recycling of older sandstones from the cratonic interior, and erosion of the Appalachian orogen starting in the Late Mississippian. Although a similar mixed system is also recorded in the Lower Pennsylvanian strata of the central and northern Arkoma Basin (Allred and Blum, 2021), one Upper Mississippian sample from the Stanley Group in the southeastern Arkoma Basin contains significant traces of Gondwanan sediment (McGuire, 2017), indicating that some areas along the southern midcontinent were also being influenced by the Ouachita orogen.

A southern influence from the Ouachita orogen is also recorded in Atokan sandstones (Lower-Middle Pennsylvanian) of the Arkoma Basin. Sharrah (2006) conducted a comparative study on two submarine fan systems in the frontal thrust sheets of the Ouachita Mountains in eastern Oklahoma and Arkansas (southwestern part of the Arkoma Basin) (Figure 1), which were receiving sediment from opposing directions. The Choctaw thrust sheet has northeast- to east-directed paleocurrent indicators in an offshore shelf environment, and the Ti Valley thrust sheet has west- to south-directed paleocurrent indicators in a deep-water environment. His detrital zircon U-Pb data showed different distributions between the two systems and thus a different sediment provenance. Northeast-directed sands were interpreted to be significantly sourced from the Sabine terrane (Gondwana) which had likely collided with the Laurentian margin by that time. The sands with west- to south-directed

paleocurrents had an Appalachian signature and no indication of Gondwanan provenance (Sharrah, 2006).

Further southwest in the Fort Worth Basin (Figures 1 and 2), it is well documented that a significant Gondwanan influence is present in Middle Pennsylvanian sandstones (Alsalem et al., 2017; Thomas et al., 2020b), but an investigation of Upper Mississippian-Lower Pennsylvanian rocks has not been conducted. The Anadarko Basin has had one study done using detrital zircon U-Pb and $^{40}Ar/^{39}Ar$ muscovite geochronology which revealed that in the Middle Pennsylvanian, the northwestern part of the basin was dominantly sourced by the adjacent Amarillo Uplift (Figure 2), and not by a regional system (Hollingworth et al., 2021). Although that area of the Anadarko Basin was heavily influenced by sediment from the nascent basin-bounding uplift, there is likely much to uncover about regional drainages in the deeper, southeastern part of the basin.

Studies in the Hugoton Embayment, the shallow northern extension of the Anadarko Basin, document a shift in sediment fill from a predominant Appalachian signature in the Late Mississippian to a combination of both Appalachian orogen and Ancestral Rocky Mountains signatures in the Early Pennsylvanian (Figure 1) (Wang and Bidgoli, 2019; Wang et al., 2022). This change represents the introduction of an emerging sediment system in the Ancestral Rocky Mountains. The eastern reach of detritus from the nascent intracratonic belt in the Early Pennsylvanian is unclear. However, coeval samples in the Arkoma Basin do reveal that a strong influence from the Ancestral Rocky Mountains is not present (Wang and Bidgoli, 2019).

2.4. Previous provenance analyses of the Ardmore Basin

There has been no detrital zircon geochronology study conducted in the Ardmore Basin prior to the present work. Other studies of provenance that have been completed are based on facies distributions and heavy mineral and petrographic analyses, which all reveal compositional changes near the Mississippian-Pennsylvanian boundary (Johnson et al., 1989; McBride, 1986; Meek, 1983). Meek (1983) conducted a lithostratigraphy study on the Springer Formation and basal unit of the Golf Course Formation (Figure 3), an Upper Mississippian-Lower Pennsylvanian interval ~800 m thick, with a primary sediment source coming from the northwest and local inputs from the southwest and north. The inputs from the southwest and north are more evident in younger Morrowan (Lower Pennsylvanian) strata than Chesterian (Upper Mississippian) strata. The Lake Ardmore Sandstone (Morrowan) contains conglomerates composed of Ordovician to Lower Mississippian pebbles likely indicating rapid uplift of the Criner Hills during deposition (Meek, 1983). Johnson et al. (1989) pointed out evidence of older Criner Hills deformation indicated by the presence of two thin conglomerates seen in the lower Springer Formation (Rod Club or Overbrook Members).

McBride (1986) conducted a diagenetic and petrologic analysis of the Rod Club, Overbrook, Lake Ardmore, and Primrose Sandstone Members which showed a clear shift in Upper Mississippian-Lower Pennsylvanian sediments based on quartz-feldspar-rock fragment (QFR) proportions. The Rod Club Sandstone (Chesterian) samples analyzed were all classified as well-sorted quartzarenites. The younger Overbrook Sandstone (Chesterian) samples differ with a higher feldspar content, falling under the subarkose sandstone category. The younger Lake Ardmore and Primrose Sandstones (Morrowan), however, contained much

greater amounts of glauconite, fossil fragments, and lithic grains than the Rod Club and Overbrook Sandstones and were classified as sublitharenite to litharenite. Overall, these studies in the Ardmore Basin reveal a shift in lithic compositions between Chesterian and Morrowan sandstones and a dominant source direction from the northwest with varying northern and southern sediment influences, including the local contributions from the Criner Hills as early as the basal Springer Formation (Figure 3).

3. METHODS

3.1. Sampling, mineral separation, and preparation

Sampling sites in the Ardmore Basin were chosen based on outcrop accessibility with the goal of acquiring multiple Mississippian-Pennsylvanian sandstones. Field guides by Hemish and Andrews (2001) and Meek et al. (1988) were used to locate most outcrop sites. Also, the most updated geologic map of the area by Stanley and Chang (2012) was used to cross-check sampling sites. Nine sandstone samples weighing ~2.5 kg each were collected from roadcuts and local exposures. They include one northern and one southern sample of the Rod Club Sandstone, one central sample of the Overbrook Sandstone, three samples of the Lake Ardmore Sandstone (one from the north and two from the south), two northern samples of the Primrose Member, and one southern sample from an unnamed sandstone unit of the Lake Murray Formation (Figure 3 and 4; Table 1).

Detrital zircon grains were extracted from rock samples with standard mineral separation methods (e.g., Gehrels et al., 2006). The process started with cleaning of samples with water, followed by crushing of whole rocks with a hammer, then grinding using a disc

mill. Silt and low-density minerals were separated through repeated washing of ground samples, followed by magnetic susceptibility separation using a Frantz-LB-1 Magnetic Separator. Nonmagnetic grains were further separated using heavy-liquid LST with density at ~3.0 g/cm^3. Grains with density over 3.0 g/cm^3 were inspected under a binocular microscope. Non-zircon grains were removed, and the remaining grains were separated, packaged, and sent to the UTChron Laboratory at UT Austin for analyses using Laser Ablation Inductively Coupled Plasma Mass Spectrometry (LA-ICP-MS).

Table 1: U-Pb detrital zircon sampling sites

Sample ID	Sample name	Formation	Latitude (° N)	Longitude (° W)
1. RCS	Rod Club South	Springer	34.0712	97.1371
2. LAW	Lake Ardmore West	Springer	34.0711	97.1332
3. LAE	Lake Ardmore East	Springer	34.0711	97.1321
4. ATOKA	Atoka Sandstone	Lake Murray	34.0711	97.1240
5. OVB	Overbrook	Springer	34.2238	97.1493
6. LAN	Lake Ardmore North	Springer	34.3213	97.0426
7. PRL	Primrose Lower	Golf Course	34.3214	97.0428
8. PRU	Primrose Upper	Golf Course	34.3218	97.0429
9. RCN	Rod Club North	Springer	34.3348	97.1977

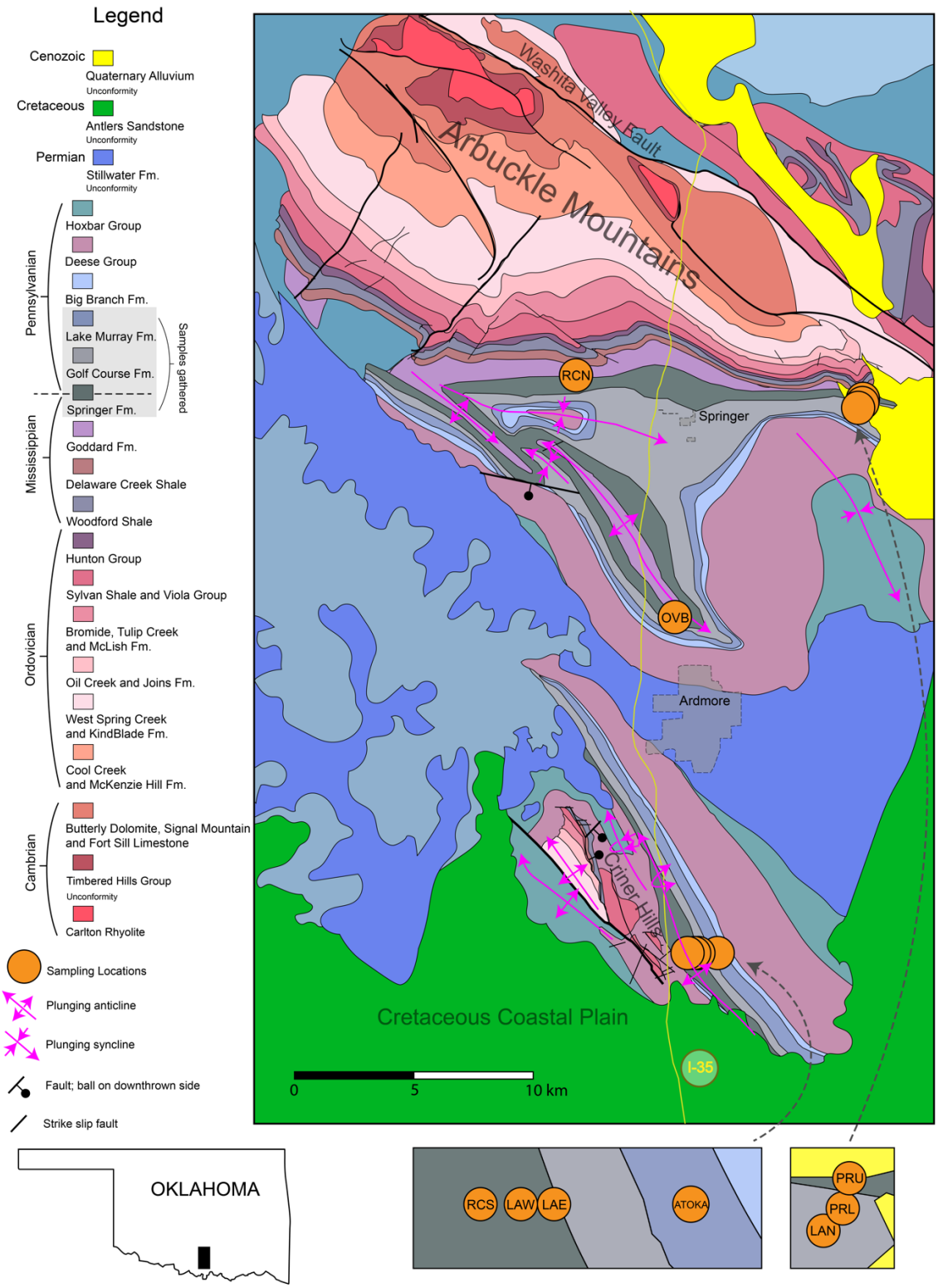

Figure 4: Sampling locations and geologic map of part of south-central Oklahoma after Stanley and Chang (2012). Symbols for samples are shown in Table 1.

3.2. Analytical methodology

Zircons were placed on epoxy resin mounts and randomly chosen for analysis using LA-ICP-MS. A minimum of 120 grains per sample were used for analysis to ensure a statistically strong study (Vermeesch, 2004). Geochronology analyses were performed on a Thermo Element2 mass spectrometer with a connected PhotonMachine Analyte G.2 excimer laser (e.g., Hart et al., 2016). Helium was the carrier gas utilized and combined with argon prior to going into the mass spectrometer. The diameter of the laser beam was 25-30µm, and operated at an energy density of 2.10 J/cm^2 and a pulse rate of 10 Hz. Each individual analysis used 4 preablation cleaning shots, 30 seconds of ablation and baseline data collection, and 30 seconds of washout. The ablation rate of ~0.5µm/second resulted in analysis of the outer 15-17µm per zircon and provided depth profiles permitting the identification of possible growth zones for individual grains to enhance provenance interpretations based on rim and core ages (Stockli and Stockli, 2013).

Elemental and isotopic fractionation were corrected with the use of interspersed analysis of two zircon standards. The primary reference standard used is GJ1 (601.7 ± 1 Ma) (Jackson et al., 2004) and a secondary standard was Pak1 (43.0 ± 0.01 Ma), a zircon standard from Pakistan used at UTChron. For quality control, analyses were performed in repeated sequences of one standard followed by 5 unknowns. Age calculations from analytical data were performed using Iolite3.7 data reduction software (Paton et al., 2011) and VizualAge (Petrus and Kamber, 2012).

For provenance analyses, $^{206}Pb/^{238}U$ ages were used for grains under 850 Ma, and $^{207}Pb/^{206}Pb$ ages were used with grains greater than 850 Ma. Ages documented in this study use 2σ absolute propagated uncertainties with $^{207}Pb/^{206}Pb$ ages being <25% discordant, and

$^{206}Pb/^{238}U$ ages being <15% discordant. The discordance was calculated with $^{206}Pb/^{238}U$ and $^{207}Pb/^{235}U$ ages if younger than 1200 Ma and $^{206}Pb/^{238}U$ and $^{207}Pb/^{206}Pb$ ages if older than 1200 Ma (e.g., Hart et. al, 2016).

Data visualization for relative probability distributions was completed using detritalPy Python scripts (Sharman et al., 2018) as Kernel Density Estimation (KDE) plots, which is a method of visualizing the distribution of observations in a dataset similar to a histogram. Multidimensional Scaling (MDS) plots were generated using an R package for statistical provenance analysis (Vermeesch et al., 2016) to plot dissimilarity amongst different samples. The degree of similarity is larger for samples that plot near each other and lower in those further apart (Vermeesch et al., 2016).

4. RESULTS

4.1. U-Pb detrital zircon data

Of the 1135 concordant detrital zircon U-Pb ages obtained, there are 23 core/rim age pairs. Zircon grain ages range from 3688 Ma to 346 Ma and are divided into seven characteristic age groups based on regional geochronological provinces (Alsalem et al., 2017; Xie et al., 2019). The groups include Paleoproterozoic and older (> ~1825 Ma), late Paleoproterozoic (~1825-1600 Ma), early Mesoproterozoic (~ <1600-1300 Ma), middle to late Mesoproterozoic (~1300-920 Ma), Neoproterozoic to Cambrian (~800-510 Ma) and middle Paleozoic (~490-340 Ma) (Figure 5; Table 2).

Upper Mississippian (Chesterian) Rod Club Sandstone: Two samples for the Rod Club Sandstone, the southern sample (RCS) and the northern sample (RCN), were collected

based on the field guide by Hemish and Andrews (2001) (see their Stops 1 and 4 and Figure 5). Both samples are fine-grained, well-sorted quartzarenites but are slightly different in color. RCN was collected ~18 km north of the city of Ardmore (Figure 6), off a dirt road at a highly weathered outcrop on the ground surface. The RCN sample has green-dark gray color on weathered surfaces and tan to orange color on fresh surfaces. The RCS sample was collected from an outcrop ~8 km south of the southern edge of the city of Ardmore (Figure 6) along the east-west oriented highway S.H. 77S at the bottom of the well exposed, northern side of the road cut. The RCS sample is white to tan in color.

Age distributions of both samples exhibit similar patterns with major middle to late Mesoproterozoic (~39%) and middle Paleozoic (~20.5%) age groups with peaks at 441 Ma and 1058 Ma (RCS), and 444 Ma and 1045 Ma (RCN). Minor groups have late Paleoproterozoic (~10%) and Archean-Paleoproterozoic (~8%) ages. The only age group in which the two samples significantly differ is the early Mesoproterozoic group with an 8% difference (~22% for RCS and ~14% for RCN).

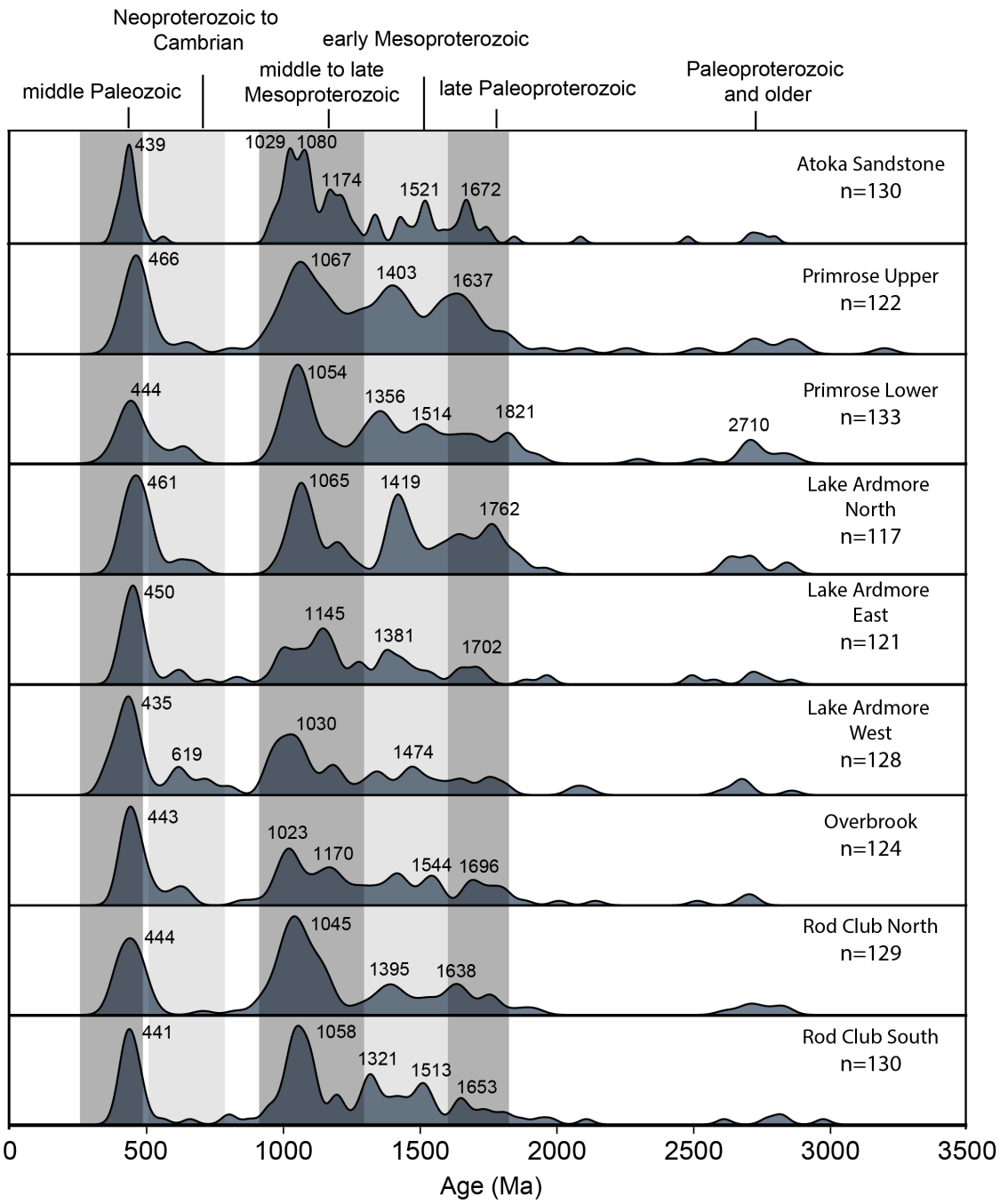

Figure 5: KDE plots of samples analyzed in this study

Table 2: Statistical analyses of detrital zircon U-Pb ages from Ardmore Basin

	Late Mississippian			Early Pennsylvanian					
Age group	RCS	RCN	OVB	LAW	LAE	LAN	PRL	PRU	ATOKA
490-340 Ma	*20%*	*21%*	*24%*	*27%*	*26%*	*18%*	*14%*	*15%*	*18%*
800-510 Ma	*2%*	*2%*	*7%*	*9%*	*5%*	*6%*	*6%*	*3%*	*1%*
1300-920 Ma	*37%*	*41%*	*31%*	*31%*	*35%*	*26%*	*32%*	*33%*	*48%*
1600-1300 Ma	*22%*	*14%*	*19%*	*14%*	*15%*	*21%*	*23%*	*23%*	*16%*
1825-1600 Ma	*9%*	*11%*	*10%*	*9%*	*7%*	*17%*	*13%*	*14%*	*10%*
> 1825 Ma	*7%*	*8%*	*6%*	*7%*	*10%*	*10%*	*12%*	*10%*	*5%*

Figure 6: Outcrop photographs of Rod Club North sample (Left) and Rod Club South sample (Right).

Upper Mississippian (Chesterian) Overbrook Sandstone: One sample of the Overbrook member was obtained from the central area of the Ardmore Basin (OVB) (Location 2 described by Meek et al. (1988)). The sample was obtained from an east-striking outcrop dipping ~65° south, within the Water Treatment Plant of the City of Ardmore (Figure 7). The weathered surface of the outcrop is dark gray-green and the fresh surface shows a clean, well-sorted, light gray-tan-orange, fine-grained sandstone. Like RCS and RCN, prominent age groups in OVB are middle to late Mesoproterozoic (~31%) and middle Paleozoic (~24%) with a principal age peak at 443 Ma and minor age peaks at 1023 Ma and 1170 Ma. Other minor groups are early Mesoproterozoic (~19%), late Paleoproterozoic (~10%), Archean-Paleoproterozoic (~6%) and Neoproterozoic to Cambrian (~7%).

Figure 7: Outcrop photograph of south-dipping surface of the Overbrook Sandstone in the Water Treatment Plant of Ardmore, OK.

Lower Pennsylvanian (Morrowan) Lake Ardmore Sandstone: Three samples of the Lake Ardmore Member were collected, including two samples ~100 meters apart from each other in the southern area of the Ardmore Basin (LAW and LAE) and one sample from the northern Ardmore Basin (LAN). One southern sample, LAW, was collected from measured section 409 in Meek (1983). The other southern sample, LAE, was collected from the same thick section ~100 m east of LAW (Figure 8). LAW is stratigraphically beneath LAE. Both southern samples were collected from east dipping beds along highway S.H. 77S. The weathered surfaces of LAW and LAE are gray to tan/yellow and the fresh surfaces of the samples are tan-orange. The northern sample, LAN, was acquired from an outcrop ~28 km north of the southern samples, or ~12 km north of the city of Ardmore, along a north-south

trending creek, from a nearly vertical bed (see Stop 3 described by Hemish and Andrews (2001) and Figure 8). The LAN sample is a well-sorted, fine grained, dark gray sandstone that does not closely resemble the LAW and LAE samples

Both southern samples have age distributions with dominant middle to late Mesoproterozoic (~33%) and middle Paleozoic (~26.5%) age groups with peaks at 435 Ma and 1030 Ma (LAW) and 450 Ma and 1145 Ma (LAE). Minor age groups include early Mesoproterozoic (~14.5%), late Paleoproterozoic (~8%), Archean-Paleoproterozoic (~8.5%), and Neoproterozoic to Cambrian (~7%). Middle to late Mesoproterozoic (~26%) and middle Paleozoic (~18%) age groups are smaller in LAN, with peaks at 461 Ma and 1065 Ma, but the sample shows larger early Mesoproterozoic (~21%) and late Paleoproterozoic (~17%) age groups, with peaks respectively at 1419 Ma and 1762 Ma. Archean-Paleoproterozoic (~10%) and Neoproterozoic to Cambrian (~6%) age groups of LAN are similar to the two southern Lake Ardmore samples.

Figure 8: Outcrop photographs of Lake Ardmore East sample (Left) and Lake Ardmore North sample (Right).

Lower Pennsylvanian (Morrowan) Primrose Sandstone: Two samples of the Primrose Member were acquired approximately 40 meters apart, from the north-central area of the Ardmore Basin at an outcrop along a north-south-trending creek (Figure 9), based on Stop 3 described by Hemish and Andrews (2001). Primrose Upper (PRU) is stratigraphically higher, or younger, than Primrose Lower (PRL). Both PRU and PRL are well-sorted, fine fine grained, tan to gray sandstones. Zircon grains for both samples fall mainly within the Middle to late Mesoproterozoic (~32.5%) and early Mesoproterozoic (~23%) age groups with a primary peak at 1054 Ma, and minor peaks at 1356 Ma for PRL and 1067 Ma and 1403 Ma for PRU. The minor age groups are middle Paleozoic (~14.5%) with notable peaks at 444 Ma (PRL) and 466 Ma (PRU), late Paleoproterozoic (~13%) with a peak at 1637 Ma, Archean-Paleoproterozoic (~11.5%), and Neoproterozoic to Cambrian (~4.5%).

Figure 9: Outcrop photographs of Primrose Upper sample (Left) and Primrose Lower sample (Right).

Lower Pennsylvanian (Atokan) Lake Murray Sandstone: One sample from an Atokan sandstone interval of the Lake Murray Formation was collected from an east-dipping outcrop in the south-central area of the Ardmore Basin (ATOKA) directly next to a bed of conglomerate (Figure 10). This sample was collected based on unit descriptions and relative positions from the Ardmore Geological Society field guide (Lang, 1966), cross-checked with the geologic map of the region (Stanley and Chang, 2012). It is a tan to orange, moderately sorted, medium- to coarse-grained sandstone with traces of dark-colored detritus. The primary age group seen in ATOKA is the middle to late Mesoproterozoic (~48%) one, representing the largest concentration for a single age group in any of the nine samples, with peaks at 1029 Ma, 1080 Ma and 1174 Ma. The secondary group is middle Paleozoic (~18%) with a major peak at 439 Ma, followed by minor groups of early Mesoproterozoic age (~16%) with a distinct peak at 1521 Ma, late Paleoproterozoic age (~10%) with a distinct peak at 1672 Ma, and Paleoproterozoic and older ages (~5%).

Figure 10: Outcrop photographs of Lake Murray Sandstone. Photograph on the left is a wider view of the outcrop and the photo on the right is a closer view of the sandstones.

4.2. Results of Core-Rim age dating

Depth-profiling analysis of zircon grains provided 23 concordant core-rim age pairs. Only ~4% (46 out of 1135) of the values reported are core-rim ages; however, the age pairs add supplementary evidence for provenance interpretations presented herein. Two prominent clusters are evident in the core-rim data plot (Figure 11): Group 1) four early Paleozoic (~490-340 Ma) rim ages with middle to late Mesoproterozoic (~1300-920 Ma) cores, and Group 2) ten grains with middle to late Mesoproterozoic (~1300-920 Ma) rim ages and early Mesoproterozoic (~1600-1300 Ma) to late Paleoproterozoic (~1825-1600 Ma) core ages. The four grains of the Group 1 belong to samples OVB, LAW, LAN and PRL. The youngest sandstone member of the study, the Atokan Lake Murray sandstone, contains three of the ten

grains in Group 2. Sample PRL also contains three grains and samples PRU, LAN, OVB and RCN each contain one grain of Group 2.

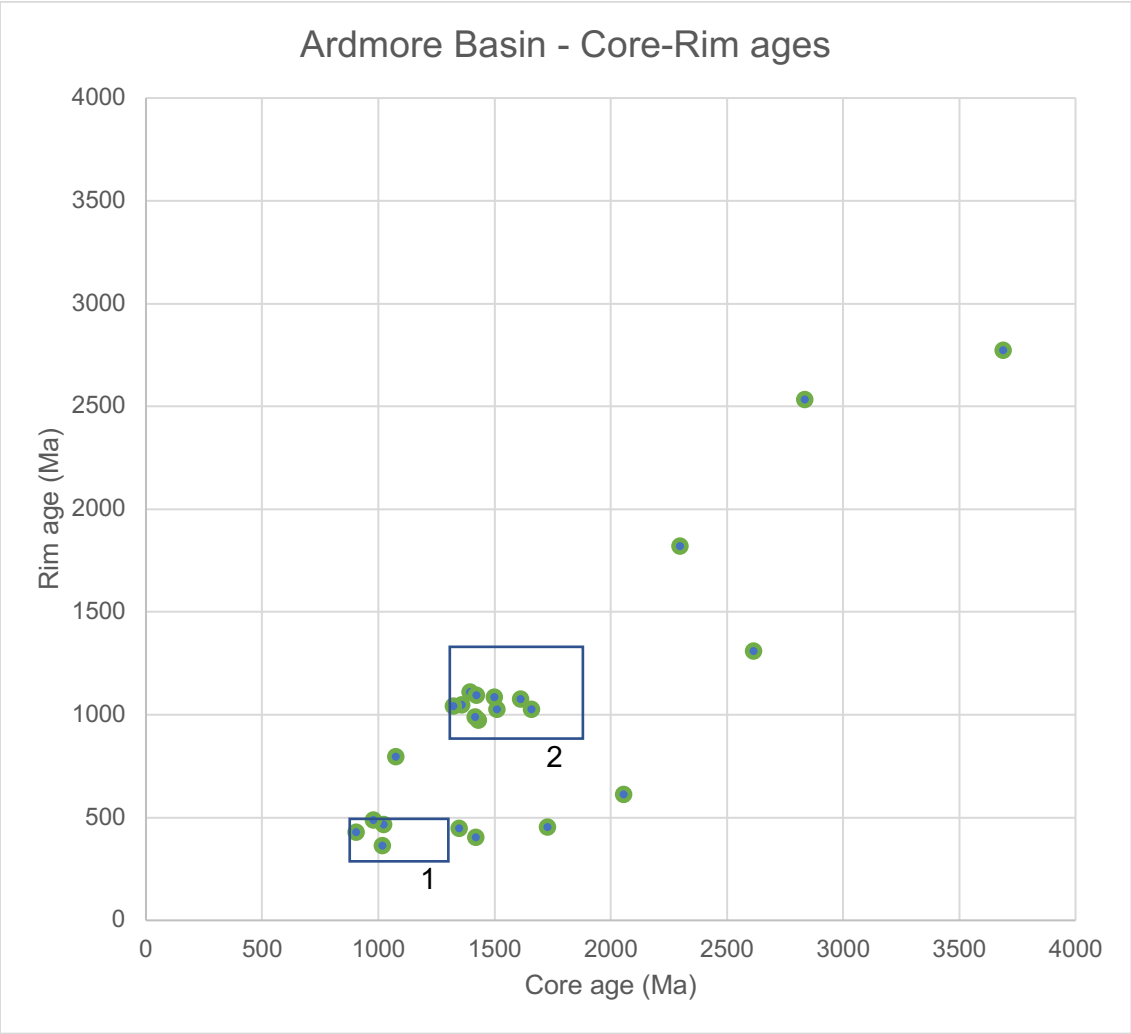

Figure 11: Core vs. rim age plot for 23 age pairs from this study. The two prominent clusters are indicated.

The remaining nine core-rim ages are not in either of the two groups and include two grains with middle Paleozoic (~490-340 Ma) rims and early Mesoproterozoic (~1600-1300 Ma) cores, one grain with a middle Paleozoic rim and a late Paleoproterozoic (~1825-1600 Ma) core, one grain with a Neoproterozoic to Cambrian (~800-510 Ma) rim with a

Paleoproterozoic and older (> ~1825 Ma) core, one grain with an early Mesoproterozoic (~ 1600-1300 Ma) rim with a Paleoproterozoic and older (> ~1825 Ma) core, one grain with a late Paleoproterozoic (~1825-1600 Ma) rim with a Paleoproterozoic and older (> ~1825 Ma) core, two grains with Paleoproterozoic and older (~1825-1600 Ma) cores and rims, and one grain with a rim age 796 Ma with a middle to late Mesoproterozoic (~1300-920 Ma) core.

5. GEOCHRONOLOGIC PROVINCES

5.1. Laurentian basement provinces

5.1.1. Laurentian Craton Interior Provinces

The core of Laurentia, the Canadian Shield, formed in the Paleoproterozoic (~1960-1800 Ma) during the collision of continental blocks of Archean age (>2500 Ma). The Trans-Hudson province resulted from the collision between the Wyoming (~2700-2500 Ma) and Superior (~2800-2700 Ma and ~3500 Ma) cratons and is composed of reworked Archean crust and volcanic rocks with ages of ~1,900-1,800 Ma (Figure 12) (Hoffman, 1989). The younger Penokean orogen on the southern end of the Superior province makes up part of the southern end of the Canadian Shield and is attributed to a microcontinent collision at ~1900-1800 Ma (Hoffman, 1989).

The central provinces of Laurentia include the Yavapai province which is composed of volcanic arc terranes with ages of ~1760-1700 Ma accreted to the south of the Canadian Shield at ~1700 Ma (Van Schmus et al., 1996) and the Mazatzal province, a separate assemblage of arc terranes (~1700-1800 Ma) south of the Yavapai province which collided at ~1600-1660 Ma (Amato et al., 2008; Bennett and Depaolo, 1987). Collectively the Yavapai

and Mazatzal provinces yield Late Paleoproterozoic detrital zircon grains (~1800-1600 Ma) (Figure 11). The formation of the Yavapai-Mazatzal provinces was followed by the intracratonic magmatism of the Granite-Rhyolite province at ~1500-1300 Ma (Whitmeyer and Karlstrom, 2007).

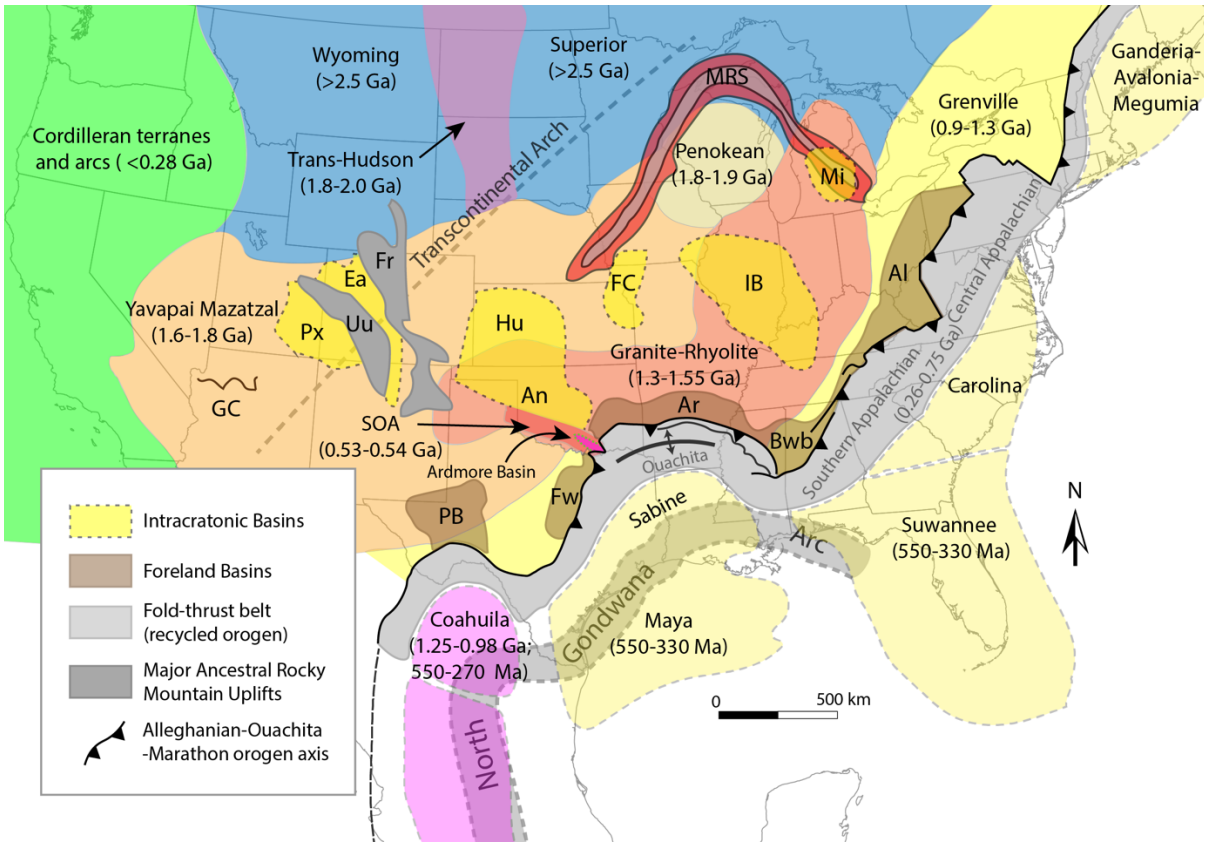

Figure 12: Basement provinces of Laurentia and Gondwanan terranes adjacent to the Appalachian-Ouachita orogen adapted from Lawton et al. (2021) and Wang and Bidgoli (2019). Al: Appalachian Basin; An: Anadarko Basin; Ar: Arkoma Basin; Bwb: Black Warrior Basin; Ea: Eagle Basin; FC: Forest City Basin; FR: Front Range; FW: Fort Worth Basin; GC: Grand Canyon; Hu: Hugoton Embayment; IB: Illinois Basin; MRS: Midcontinent Rift System; Mi: Michigan Basin; PB: Permian Basin; Px: Paradox Basin; SOA: Southern Oklahoma Aulacogen; Uu: Uncompahgre Uplift.

5.1.2. Sources from the Appalachian region

The Appalachian region records various tectonic developments starting in Paleoproterozoic and ending in the late Paleozoic. The Grenville Orogeny is the oldest of the recorded events. Rifting of Rodinia followed in the Neoproterozoic, and then the Taconic, Acadian and Alleghanian orogenies in the Paleozoic (Park et al., 2010; Wang and Bidgoli, 2019). The Grenville orogen was a result of continent collisions leading to the suturing of Rodinia during ~1300-900 Ma. The orogen comprises a significant part of the basement of eastern Laurentia (Park et al., 2010) (Figure 12). Neoproterozoic (~700-550 Ma) polyphase rift successions and associated magmatic rocks east of the Grenville province in the Appalachian region represent the separation of Rodinia and formation of the Iapetus Ocean (Hoffman, 1989). The Appalachian orogen is composed of the Taconic belt (Ordovician) with ages of ~470-450 Ma, the Acadian belt (Early Devonian to Early Mississippian) with ages of ~400-350 Ma, and the Alleghanian belt (Late Mississippian to middle Permian), which did not did not supply significant amounts of zircon grains to the late Paleozoic Appalachian basin fill (Becker et al., 2005; Drake et al., 1989; Park et al., 2010; Thomas et al., 2017) .

5.1.3. Other sources

Rocks of the Mesoproterozoic Midcontinent Rift System (MRS) of North America and the aforementioned late Neoproterozoic-Cambrian Wichita Igneous Province (WIP) were also considered as potential contributors to regional sedimentary accumulations (Thomas et al., 2016; Wang and Bidgoli, 2019; Xie and Manger, 2022). The MRS formed from magmatism associated with back-arc extension during the Grenville orogen and cut through

various crustal provinces (Figure 12). It consists of bimodal igneous rocks with ages of 1115-1085 Ma (Craddock et al., 2013). The U-Pb ages of detrital zircon contributions from both the MRS and WIP fall within narrow time frames. The WIP, which underlies the Ardmore Basin and basin-bounding southern uplifts (Criner-Wichita Uplifts), yields ages of ~540-530 Ma (Hanson et al., 2013; Wall et al., 2020).

5.2. Gondwanan and peri-Gondwanan provinces:

Crustal provinces adjacent to the Laurentian eastern and southern margins and the Gondwanan northern margin (Figure 12), include the Avalonia, Carolina, Suwanee, Sabine, Maya and Coahuila terranes. These provinces have various interpreted origins and ages, including magmatic arc terranes which collided with Gondwana and then separated from it, or separate intervening island arcs between Laurentia and Gondwana. Some of these terranes contain Neoproterozoic to Cambrian (~800-510 Ma) and Grenville (~1300-920 Ma) crust, and other terranes have different age distributions (Lawton et al., 2021). Such terranes include the Carolina terrane with documented basement ages of ~635-535 Ma (Wortman et al., 2000), the Avalonia terrane with basement ages of ~763-586 Ma (Krogh et al., 1988), and the Suwannee terrane with basement ages of ~2250-1900 Ma and ~680-500 Ma (Mueller et al., 2014; Mueller et al., 1994).

The Coahuila terrane is unlike Gondwanan terranes since its timing of amalgamation to Gondwana is unconfirmed and parts of it have Grenville-aged basement (Lawton et al., 2021). The terrane most proximal to the Ardmore Basin is the Sabine terrane, which is covered by the Gulf Coastal Plain and has an unknown composition and age (Thomas et al., 2020). However, it is inferred to have supplied detritus to the Ouachita foreland and likely

yielded the “North Gondwana signature” which contains dominant Neoproterozoic-Cambrian (peri-Gondwanan) ages (Lawton et al., 2021).

5.3. Sources from recycled sediment

Recycled sedimentary units exposed in both intracontinental uplifts and the Appalachian-Ouachita fold and thrust belt have been considered primary contributors to sedimentary systems in regional studies. Repeating age groups present in sedimentary strata and basement rocks pose a challenge for detrital zircon U-Pb geochronologic studies. However, distinctive detrital zircon age distributions or “signatures” established by previous studies (Lawton et al., 2021; Thomas et al., 2017), along with data from older strata deposited across vast areas of the continental interior (Konstantinou et al., 2014; Lovell and Bowen, 2013; Pickell, 2012), provide insights for distinguishing provenance.

The “Appalachian signature” proposed by Thomas et al. (2017) represents the general pattern of detrital zircon U-Pb ages derived from the Appalachian orogen. It includes ages from the uplifted sedimentary strata in the thrust belt, exposed basement, and igneous rocks (Becker et al., 2005; Eriksson et al., 2004; Park et al., 2010; Thomas et al., 2004). The signature includes a dominant Grenville (~1300-900 Ma) population (with two major peaks at ~1065 Ma and ~1165 Ma) from either recycled strata or directly from Grenville basement (Becker et al., 2005), a limited population of grains older than 1500 Ma, a general absence of Neoproterozoic to Cambrian (~800-500 Ma) ages, a significant amount of Taconic and Acadian (Paleozoic) (~490-340 Ma) ages, and absence of Alleghanian-aged (330-270 Ma) grains (Thomas et al., 2017). Samples from Ordovician-Pennsylvanian sandstones of the

Appalachian Basin representative of the Appalachian signature are compiled and plotted in Figure 13.

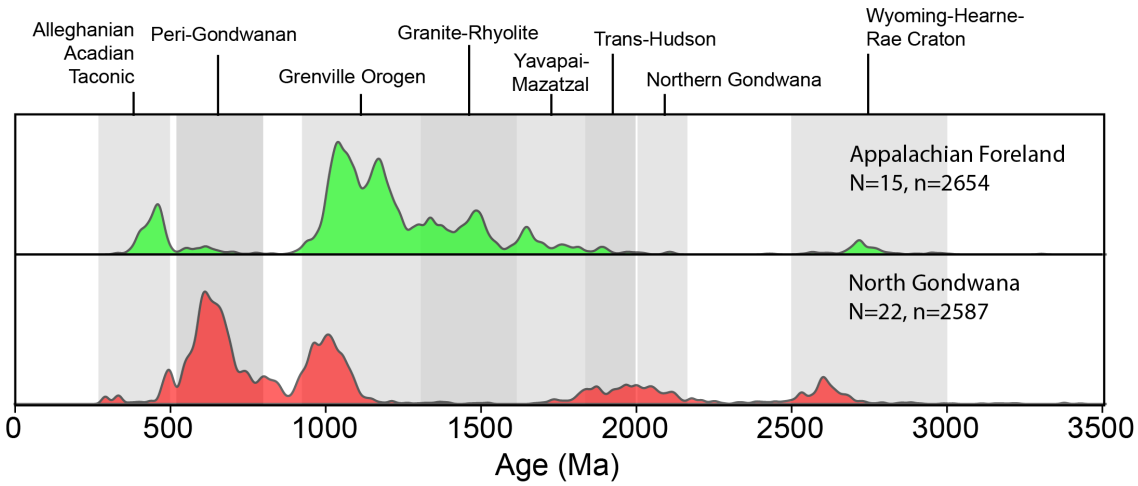

Figure 13: Comparison of detrital zircon ages from Northern Gondwana and the Appalachian Foreland, including Paleozoic Appalachian samples from the Appalachian Basin (Park et al., 2010; Thomas et al., 2017) and Paleozoic sandstones of northern Gondwana (Pastor-Galan et al., 2013; Shaw et al., 2014).

Sediments that have been interpreted as derived from peri-Gondwanan terranes, through the Ouachita and Appalachian orogens, including the Upper Mississippian sandstones of the Arkoma Basin (McGuire, 2017), the Middle Pennsylvanian sandstones of the Fort Worth Basin (Alsalem et al., 2017), and the lower Permian sandstones of the Permian Basin (Liu and Stockli, 2020) and throughout the southern midcontinent in younger deposits, show a unique signature that is characterized by the dominant Neoproterozoic to Cambrian (~850-510 Ma) age group besides age groups seen in the Appalachian signature, namely the Grenville, Archean and early Paleozoic age groups (Figure 13) (Pastor-Galan et al., 2013; Shaw et al., 2014; Waite et al., 2020).

Other potential recycled sources include sedimentary and metasedimentary units of the northern midcontinent. The Cambrian sandstones have a characteristic Archean-age population, and the Ordovician sandstones have a strong Archean group but also high Grenville and significant Granite-Rhyolite populations (Figure 14) (Konstantinou et al., 2014; Lovell and Bowen, 2013). Mesoproterozoic-aged Baraboo quartzites from the Lake Superior region have a dominant zircon population with ages characteristic of the Yavapai, Mazatzal and Penokean-Trans Hudson provinces (Figure 14) (Medaris et al., 2021). Sedimentary rocks of the MRS (Figure 12) contain zircons with Grenville, Trans-Hudson/Penokean and Superior province signatures (Figure 14) (Craddock et al., 2013). A more proximal potential source for the Ardmore Basin is the Ordovician sandstones of the southern midcontinent (Pickell, 2012; Thomas et al., 2016). These sandstones have a dominant Archean age group, and minor amounts of Grenville, Granite Rhyolite and Yavapai-Mazatzal groups (Figure 14) (Pickell, 2012).

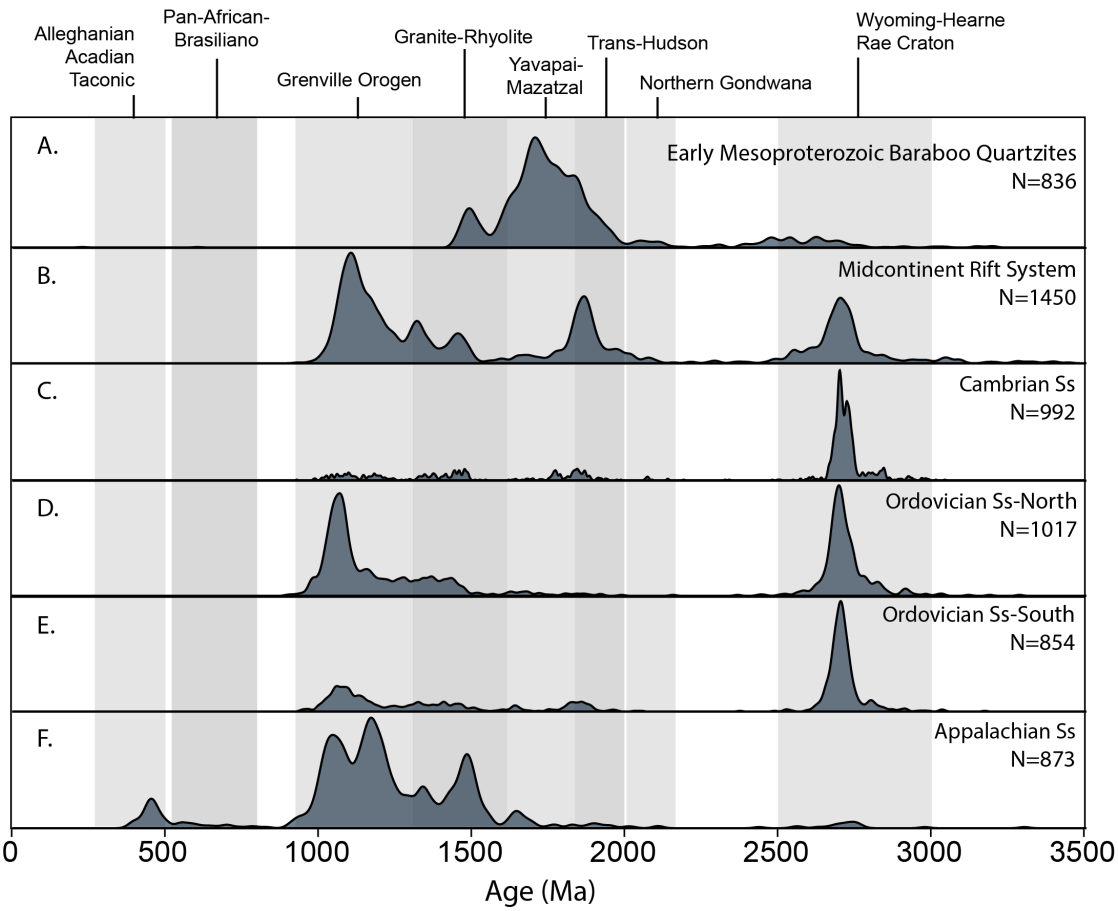

Figure 14: Kernel Density Estimation plots of potential recycled sources after Xie and Manger (2022). See citation details in the text.

6. DISCUSSION

6.1. Provenance of the Upper Mississippian sandstones

The relative similarity among the three Upper Mississippian sandstone samples of the Springer Formation (Figure 5; Table 2) suggests they likely had similar sources. Given the large geographic distance between the Ardmore Basin and the corresponding crustal province sources of the detrital zircons, and the lack of a unique unimodal age group, the sedimentation in the Ardmore Basin was primarily controlled by recycled pre-existing sedimentary rocks during this time.

MDS comparison of detrital zircon ages from the Ardmore Basin with those of potential recycled sources reveals a similarity between Ordovician-Upper Devonian strata of the Appalachian region and samples herein (Figure 15). Comparison of detrital zircon ages of coeval sedimentary deposits in the Appalachian Basin (Figure 16), which received most of their sediment from the active orogen, reveals a substantial mismatch in age groups including the middle Paleozoic (Appalachian), early Mesoproterozoic (Granite-Rhyolite) and late Paleoproterozoic (Yavapai-Mazatzal), as well as subtle mismatches in the Neoproterozoic to Cambrian (peri-Gondwanan) (Figure 5 and Table 2). These dissimilarities can be explained by an intermixing of Appalachian-derived sediment with other sources from the northern midcontinent (Figure 14), and in the case of the Overbrook Sandstone, the Ouachita orogen to the south.

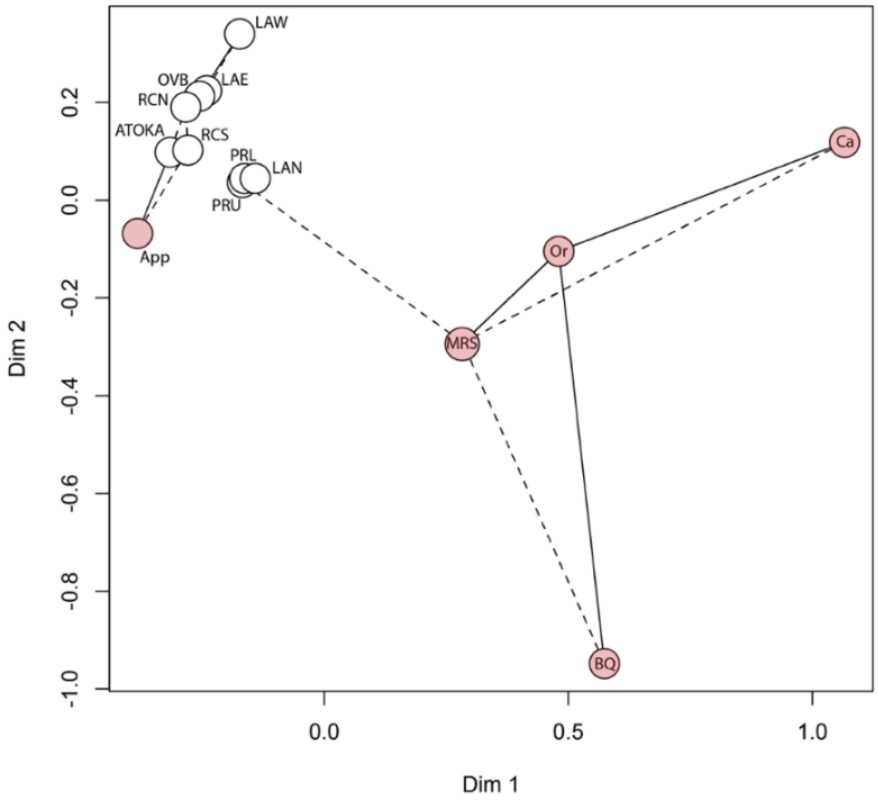

Figure 15: Multidimensional Scaling (MDS) plot of detrital zircon U-Pb ages from the Ardmore Basin samples and potential recycled sources of Laurentia. App: Ordovician-Devonian strata of the Appalachian Basin; BQ: Baraboo quartzites; MRS: Midcontinent Rift System; Ca: Cambrian sandstones; Or: Ordovician sandstones. See citation details in text.

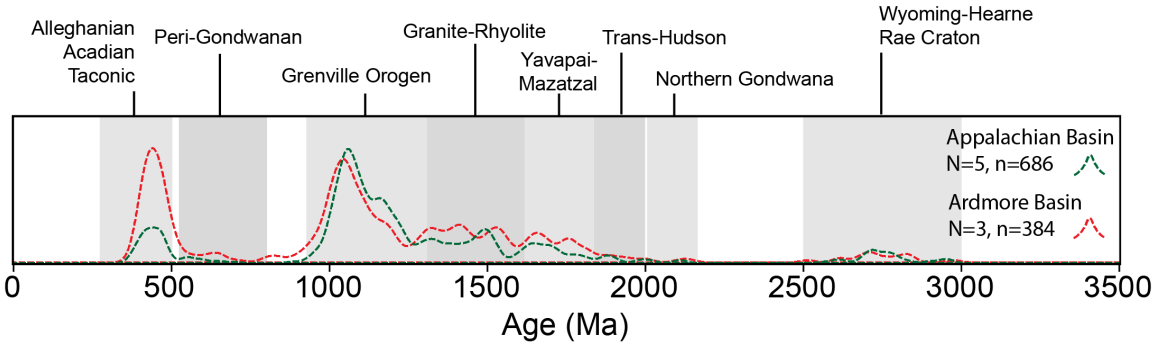

Figure 16: KDE comparing Upper Mississippian sandstones from the Ardmore Basin and Appalachian Basin. Appalachian samples are from Thomas et al. (2017) (1 sample) and Park et al. (2010) (4 samples).

The late Mesoproterozoic (Grenville) age group is inferred to be primarily derived from Appalachian sediment. The subtle trace of "double peaks" within the group seen in RCN, RCS and OVB (Figure 5) (ranging from 31% to 41%) matches well with the Appalachian signature (Thomas et al., 2017). Some of the Grenville grains in Upper Mississippian sandstones of the Ardmore Basin could also be recycled from the Ordovician and MRS sandstones (Figure 14).

The second most abundant age group, the middle Paleozoic (Appalachian) group (ranging from 20% to 24%) was likely recycled from the Appalachian sediment and/or directly derived from synorogenic igneous rocks from the Taconic and Acadian orogens. The third most abundant age group, the early Mesoproterozoic (Granite-Rhyolite) (ranging from 14% to 22%), is inferred to be sourced from the Appalachian sediment and inputs from Ordovician and MRS sandstones and possibly the Baraboo quartzites from the northern midcontinent (Figure 14). A direct contribution from the northern Granite-Rhyolite basement province of the Arbuckle Uplift is not considered since the basement was covered by sedimentary rocks during the Late Mississippian (Thomas et al., 2016).

The more minor late Paleoproterozoic (Yavapai-Mazatzal) age group (ranging from 9%-11%) can be derived from Appalachian sediment, MRS, and/or Baraboo Quartzites (Figure 14). Similarly, the Paleoproterozoic and older (> ~1825 Ma) age group (ranging from 6% to 8%) can be from the Appalachian sediment and the MRS and Ordovician sandstones (Figure 14). The Neoproterozoic to Cambrian (peri-Gondwanan) age group in RCN and RCS (2%) was likely derived from Appalachian sediment. However, OVB has 7% Neoproterozoic to Cambrian (peri-Gondwanan) grains and is possibly the first sign of influence from the emerging peri-Gondwanan sediment supply in the developing Ouachita Orogen.

Core-rim U-Pb age data herein (Figure 11) also provide supplementary evidence for an Appalachian sediment provenance. Studies show that Appalachian Grenville grains have Taconic and Acadian-aged rims (~490-440 Ma and ~420-350 Ma, respectively) and the Grenville grains derived from the south have rims of Neoproterozoic to Cambrian age (~750-500 Ma) (Liu et al., 2022). Of the 23 concordant core-rim pairs in our dataset, four grains fall within the Appalachian Grenville group (Group 1 in Figure 11), and no grain falls within the southern Grenville group. These grains belong to Upper Mississippian OVB and Lower Pennsylvanian LAW, LAN and PRL samples, which indicates a continuous supply of Appalachian sediment into the Early Pennsylvanian.

In short, Upper Mississippian sandstones of the Ardmore Basin are interpreted to be primarily derived from the Appalachian sediment and exposed igneous rocks from the Taconic and Acadian orogens with minor contributions from the northern midcontinent. The increase of the Neoproterozoic to Cambrian (peri-Gondwanan) age group (from 2% to 7%) during the deposition of the Overbrook Sandstone and the clear shift in petrologic characteristics from mature quartzarenites of the Rod Club to a higher lithic composition recorded in the younger Overbrook Sandstone (McBride, 1986) may imply that the Ardmore Basin started to receive sediment from an active orogen and indicates initial traces of peri-Gondwanan sediment from the south.

6.2. Provenance of the Lower Pennsylvanian sandstones

Visual comparison of MDS and KDE plots and statistical analyses reveal significant differences between the Lower Pennsylvanian samples of the northern part of the basin (PRL, PRU, LAN) and the southern part (LAW, LAE, ATOKA) (Figures 5 and 17; Table 2). In

particular, the southern samples contain higher percentages of middle Paleozoic (Appalachian) and Neoproterozoic to Cambrian (peri-Gondwanan) age groups and low percentages of early Mesoproterozoic (Granite-Rhyolite) and late Paleoproterozoic (Yavapai-Mazatzal) age groups.

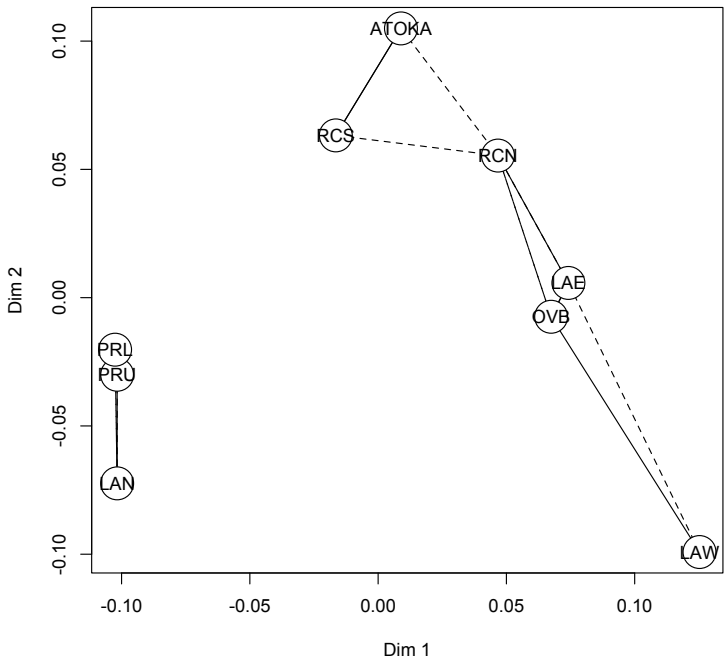

Figure 17: MDS plot of all Ardmore Basin samples.

Considering the similarity in age distributions to the Upper Mississippian sandstones, the samples from the southern part of the basin likely continued receiving sediment from the Appalachian sediment to the east, recycled sources from the northern midcontinent, and small contributions from the Ouachita Orogen to the south. In contrast, the northern area of the basin likely received sediment from a newly introduced system to the west besides receiving detritus from the Appalachian sediment. The significant increase in the midcontinent Granite-Rhyolite and Yavapai-Mazatzal age groups between the southern (LAW and LAE) and the northern Morrowan samples (LAN, PRL, and PRU) (~14.5% to

~22.5%, and ~8% to ~15%, respectively) (Figure 18; Table 2) is likely caused from the nascent influence of the basement uplifts in the Ancestral Rocky Mountains to the west (Figure 12). A similar shift in detrital zircon U-Pb ages has been reported in Morrowan sandstones of the Hugoton Embayment proximal to the orogen front and up-dip of the Ardmore Basin (Figure 18) (Wang et al., 2022). In addition, Meek (1983) proposed a primary source of sediment from the northwest in his study.

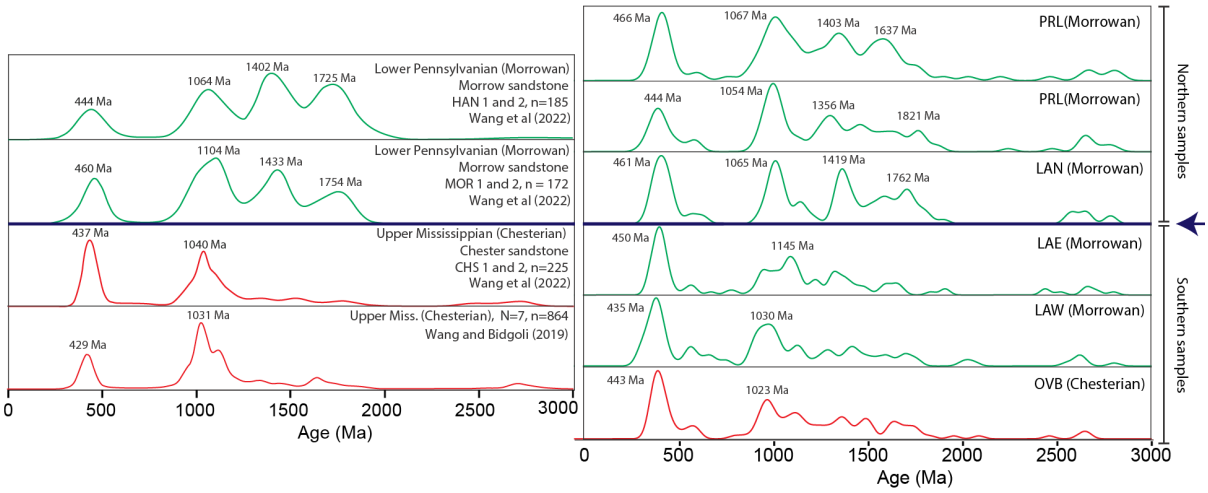

Figure 18: Comparison of Chesterian and Morrowan samples from Wang et al. (2022) and Wang and Bidgoli (2019) (left side), and samples herein (right side). Blue line represents the shift in age group distributions.

Following the deposition of the Lake Ardmore and Primrose sandstones, the younger Lake Murray Sandstone sample (Atokan age) records a characteristic Appalachian signature with dominant late Mesoproterozoic (Grenville) and middle Paleozoic (Appalachian) groups (Figure 5; Table 2). The Lake Murray Sandstone was collected stratigraphically above a thick (~3 meters) unit of conglomerate likely deposited after an episode of significant local uplift in the Criner Hills. Atokan time is indeed a period of extensive deformation in the Ardmore Basin and surrounding areas (Johnson et al., 1989). The sample has limited Neoproterozoic

grains (~1%) so an influence from the approaching Ouachita orogen seen in older samples (OVB, LAW, LAE, LAN, PRL, PRU) is not favored. The increased early Mesoproterozoic (Granite-Rhyolite) and late Paleoproterozoic (Yavapai-Mazatzal) age groups seen in the northern group (LAN, PRL, and PRU) is also not present. However, the Lake Murray Sandstone sample shows very similar detrital zircon U-Pb age distributions to the Upper Mississippian Rod Club sandstones, especially the southern sample, RCS (Figure 5 and 17). Since this sample was collected above a unit of conglomerate, it is possible that instead of recording regional sources, it reflects an overwhelming contribution of detritus from erosion of local uplift. Further studies are needed help better understand this change.

6.3. Late Mississippian to Early Pennsylvanian sediment routing in the southern midcontinent

MDS plots with coeval sandstones between the Appalachian orogen and the central and southern midcontinent provide insights into the routing of sediment (Figure 19). The sediments of the Ardmore Basin are statistically closer to the Mauch Chunk-Pottsville clastic wedge and the longitudinal system headed in the northern Appalachian foreland than to the southern Pennington-Lee clastic wedge (Figure 1). Chesterian samples of the Hugoton Embayment and the Ardmore Basin plot closely together. This may indicate that during this time, the Hugoton Embayment and Ardmore Basin were receiving sediment from a similar provenance. The other recycled sediments from the northern midcontinent including Ordovician sandstones, Baraboo quartzites, and MRS sandstones were also possibly incorporated into associated dispersal systems.

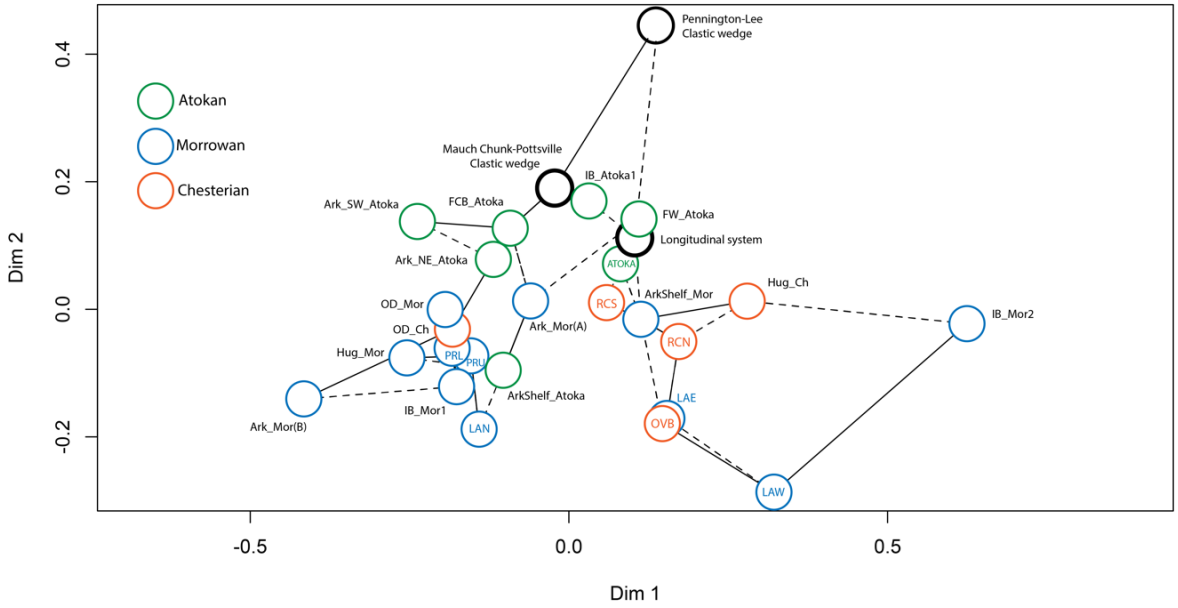

Figure 19: MDS plot of Ardmore Basin samples and regional coeval sandstones. ArkShelf_Atoka: Atokan sandstones of the Arkoma Shelf (Wang et al., 2022); ArkShelf_Mor: Morrowan sandstones of the Arkoma Shelf (Wang et al., 2022); Ark_Mor(A): Morrowan sandstones of the Arkoma Basin (Allred and Blum, 2019); Ark_Mor(B): Morrowan sandstones of the Arkoma Basin (Allred and Blum, 2019); Ark_NE_Atoka: Arkoma Basin sandstones with a northeast directed paleoflow (Sharrah, 2006); Ark_SW_Atoka: Arkoma Basin sandstones with a southwest directed paleoflow; FCB_Atoka: Atokan sandstones of the Forest City Basin (Kissock et al., 2017); FW_Atoka: Atokan sandstone from the Fort Worth Basin (Alsalem et al., 2017); Hug_Ch: Chesterian sandstones of the Hugoton Embayment (HE) (Wang and Bidgoli, 2019; Wang et al., 2022); Hug_Mor: Morrowan sandstones from the HE (Wang and Bidgoli, 2019; Wang et al., 2022); IB_Atoka1: Atokan sandstone from the Illinois Basin (IB); IB_Mor1 and IB_Mor2: Morrowan sandstones from the IB (Kissock et al., 2017); OD_Mor: Lower Pennsylvanian sandstone from northwest Arkansas (Xie and Manger, 2022); OD_Ch: Upper Mississippian Sandstones from northwest Arkansas (Xie and Manger, 2022). Longitudinal System: Pennsylvanian sandstones of the Appalachian longitudinal system (Thomas et al., 2017); Pennington Lee Clastic wedge (Becker et al., 200; Thomas et al., 2017); Mauch Chunk-Pottsville Clastic wedge (Thomas et al., 2017; Park et al., 2010).

Morrowan samples of the Ardmore Basin plot into two separate groups. The northern group (LAN, PRL, and PRU) shares similarities with coeval samples from the Illinois Basin, Hugoton Embayment, and Arkoma Shelf (southern Ozark Dome area) (Figure 19). This

possibly indicates that the Appalachian sediment systems feeding the Illinois Basin also delivered to the Ardmore Basin, Hugoton Embayment, and the Arkoma shelf. In contrast, the southern group of Morrowan samples (LAW and LAE) are relatively dissimilar from the aforementioned areas related to the northern group, which indicates that although displaying an Appalachian provenance signature, a different source not reaching the more northern zones - likely the Ouachita orogen - was supplying sediment. Therefore, the southern area of the Ardmore Basin was likely still receiving Appalachian sediment but also started to receive sediment from the Ouachita orogen in the south-southeast.

In summary, the Ardmore Basin likely received Appalachian-derived sediment as the Alleghenian orogeny and associated deformation developed in the Late Mississippian during the deposition of the Rod Club and Overbrook Sandstones. Sediments of Appalachian origin likely had headwaters in the northern areas of the orogen or were reworked from topographically high Appalachian sediment-rich strata in the northeastern midcontinent (Kissock et al., 2017), then they traveled west until deflected southward through the midcontinent due to the topographic barrier of the Transcontinental Arch (Figure 20) (Lawton et al., 2021). The southward-flowing sediment moved through the midcontinent via various pathways possibly including the incised valleys of the Hugoton Embayment (Wang and Bidgoli, 2019) and likely travelled into the depocenter, or southeastern corner, of the Anadarko Basin and the adjacent Ardmore Basin (Figure 20). Other smaller-scale contributions from recycled sediment of the midcontinent such as Ordovician and MRS sandstones and Baraboo quartzites were likely incorporated into the same north to south drainages. During the deposition of the latest Mississippian sandstone in the Ardmore Basin, the Overbrook, the basin began to receive Neoproterozoic to Cambrian (peri-Gondwanan)

sediment from the active Ouachita Orogen to the southeast. Sea level fluctuations resulted in various sediment delivery mechanisms including fluvial and littoral transport (Chapman and Laskowski, 2019; Lawton et al., 2021).

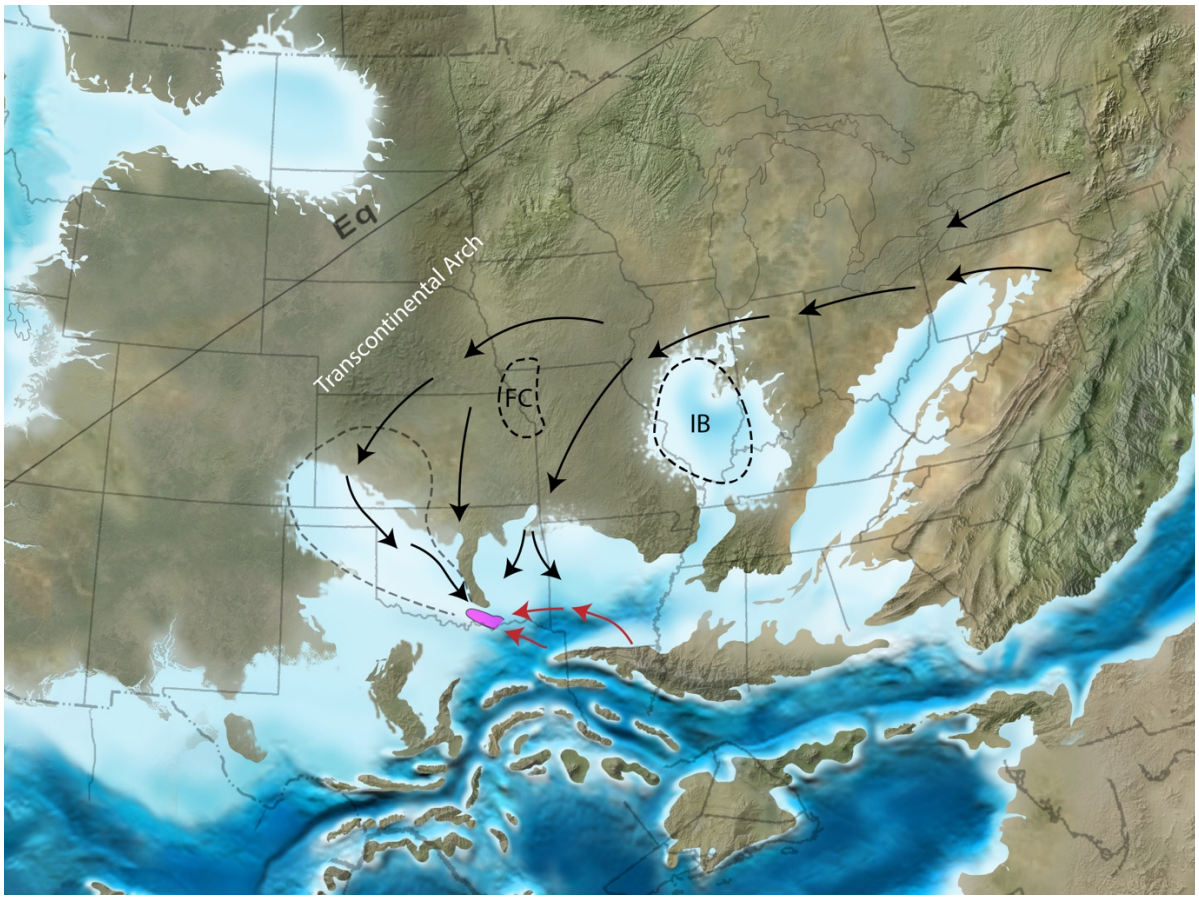

Figure 20: Proposed sediment delivery routing systems during the Late Mississippian, drafted onto a paleogeographic map (Blakey, 2013). Black arrows represent interpreted Appalachian and midcontinent sediment transport, red arrows represent influence from the Ouachita orogen specifically for sample OVB. Purple shape represents outline of the Ardmore Basin.

The provenance of sediment in the northern Ardmore Basin shifted in the Early Pennsylvanian. Influence from the rising Ancestral Rocky Mountains included increases in midcontinent age groups (~14.5% to ~21% in the Granite-Rhyolite age group, and ~8% to ~17% in the Yavapai-Mazatzal age group) which were first seen during the deposition of

LAN, the northern sample of the Morrowan Lake Ardmore Sandstone. Sediment from the Ancestral Rocky Mountains traveled south-southeastward into the Hugoton Embayment and into topographic lows of the southeastern Anadarko Basin and the Ardmore Basin. The influence from the Ancestral Rocky Mountains did not reach the coeval Lake Ardmore Sandstone samples collected in the southern Ardmore Basin (LAW and LAE), which instead remained relatively consistent with the Upper Mississippian samples with a dominant Appalachian signature and traces of recycled midcontinent strata. This implies that during the Morrowan the Ardmore Basin was receiving sediment from (at least) two separate systems, a system coming from the northwest and a system entering through the east-northeast of the basin with southern inputs from the approaching Ouachita orogen (Figure 21). Finally, in Early Pennsylvanian (Atokan) time, the southern part of the Ardmore Basin proximal to the present-day Criner Hills was supplied by recycled sediment from the local uplift.

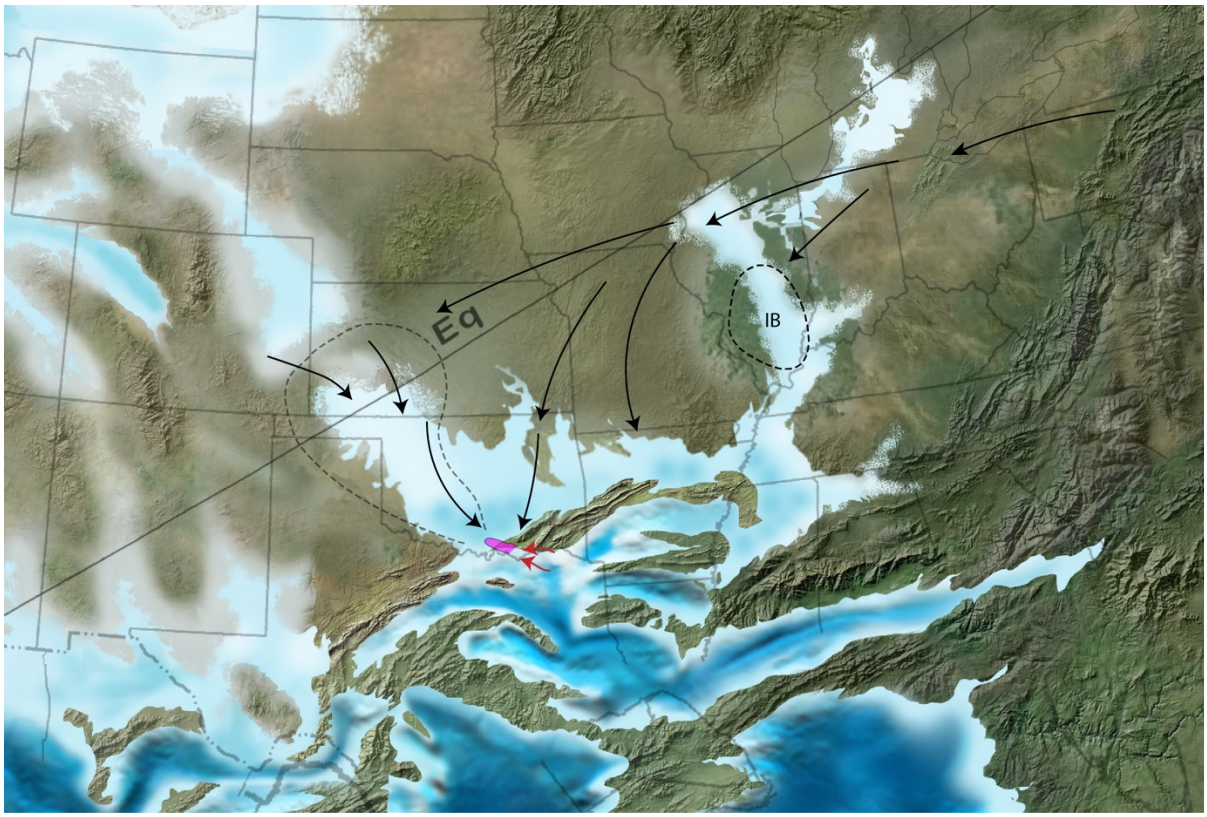

Figure 21: Proposed sediment delivery routing systems during the Early Pennsylvanian, drafted onto a paleogeographic map (Blakey, 2013). Black arrows represent interpreted Appalachian and midcontinent sediment transport, red arrows represent Gondwana influence specifically for sample OVB. Purple shape represents outline of the Ardmore Basin.

7. CONCLUSIONS

In this study, nine samples of Late Mississippian to Early Pennsylvanian age from the Ardmore Basin were collected, processed, and analyzed using U-Pb detrital zircon geochronology. The data reveal changing conditions in this timeframe. The main conclusions reached in this study include:

1. Detrital zircon U-Pb signatures of the Upper Mississippian (Chesterian) Rod Club Sandstones (RCS and RCN) and Overbrook Sandstone (OVB) are characterized by a

predominant middle to late Mesoproterozoic (Grenville) population, secondary middle Paleozoic (Appalachian), early Mesoproterozoic (Granite-Rhyolite), and late Paleoproterozoic (Yavapai-Mazatzal) populations, and minor Neoproterozoic to Cambrian (peri-Gondwanan) and Paleoproterozoic and older (> ~1825 Ma) age groups. These age groups were mostly derived from an Appalachian source and partially from pre-existing sediments of the northern midcontinent. Along with the Appalachian and midcontinent sources, the Overbrook Sandstone records an introduction of peri-Gondwanan sediment influence from the emerging Ouachita orogen.

2. Lower Pennsylvanian (Morrowan) sandstones displayed varied detrital zircon U-Pb age distributions. The samples collected in the southern part of the basin are characterized by the same age groups as the Upper Mississippian sandstones and thus represent a similar primary Appalachian source and minor contributions from pre-existing sediments of the northern midcontinent and continued influence from the Ouachita Orogen. The northern samples record an intermixed system of Appalachian sources and an introduced influence from the Ancestral Rocky Mountains to the northwest as indicated by abrupt changes in early Mesoproterozoic (Granite-Rhyolite), and late Paleoproterozoic (Yavapai-Mazatzal) age groups, and decreases in total percentages of the Appalachian-characteristic age groups, including the middle to late Mesoproterozoic (Grenville) and middle Paleozoic (Appalachian) populations. The signature of Ouachita influence is also less dominant in the northern samples.

3. The Lower Pennsylvanian (Atokan) sandstone collected from the southern part of the basin has the same characteristic ages as the Upper Mississippian sandstones and represents recycling from the local Criner Hills uplift.

APPENDIX

U-Pb detrital zircon geochronology data for all samples in this study.

Sample Name: ATOKA							207/235		206/238		207/206		Best age			
Grain #	[U] ppm	U/Th	207/235	2σ error	206/238	2σ error	Age (Ma)	2σ error	Age (Ma)	2σ error	Age (Ma)	2σ error	(Ma)	2σ error	% Disc*	Rim/ Core
ATOKA_1.FIN2	366	4.87	0.552	0.014	0.0703	0.0013	445.9	9.2	438	7.8	488	50	438.0	7.8	1.8	
ATOKA_2.FIN2	230	0.86	0.4677	0.009	0.06268	0.00056	388.9	6.3	391.8	3.4	353	43	391.8	3.4	0.7	
ATOKA_3.FIN2	108.1	0.83	14.46	0.12	0.5455	0.0044	2780.4	8.1	2805	19	2758	12	2758.0	12.0	1.7	
ATOKA_4.FIN2	338	2.05	3.004	0.027	0.2476	0.0022	1407.7	6.8	1426	11	1377	15	1426.0	11.0	1.3	
ATOKA_5.FIN2	231	1.76	4.485	0.048	0.317	0.0033	1727.1	8.9	1775	16	1668	16	1668.0	16.0	6.4	
ATOKA_6.FIN2	206.6	1.96	4.825	0.051	0.3294	0.0033	1789.2	9.1	1835	16	1731	18	1731.0	18.0	6.0	
ATOKA_7.FIN2	171.4	1.19	0.556	0.017	0.0708	0.0017	449	11	441	10	499	90	441.0	10.0	1.8	
ATOKA_8.FIN2	416	1.84	1.886	0.019	0.1837	0.0016	1075.5	6.8	1087.2	8.5	1044	19	1087.2	8.5	1.1	
ATOKA_9.FIN2	118.4	0.95	4.25	0.089	0.2974	0.0057	1682	18	1677	28	1679	37	1679.0	37.0	0.1	
ATOKA_10.FIN2	82.5	0.76	1.854	0.031	0.1822	0.002	1063	11	1079	11	1024	36	1079.0	11.0	1.5	
ATOKA_11.FIN2	256	4.78	3.197	0.055	0.2553	0.0032	1455	13	1465	17	1430	24	1465.0	17.0	0.7	
ATOKA_12.FIN2	216.4	1.78	2.319	0.034	0.2113	0.0026	1217	10	1236	14	1180	28	1236.0	14.0	1.6	
ATOKA_13.FIN2	323	0.38	4.069	0.053	0.2839	0.0036	1648	11	1610	18	1695	16	1695.0	16.0	5.0	
ATOKA_14.FIN2	121	2.27	2.243	0.037	0.2076	0.0025	1192	12	1215	13	1143	31	1215.0	13.0	1.9	
ATOKA_15.FIN2	107.1	1.83	3.838	0.044	0.2806	0.0027	1599.4	9.2	1594	13	1598	20	1594.0	13.0	0.3	
ATOKA_16.FIN2	147.4	1.31	0.547	0.01	0.07168	0.00075	442.8	7	446.2	4.5	416	42	446.2	4.5	0.8	
ATOKA_17.FIN2	376	1.35	0.49	0.01	0.06398	0.00078	404.2	6.9	399.8	4.7	423	48	399.8	4.7	1.1	
ATOKA_19.FIN2	60.2	0.89	2.781	0.054	0.2332	0.003	1348	14	1351	16	1336	36	1351.0	16.0	0.2	
ATOKA_21.FIN2	86.9	1.44	3.476	0.043	0.2677	0.0027	1520.3	9.8	1529	14	1505	24	1529.0	14.0	0.6	
ATOKA_22.FIN2	253.4	0.82	5.366	0.046	0.344	0.0023	1878.5	7.4	1906	11	1847	13	1847.0	13.0	3.2	

ATOKA_23.FIN2	259	1.06	2.174	0.03	0.1936	0.0027	1171.1	9.5	1140	14	1230	25	1140.0	14.0	2.7	
ATOKA_24.FIN2	143.8	1.82	2.274	0.032	0.2057	0.0022	1202.4	9.9	1206	12	1193	26	1206.0	12.0	0.3	
ATOKA_25.FIN2	197.2	3.17	1.803	0.053	0.1726	0.0051	1046	19	1026	28	1081	51	1026.0	28.0	1.9	Rim
ATOKA_25.FIN2	285.3	1.69	4.193	0.047	0.2981	0.003	1671.5	9.2	1681	15	1659	18	1659.0	18.0	1.3	Core
ATOKA_26.FIN2	495.3	0.94	0.4847	0.0064	0.06384	0.00053	400.9	4.4	398.9	3.2	399	30	398.9	3.2	0.5	
ATOKA_27.FIN2	279.1	2.82	1.666	0.017	0.1647	0.0012	994.8	6.6	982.9	6.5	1013	19	982.9	6.5	1.2	
ATOKA_28.FIN2	185.5	3.22	2.149	0.024	0.1982	0.0016	1164.7	7.4	1165.5	8.4	1154	21	1165.5	8.4	0.1	
ATOKA_29.FIN2	152.1	1.93	0.527	0.011	0.06913	0.00075	429	7.5	430.9	4.5	394	48	430.9	4.5	0.4	
ATOKA_30.FIN2	280.5	2.48	3.503	0.038	0.2631	0.0026	1526.4	8.6	1505	13	1544	17	1505.0	13.0	1.4	
ATOKA_31.FIN2	127	0.99	2.185	0.031	0.1988	0.002	1176	10	1169	11	1177	31	1169.0	11.0	0.6	
ATOKA_32.FIN2	324	2.52	1.861	0.02	0.1796	0.0015	1066.4	7.3	1064.3	8.3	1054	20	1064.3	8.3	0.2	
ATOKA_33.FIN2	56.3	0.97	0.555	0.021	0.0692	0.0012	448	13	431.3	7	484	82	431.3	7.0	3.7	
ATOKA_34.FIN2	58.3	0.92	1.838	0.041	0.1761	0.0022	1055	15	1047	12	1046	43	1047.0	12.0	0.8	
ATOKA_35.FIN2	337	3.17	2.229	0.021	0.2014	0.0016	1189.5	6.5	1182.4	8.8	1188	18	1182.4	8.8	0.6	
ATOKA_36.FIN2	20.45	1.73	4.089	0.087	0.2935	0.0043	1651	18	1658	21	1621	44	1621.0	44.0	2.3	
ATOKA_37.FIN2	790	6.55	2.002	0.03	0.1854	0.0021	1116	10	1097	11	1148	24	1097.0	11.0	1.7	
ATOKA_38.FIN2	247.3	1.71	0.5499	0.0091	0.07037	0.00061	444.3	6	438.3	3.7	454	36	438.3	3.7	1.4	
ATOKA_39.FIN2	329	3.93	2.183	0.02	0.2001	0.0014	1174.9	6.3	1175.9	7.7	1169	17	1175.9	7.7	0.1	
ATOKA_40.FIN2	115	1.93	1.789	0.029	0.1734	0.0022	1039	11	1030	12	1048	35	1030.0	12.0	0.9	
ATOKA_41.FIN2	176.9	1.26	3.536	0.055	0.257	0.0029	1534	12	1474	15	1611	29	1474.0	15.0	3.9	
ATOKA_42.FIN2	226	2.43	3.568	0.057	0.2657	0.0043	1540	12	1517	22	1573	18	1517.0	22.0	1.5	
ATOKA_43.FIN2	91.7	2.73	1.946	0.037	0.1854	0.0024	1094	13	1098	13	1083	33	1098.0	13.0	0.4	
ATOKA_44.FIN2	22.6	1.25	1.592	0.051	0.1592	0.0027	961	20	952	15	960	73	952.0	15.0	0.9	
ATOKA_45.FIN2	332	2.96	2.383	0.031	0.2101	0.0021	1236.3	9.3	1229	11	1245	19	1229.0	11.0	0.6	
ATOKA_46.FIN2	41	1.23	1.755	0.041	0.1728	0.002	1025	15	1027	11	1005	49	1027.0	11.0	0.2	
ATOKA_47.FIN2	228.7	1.32	4.408	0.038	0.3082	0.0025	1713.9	7.3	1731	12	1691	15	1691.0	15.0	2.4	
ATOKA_48.FIN2	270	1.02	0.528	0.01	0.06674	0.0007	430	6.8	416.4	4.2	490	41	416.4	4.2	3.2	
ATOKA_49.FIN2	255	4.21	0.619	0.034	0.0731	0.0018	488	21	455	11	630	120	455.0	11.0	6.8	

ATOKA_50.FIN2	84	0.87	2.774	0.053	0.2288	0.0029	1345	14	1327	15	1366	33	1327.0	15.0	1.3
ATOKA_51.FIN2	154.8	0.71	14.19	0.11	0.5442	0.0045	2761.8	7.6	2800	19	2729	12	2729.0	12.0	2.6
ATOKA_52.FIN2	498	2.70	3.469	0.063	0.2468	0.0049	1519	14	1422	26	1657	28	1422.0	26.0	6.4
ATOKA_53.FIN2	238.7	1.32	1.937	0.022	0.1853	0.0018	1094	7.4	1095.6	9.7	1088	22	1095.6	9.7	0.1
ATOKA_54.FIN2	271.8	1.45	1.661	0.017	0.168	0.0013	993	6.5	1001.8	7.5	966	22	1001.8	7.5	0.9
ATOKA_55.FIN2	219.6	2.22	4.67	0.048	0.316	0.0028	1760.7	8.5	1770	14	1745	15	1745.0	15.0	1.4
ATOKA_56.FIN2	230	4.00	2.822	0.063	0.2315	0.0036	1356	17	1341	19	1376	24	1341.0	19.0	1.1
ATOKA_57.FIN2	47.8	0.95	2.019	0.052	0.1912	0.0025	1121	18	1127	14	1092	50	1127.0	14.0	0.5
ATOKA_58.FIN2	105.2	1.20	3.436	0.044	0.2667	0.0028	1511	10	1524	14	1486	21	1524.0	14.0	0.9
ATOKA_59.FIN2	288	1.18	4.242	0.051	0.2985	0.0035	1680.7	9.9	1683	17	1668	17	1668.0	17.0	0.9
ATOKA_60.FIN2	274	2.26	1.828	0.023	0.1796	0.0021	1054.4	8.4	1065	12	1024	22	1065.0	12.0	1.0
ATOKA_61.FIN2	172.6	2.11	2.226	0.028	0.2046	0.0021	1188	8.9	1199	11	1156	23	1199.0	11.0	0.9
ATOKA_62.FIN2	149.8	1.70	2.391	0.037	0.2134	0.0024	1239	11	1247	13	1219	27	1247.0	13.0	0.6
ATOKA_63.FIN2	463	0.76	0.5783	0.009	0.07196	0.0009	462.8	5.8	447.9	5.4	526	29	447.9	5.4	3.2
ATOKA_64.FIN2	81.4	2.52	1.664	0.029	0.1653	0.0017	993	11	985.9	9.4	989	35	985.9	9.4	0.7
ATOKA_65.FIN2	456.9	1.43	0.602	0.021	0.0736	0.0016	478	13	458	9.4	556	73	458.0	9.4	4.2
ATOKA_66.FIN2	551	1.71	0.5486	0.0079	0.06918	0.00066	443.7	5.2	431.2	4	498	31	431.2	4.0	2.8
ATOKA_67.FIN2	147.7	1.76	1.686	0.024	0.171	0.0014	1001.9	9	1017.2	7.8	956	30	1017.2	7.8	1.5
ATOKA_68.FIN2	59.42	1.89	1.88	0.032	0.1811	0.0016	1071	11	1072.9	8.9	1053	36	1072.9	8.9	0.2
ATOKA_69.FIN2	53.8	1.52	2.174	0.049	0.2096	0.0029	1171	15	1226	15	1053	42	1226.0	15.0	4.7
ATOKA_70.FIN2	120.4	0.52	13.78	0.12	0.5345	0.0039	2733.5	8	2759	17	2704	12	2704.0	12.0	2.0
ATOKA_71.FIN2	180.9	1.88	2.569	0.04	0.2188	0.0034	1290	12	1277	17	1316	28	1277.0	17.0	1.0
ATOKA_72.FIN2	185	2.16	1.883	0.038	0.1773	0.002	1073	13	1052	11	1111	36	1052.0	11.0	2.0
ATOKA_73.FIN2	342	21.40	2.128	0.037	0.1986	0.0029	1155	12	1167	15	1129	24	1167.0	15.0	1.0
ATOKA_74.FIN2	149.9	1.04	2.658	0.031	0.2289	0.0021	1316.7	8.9	1328	11	1301	23	1328.0	11.0	0.9
ATOKA_75.FIN2	213	0.72	0.599	0.016	0.0756	0.0011	475.8	9.9	469.7	6.7	498	65	469.7	6.7	1.3
ATOKA_76.FIN2	372.8	0.99	0.533	0.015	0.0684	0.0011	433.4	9.8	426.5	6.8	474	71	426.5	6.8	1.6
ATOKA_77.FIN2	92.5	0.72	4.235	0.053	0.3063	0.003	1680	11	1722	15	1634	22	1634.0	22.0	5.4

ATOKA_78.FIN2	175.8	1.81	2.173	0.028	0.2012	0.0022	1171.2	8.9	1183	12	1159	23	1183.0	12.0	1.0
ATOKA_79.FIN2	271.4	1.00	1.908	0.023	0.1825	0.0016	1082.8	8.1	1080.4	9	1100	17	1080.4	9.0	0.2
ATOKA_80.FIN2	215.4	2.99	1.748	0.022	0.1752	0.0022	1025.4	8.1	1040	12	1008	27	1040.0	12.0	1.4
ATOKA_81.FIN2	107.8	1.85	1.945	0.028	0.1861	0.0019	1095.2	9.5	1100	10	1097	28	1100.0	10.0	0.4
ATOKA_82.FIN2	20.81	3.74	1.908	0.058	0.1845	0.0032	1079	21	1091	17	1059	62	1091.0	17.0	1.1
ATOKA_83.FIN2	190	2.45	2.21	0.031	0.2065	0.0022	1184	9.3	1210	12	1135	24	1210.0	12.0	2.2
ATOKA_84.FIN2	225.4	0.93	0.57	0.011	0.07151	0.0008	458.2	7.2	445.2	4.8	530	42	445.2	4.8	2.8
ATOKA_85.FIN2	422	1.77	1.834	0.019	0.1785	0.0017	1056.9	6.7	1058.7	9.2	1064	18	1058.7	9.2	0.2
ATOKA_86.FIN2	447	1.92	0.5413	0.007	0.07044	0.00067	438.9	4.6	438.8	4	444	28	438.8	4.0	0.0
ATOKA_87.FIN2	250.5	1.49	4.603	0.044	0.3112	0.0032	1750.2	7.8	1746	16	1759	21	1759.0	21.0	0.7
ATOKA_88.FIN2	153.2	2.04	2.103	0.029	0.1965	0.0019	1148	9.6	1156	10	1135	25	1156.0	10.0	0.7
ATOKA_89.FIN2	922	2.55	1.761	0.024	0.1736	0.0027	1032.4	8.3	1032	15	1031	23	1032.0	15.0	0.0
ATOKA_90.FIN2	14.46	1.58	1.832	0.069	0.1725	0.0031	1045	25	1025	17	1061	77	1025.0	17.0	1.9
ATOKA_91.FIN2	190.2	0.84	1.784	0.026	0.1721	0.002	1038.4	9.4	1023	11	1066	28	1023.0	11.0	1.5
ATOKA_92.FIN2	190	2.59	1.582	0.022	0.1592	0.0016	961.6	8.6	954	8.2	981	28	954.0	8.2	0.8
ATOKA_93.FIN2	190.7	1.56	10.755	0.097	0.4788	0.0041	2501	8.4	2521	18	2482	13	2482.0	13.0	1.6
ATOKA_94.FIN2	129.5	2.25	2.813	0.043	0.2324	0.004	1359	12	1346	21	1371	31	1346.0	21.0	1.0
ATOKA_95.FIN2	254	1.06	0.538	0.013	0.07005	0.00098	437.4	8.3	436.4	5.9	427	49	436.4	5.9	0.2
ATOKA_96.FIN2	202	1.57	4.128	0.055	0.2932	0.0032	1659	11	1657	16	1663	23	1663.0	23.0	0.4
ATOKA_97.FIN2	116.3	1.92	1.966	0.032	0.1913	0.0023	1102	11	1128	12	1045	31	1128.0	12.0	2.4
ATOKA_98.FIN2	342.4	1.99	1.86	0.019	0.1791	0.0017	1066.3	6.7	1061.7	9.1	1070	18	1061.7	9.1	0.4
ATOKA_99.FIN2	127.9	4.78	0.567	0.017	0.0712	0.0011	455	11	443.1	6.6	495	70	443.1	6.6	2.6
ATOKA_100.FIN2	233	1.22	6.837	0.062	0.3824	0.0031	2089.4	8	2087	14	2089	13	2089.0	13.0	0.1
ATOKA_101.FIN2	822	1.70	1.717	0.017	0.1708	0.0016	1014.1	6.4	1016.5	9	1004	18	1016.5	9.0	0.2
ATOKA_102.FIN2	200	1.83	3.653	0.043	0.2711	0.0034	1560.4	9.4	1546	17	1575	24	1546.0	17.0	0.9
ATOKA_103.FIN2	184.5	3.57	2.427	0.047	0.217	0.0039	1253	15	1266	21	1216	41	1266.0	21.0	1.0
ATOKA_104.FIN2	421.2	3.66	1.684	0.021	0.1687	0.0017	1001.7	8	1004.9	9.3	989	20	1004.9	9.3	0.3

ATOKA_105.FIN2	243.7	2.05	1.844	0.025	0.1744	0.002	1060.9	8.6	1036	11	1097	24	1036.0	11.0	2.3	
ATOKA_106.FIN2	262	1.67	3.758	0.049	0.2774	0.0031	1583	11	1578	16	1580	21	1578.0	16.0	0.3	
ATOKA_107.FIN2	127.2	1.90	1.928	0.028	0.1816	0.002	1090.2	9.9	1076	11	1110	25	1076.0	11.0	1.3	
ATOKA_108.FIN2	215	2.97	1.927	0.028	0.1851	0.0019	1088.9	9.7	1095	10	1072	27	1095.0	10.0	0.6	
ATOKA_109.FIN2	62.1	0.90	15.79	0.15	0.5784	0.0055	2862.4	9.3	2941	22	2800	14	2800.0	14.0	5.0	
ATOKA_110.FIN2	585	1.63	3.537	0.031	0.269	0.0023	1534.7	7	1535	11	1530	16	1535.0	11.0	0.0	
ATOKA_111.FIN2	319	0.96	1.789	0.023	0.1723	0.0021	1042	8.5	1025	12	1072	24	1025.0	12.0	1.6	
ATOKA_112.FIN2	103.1	1.83	1.831	0.027	0.1797	0.002	1055	9.6	1065	11	1026	29	1065.0	11.0	0.9	
ATOKA_113.FIN2	1320	19.67	1.774	0.029	0.1726	0.0029	1035	11	1026	16	1057	23	1026.0	16.0	0.9	Rim
ATOKA_113.FIN2	188.5	2.55	3.347	0.067	0.2641	0.0036	1490	16	1510	19	1461	31	1510.0	19.0	1.3	Core
ATOKA_114.FIN2	79.8	1.87	2.155	0.041	0.1988	0.0024	1164	13	1169	13	1149	36	1169.0	13.0	0.4	
ATOKA_115.FIN2	202.9	1.81	2.264	0.03	0.2072	0.0026	1200	9.3	1214	14	1164	25	1214.0	14.0	1.2	
ATOKA_116.FIN2	80.5	0.57	3.339	0.044	0.2657	0.0033	1491	11	1518	17	1452	24	1518.0	17.0	1.8	
ATOKA_117.FIN2	138.1	1.71	0.46	0.011	0.06132	0.00069	383	7.7	383.6	4.2	361	55	383.6	4.2	0.2	
ATOKA_118.FIN2	632	1.60	0.666	0.011	0.0794	0.0013	518	7	492.6	7.5	624	51	492.6	7.5	4.9	
ATOKA_119.FIN2	387	1.33	0.6222	0.0093	0.07881	0.00082	490.6	5.8	489	4.9	485	31	489.0	4.9	0.3	
ATOKA_120.FIN2	903	54.80	3.159	0.032	0.2498	0.0028	1446.6	7.9	1437	15	1456	17	1437.0	15.0	0.7	
ATOKA_121.FIN2	485.3	1.62	0.618	0.013	0.0745	0.0011	487.8	8.5	463.2	6.6	614	46	463.2	6.6	5.0	
ATOKA_122.FIN2	113.1	2.37	1.977	0.044	0.1835	0.0029	1105	15	1086	16	1142	36	1086.0	16.0	1.7	
ATOKA_123.FIN2	92.9	1.99	1.741	0.049	0.1637	0.0037	1021	18	976	21	1107	54	976.0	21.0	4.4	
ATOKA_124.FIN2	251.7	1.54	0.7414	0.0099	0.09126	0.00076	563.3	5.9	562.9	4.5	551	28	562.9	4.5	0.1	
ATOKA_126.FIN2	1443	13.60	1.773	0.042	0.163	0.0042	1035	15	973	23	1160	51	973.0	23.0	6.0	Rim
ATOKA_126.FIN2	127.2	1.98	3.02	0.05	0.2487	0.0024	1411	13	1432	13	1374	30	1432.0	13.0	1.5	Core

ATOKA_127.FIN2	387	1.85	1.68	0.018	0.1697	0.0014	1000.1	6.7	1010.4	7.4	973	19	1010.4	7.4	1.0
ATOKA_128.FIN2	214.9	1.40	4.228	0.041	0.2974	0.0028	1678.3	7.9	1678	14	1675	17	1675.0	17.0	0.2
ATOKA_129.FIN2	858	2.82	0.5181	0.0068	0.06579	0.00093	423.7	4.6	410.7	5.6	491	34	410.7	5.6	3.1
ATOKA_130.FIN2	139.1	1.96	1.962	0.028	0.1852	0.0017	1100.9	9.7	1095.3	9.2	1107	27	1095.3	9.2	0.5

Sample Name: PRU							207/235		206/238		207/206		Best age			
Grain #	[U] ppm	U/Th	207/235	2σ error	206/238	2σ error	Age (Ma)	2σ error	Age (Ma)	2σ error	Age (Ma)	2σ error	(Ma)	2σ error	% Disc*	Rim/ Core
PRU_1.FIN2	153	3.31	1.829	0.033	0.1768	0.0019	1053	12	1049	11	1055	36	1049.0	11.0	0.4	
PRU_2.FIN2	224.4	3.84	4.428	0.065	0.3023	0.0046	1716	12	1702	23	1740	27	1740.0	27.0	2.2	
PRU_3.FIN2	161.6	6.12	2.99	0.15	0.2393	0.0087	1390	37	1380	45	1412	41	1380.0	45.0	0.7	
PRU_4.FIN2	48.4	2.02	1.816	0.056	0.1786	0.003	1046	20	1058	17	989	65	1058.0	17.0	1.1	
PRU_5.FIN2	206.6	1.50	1.494	0.039	0.1349	0.0026	926	16	815	15	1204	59	815.0	15.0	12.0	
PRU_6.FIN2	123.5	0.84	0.605	0.02	0.07534	0.00096	479	13	468.1	5.7	498	71	468.1	5.7	2.3	
PRU_7.FIN2	260	7.83	0.516	0.015	0.06764	0.00096	420	10	421.8	5.8	395	61	421.8	5.8	0.4	
PRU_8.FIN2	197	1.55	0.578	0.016	0.0758	0.001	462	10	470.9	6.2	405	65	470.9	6.2	1.9	
PRU_9.FIN2	289	1.76	2.416	0.041	0.2115	0.0033	1245	12	1236	18	1263	28	1236.0	18.0	0.7	
PRU_10.FIN2	202	0.58	2.412	0.037	0.2175	0.0026	1245	11	1270	14	1203	30	1270.0	14.0	2.0	
PRU_11.FIN2	32.5	1.09	3.71	0.11	0.2771	0.0055	1563	23	1575	28	1524	50	1575.0	28.0	0.8	
PRU_12.FIN2	252	11.10	2.096	0.039	0.1924	0.0025	1149	13	1134	13	1170	32	1134.0	13.0	1.3	
PRU_13.FIN2	223.3	1.58	4.251	0.061	0.3015	0.0036	1682	12	1698	18	1663	22	1663.0	22.0	2.1	
PRU_14.FIN2	156	1.09	0.61	0.019	0.07871	0.00096	482	12	488.3	5.7	424	65	488.3	5.7	1.3	
PRU_15.FIN2	376	2.11	4.157	0.049	0.2936	0.0034	1663.9	9.6	1659	17	1669	21	1669.0	21.0	0.6	
PRU_16.FIN2	50	1.80	1.643	0.049	0.166	0.0028	980	19	989	15	940	66	989.0	15.0	0.9	
PRU_17.FIN2	311.1	0.85	2.85	0.1	0.1695	0.0037	1367	27	1009	21	1980	57	DISC	DISC	26.2	

PRU_18.FIN2	326	1.65	2.975	0.037	0.241	0.0024	1401.9	9.3	1391	12	1408	20	1391.0	12.0	0.8
PRU_20.FIN2	30.1	1.96	2.736	0.091	0.236	0.0046	1327	25	1364	24	1254	72	1364.0	24.0	2.8
PRU_22.FIN2	196.4	1.38	0.881	0.021	0.1057	0.0016	639	11	647.6	9.1	599	47	647.6	9.1	1.3
PRU_23.FIN2	878	22.75	0.513	0.011	0.0659	0.0011	420.2	7.4	411.5	6.7	464	43	411.5	6.7	2.1
PRU_24.FIN2	199	2.31	3.266	0.051	0.2589	0.0027	1472	12	1484	14	1454	26	1484.0	14.0	0.8
PRU_25.FIN2	96.2	0.73	3.294	0.056	0.2549	0.0035	1477	13	1463	18	1504	34	1463.0	18.0	0.9
PRU_26.FIN2	123.4	1.27	3.138	0.063	0.2537	0.0032	1438	15	1457	16	1412	34	1457.0	16.0	1.3
PRU_27.FIN2	138.8	0.49	13.09	0.16	0.5142	0.0062	2684	12	2673	26	2697	17	2697.0	17.0	0.9
PRU_28.FIN2	241	1.02	0.628	0.016	0.0792	0.001	493.2	9.8	491	6.1	492	58	491.0	6.1	0.4
PRU_29.FIN2	566	2.85	3.35	0.049	0.2143	0.0028	1491	11	1251	15	1855	23	DISC	DISC	16.1
PRU_30.FIN2	187.9	1.01	0.569	0.019	0.0724	0.0013	455	12	450.5	7.5	469	80	450.5	7.5	1.0
PRU_31.FIN2	225.3	1.82	3.93	0.06	0.2942	0.0035	1617	12	1662	18	1563	22	1563.0	18.0	2.8
PRU_32.FIN2	66.3	0.87	15.9	0.24	0.5643	0.0074	2870	14	2882	31	2864	18	2864.0	18.0	0.6
PRU_33.FIN2	83	2.64	2.118	0.056	0.1958	0.0026	1148	18	1152	14	1118	50	1152.0	14.0	0.3
PRU_34.FIN2	28.5	2.60	2.079	0.073	0.1986	0.004	1139	24	1170	22	1063	74	1170.0	22.0	2.7
PRU_35.FIN2	388	0.67	0.592	0.011	0.07611	0.00098	471.9	7.4	472.8	5.9	455	44	472.8	5.9	0.2
PRU_36.FIN2	440	6.66	1.796	0.035	0.1779	0.0028	1042	13	1055	15	1013	34	1055.0	15.0	1.2
PRU_37.FIN2	68.2	2.08	2.122	0.053	0.1971	0.0025	1153	17	1159	13	1130	47	1159.0	13.0	0.5
PRU_38.FIN2	245.5	2.66	4.637	0.076	0.3172	0.0044	1756	13	1779	22	1723	29	1723.0	29.0	3.3
PRU_39.FIN2	208	2.45	1.514	0.035	0.1574	0.0022	932	14	942	12	881	47	942.0	12.0	1.1
PRU_41.FIN2	120.6	1.23	1.85	0.039	0.1786	0.0023	1060	14	1059	13	1049	46	1059.0	13.0	0.1
PRU_42.FIN2	95.7	0.57	1.861	0.043	0.1826	0.0027	1065	15	1080	14	1013	46	1080.0	14.0	1.4
PRU_43.FIN2	234.1	1.96	4.515	0.065	0.3163	0.0038	1731	12	1773	19	1674	21	1674.0	21.0	5.9
PRU_44.FIN2	153.1	1.56	3.468	0.078	0.2678	0.0038	1517	17	1529	19	1488	43	1529.0	19.0	0.8
PRU_45.FIN2	92.6	1.24	2.624	0.052	0.2192	0.0029	1304	15	1277	15	1338	39	1277.0	15.0	2.1
PRU_46.FIN2	473	2.78	2.513	0.032	0.222	0.0022	1274.3	9.1	1292	12	1233	22	1292.0	12.0	1.4
PRU_47.FIN2	453	1.37	1.984	0.043	0.1806	0.0033	1106	15	1069	18	1160	28	1069.0	18.0	3.3
PRU_48.FIN2	296	1.28	0.551	0.012	0.07068	0.0007	444.3	7.9	440.2	4.2	443	52	440.2	4.2	0.9

PRU_49.FIN2	150.4	0.61	6.081	0.078	0.3642	0.0035	1986	11	2001	17	1958	22	1958.0	22.0	2.2
PRU_50.FIN2	85	0.99	1.89	0.054	0.1798	0.0032	1077	18	1065	17	1077	59	1065.0	17.0	1.1
PRU_51.FIN2	56.2	1.88	1.751	0.048	0.1742	0.0028	1024	18	1035	16	985	54	1035.0	16.0	1.1
PRU_52.FIN2	476	3.19	2.979	0.032	0.2434	0.0022	1402	8.4	1404	12	1384	20	1404.0	12.0	0.1
PRU_53.FIN2	187	1.26	2.942	0.05	0.2423	0.0027	1391	13	1398	14	1363	32	1398.0	14.0	0.5
PRU_56.FIN2	102.6	1.68	23.35	0.25	0.6659	0.0071	3239	10	3288	28	3202	16	3202.0	16.0	2.7
PRU_57.FIN2	253	0.83	0.601	0.015	0.0764	0.0011	477.3	9.7	474.5	6.7	468	56	474.5	6.7	0.6
PRU_58.FIN2	116.7	0.83	2.795	0.046	0.2345	0.0029	1352	12	1358	15	1351	32	1358.0	15.0	0.4
PRU_59.FIN2	124.6	1.26	4.464	0.093	0.3049	0.0047	1720	17	1714	23	1716	29	1716.0	29.0	0.1
PRU_60.FIN2	291	1.16	0.518	0.014	0.06526	0.0009	422.4	9.2	407.5	5.4	477	64	407.5	5.4	3.5
PRU_61.FIN2	293	1.37	1.558	0.029	0.1544	0.0021	952	11	925	12	1001	35	925.0	12.0	2.8
PRU_62.FIN2	484	0.86	0.608	0.014	0.0747	0.0011	481	8.6	464	6.4	548	46	464.0	6.4	3.5
PRU_63.FIN2	163	1.79	13.56	0.19	0.5197	0.0067	2717	13	2696	28	2733	17	2733.0	17.0	1.4
PRU_64.FIN2	74.5	1.12	4.005	0.073	0.2894	0.0036	1631	15	1638	18	1617	34	1617.0	34.0	1.3
PRU_66.FIN2	148.1	1.85	3.027	0.048	0.2368	0.0025	1413	12	1369	13	1480	29	1369.0	13.0	3.1
PRU_67.FIN2	154	3.19	2.23	0.039	0.2006	0.0023	1189	12	1178	12	1205	36	1178.0	12.0	0.9
PRU_68.FIN2	107	2.57	1.739	0.048	0.1714	0.0032	1019	19	1019	18	1017	57	1019.0	18.0	0.0
PRU_69.FIN2	340	1.64	2.876	0.033	0.2389	0.0026	1374.2	8.8	1380	13	1367	20	1380.0	13.0	0.4
PRU_70.FIN2	364	5.43	1.62	0.024	0.1668	0.0019	977.3	9.6	996	10	939	29	996.0	10.0	1.9
PRU_71.FIN2	82	1.42	3.15	0.1	0.2496	0.004	1441	25	1436	21	1444	57	1436.0	21.0	0.3
PRU_72.FIN2	59	4.28	8.48	0.13	0.4298	0.0056	2282	13	2303	25	2259	26	2259.0	26.0	1.9
PRU_73.FIN2	337	1.30	0.594	0.012	0.07611	0.00091	472.1	7.7	472.8	5.4	450	46	472.8	5.4	0.1
PRU_74.FIN2	78	0.50	0.578	0.022	0.0734	0.0012	460	14	457.4	7.2	448	81	457.4	7.2	0.6
PRU_75.FIN2	128.6	1.09	15.96	0.19	0.5747	0.0069	2873	12	2930	29	2837	20	2837.0	20.0	3.3
PRU_76.FIN2	131.4	2.53	2.1	0.042	0.1953	0.0028	1147	14	1149	15	1130	35	1149.0	15.0	0.2
PRU_77.FIN2	147	2.21	1.909	0.036	0.183	0.0023	1083	12	1083	13	1062	36	1083.0	13.0	0.0
PRU_78.FIN2	91.4	1.25	1.632	0.039	0.1644	0.0025	981	15	981	14	946	50	981.0	14.0	0.0
PRU_79.FIN2	274	1.60	1.805	0.027	0.1748	0.0019	1046	10	1038	10	1043	28	1038.0	10.0	0.8

PRU_80.FIN2	274	2.80	3.348	0.085	0.2445	0.0044	1489	20	1409	23	1591	40	1409.0	23.0	5.4	
PRU_81.FIN2	232.2	0.85	0.568	0.015	0.0725	0.0011	455.3	9.8	450.8	6.5	448	57	450.8	6.5	1.0	
PRU_82.FIN2	143	0.69	4.056	0.063	0.2875	0.0032	1643	13	1628	16	1646	31	1646.0	31.0	1.1	
PRU_83.FIN2	63.4	1.00	2.301	0.055	0.2112	0.0027	1212	17	1235	14	1146	49	1235.0	14.0	1.9	
PRU_84.FIN2	311	1.87	2.24	0.033	0.2037	0.0023	1194	11	1195	13	1175	29	1195.0	13.0	0.1	
PRU_85.FIN2	424	6.32	0.923	0.021	0.1078	0.0016	665	12	659.7	9	659	45	659.7	9.0	0.8	
PRU_86.FIN2	102	0.82	1.907	0.046	0.1862	0.0025	1081	16	1100	14	1024	45	1100.0	14.0	1.8	
PRU_87.FIN2	83.7	2.49	1.801	0.04	0.1756	0.0024	1042	15	1042	13	1028	48	1042.0	13.0	0.0	
PRU_88.FIN2	84.9	1.76	0.539	0.024	0.0679	0.0013	435	16	423.1	7.6	473	92	423.1	7.6	2.7	
PRU_89.FIN2	284	1.14	2.671	0.043	0.2245	0.0029	1320	12	1305	15	1334	27	1305.0	15.0	1.1	
PRU_90.FIN2	360	1.49	5.08	0.058	0.3307	0.0035	1831.1	9.6	1841	17	1815	19	1815.0	19.0	1.4	
PRU_91.FIN2	102	1.35	7.19	0.14	0.3989	0.0063	2131	17	2162	29	2089	29	2089.0	29.0	3.5	
PRU_92.FIN2	184.8	1.34	4.972	0.06	0.3248	0.0031	1813	10	1813	15	1807	21	1807.0	21.0	0.3	
PRU_93.FIN2	18.84	1.19	2.79	0.11	0.2269	0.0052	1334	31	1316	27	1353	80	1316.0	27.0	1.3	
PRU_94.FIN2	223	0.97	2.987	0.054	0.2455	0.0039	1401	14	1414	20	1390	28	1414.0	20.0	0.9	
PRU_95.FIN2	156.8	1.66	11.78	0.31	0.412	0.01	2581	24	2218	47	2891	26	2891.0	26.0	23.3	
PRU_96.FIN2	498	1.76	2.594	0.047	0.2202	0.0034	1299	14	1283	18	1333	31	1283.0	18.0	1.2	
PRU_97.FIN2	112.2	1.38	4.842	0.065	0.3207	0.0038	1791	11	1792	19	1793	26	1793.0	26.0	0.1	
PRU_98.FIN2	51.4	0.89	13.92	0.21	0.5302	0.0081	2742	14	2739	34	2743	25	2743.0	25.0	0.1	
PRU_99.FIN2	77.7	1.65	2.046	0.048	0.1909	0.0025	1126	16	1126	14	1125	48	1126.0	14.0	0.0	
PRU_100.FIN2	147	2.30	2.179	0.048	0.1979	0.0029	1172	15	1164	15	1190	44	1164.0	15.0	0.7	
PRU_101.FIN2	598	4.69	1.927	0.034	0.1836	0.003	1089	12	1086	16	1102	31	1086.0	16.0	0.3	Rim
PRU_101.FIN2	117.7	1.33	3.21	0.11	0.262	0.0053	1457	28	1500	27	1402	58	1500.0	27.0	3.0	Core
PRU_102.FIN2	104.3	2.62	4.111	0.065	0.2972	0.0039	1654	13	1676	19	1629	33	1629.0	33.0	2.9	
PRU_103.FIN2	184	1.28	4.048	0.066	0.2899	0.0037	1641	13	1640	19	1649	28	1649.0	28.0	0.5	
PRU_104.FIN2	34.6	0.98	1.676	0.065	0.1713	0.0031	992	25	1021	17	916	85	1021.0	17.0	2.9	

PRU_105.FIN2	184.6	1.83	2.934	0.041	0.2476	0.0026	1389	11	1425	14	1354	28	1425.0	14.0	2.6
PRU_106.FIN2	131.5	1.15	0.59	0.018	0.0769	0.00096	469	11	477.5	5.7	424	68	477.5	5.7	1.8
PRU_107.FIN2	186.5	1.34	2.186	0.038	0.2063	0.0027	1174	12	1209	14	1130	31	1209.0	14.0	3.0
PRU_108.FIN2	209	0.88	0.639	0.021	0.0782	0.0012	499	13	485	7.4	565	72	485.0	7.4	2.8
PRU_110.FIN2	309	1.05	0.617	0.014	0.07937	0.00094	486.6	8.8	492.3	5.6	466	49	492.3	5.6	1.2
PRU_111.FIN2	95.7	1.77	3.88	0.12	0.2845	0.0066	1607	24	1613	33	1615	55	1615.0	55.0	0.1
PRU_112.FIN2	286	0.86	1.946	0.028	0.1884	0.0022	1095.3	9.7	1112	12	1075	24	1112.0	12.0	1.5
PRU_113.FIN2	225.2	1.22	0.633	0.023	0.0831	0.0017	504	17	514.6	9.9	458	86	514.6	9.9	2.1
PRU_114.FIN2	132	1.10	5.535	0.084	0.3574	0.0045	1903	13	1969	21	1848	25	1848.0	25.0	6.5
PRU_115.FIN2	32.3	0.72	11.03	0.24	0.4852	0.0089	2520	21	2547	38	2522	34	2522.0	34.0	1.0
PRU_116.FIN2	336	0.95	0.797	0.036	0.0912	0.0022	593	20	562	13	704	78	562.0	13.0	5.2
PRU_117.FIN2	239	5.98	2.985	0.072	0.2299	0.0064	1398	19	1331	34	1522	30	1331.0	34.0	4.8
PRU_118.FIN2	211.5	0.69	4.336	0.059	0.3022	0.0034	1700	12	1701	17	1699	20	1699.0	20.0	0.1
PRU_119.FIN2	229	1.42	3.86	0.053	0.2872	0.0031	1603	11	1627	15	1571	27	1571.0	15.0	1.5
PRU_120.FIN2	212	1.01	3.265	0.053	0.2545	0.0033	1470	13	1461	17	1484	27	1461.0	17.0	0.6
PRU_121.FIN2	297	0.86	1.942	0.04	0.1867	0.003	1094	14	1103	16	1069	37	1103.0	16.0	0.8
PRU_122.FIN2	198	1.07	4.35	0.056	0.3038	0.0033	1701	11	1709	16	1684	23	1684.0	23.0	1.5
PRU_123.FIN2	24.18	0.86	4.02	0.12	0.2922	0.005	1630	24	1651	25	1595	56	1595.0	25.0	1.3
PRU_124.FIN2	173	1.44	3.81	0.059	0.2828	0.0031	1592	12	1605	16	1570	26	1570.0	16.0	0.8
PRU_125.FIN2	224.6	1.15	3.909	0.087	0.2753	0.0039	1613	18	1567	20	1667	38	1567.0	20.0	2.9
PRU_126.FIN2	153.5	1.16	0.611	0.025	0.0757	0.0015	482	16	470.1	9.3	511	88	470.1	9.3	2.5
PRU_127.FIN2	274	1.19	3.218	0.043	0.2528	0.0029	1460	10	1452	15	1468	26	1452.0	15.0	0.5
PRU_128.FIN2	264	1.95	1.724	0.031	0.164	0.002	1016	11	978	11	1098	33	978.0	11.0	3.7

PRU_129.FIN2	323.4	0.82	4.075	0.061	0.2924	0.004	1648	12	1653	20	1634	25	1634.0	25.0	1.2	
PRU_130.FIN2	70.3	1.44	1.84	0.048	0.1828	0.0024	1057	17	1082	13	977	50	1082.0	13.0	2.4	

Sample Name: PRL							207/235		206/238		207/206		Best age			
Grain #	[U] ppm	U/Th	207/235	2σ error	206/238	2σ error	Age (Ma)	2σ error	Age (Ma)	2σ error	Age (Ma)	2σ error	(Ma)	2σ error	% Disc*	Rim/ Core
PRL_1.FIN2	18.81	2.54	1.637	0.083	0.1661	0.0041	966	32	989	22	880	110	989.0	22.0	2.4	
PRL_2.FIN2	175.2	3.60	1.616	0.028	0.1602	0.0018	975	11	957	10	1007	34	957.0	10.0	1.8	
PRL_3.FIN2	142	1.17	3.359	0.053	0.2604	0.0028	1494	13	1491	14	1492	27	1491.0	14.0	0.2	
PRL_4.FIN2	97.7	1.32	2.807	0.059	0.2326	0.0029	1354	15	1348	15	1368	40	1348.0	15.0	0.4	
PRL_5.FIN2	239.1	0.95	0.739	0.022	0.0753	0.0011	560	13	467.9	6.8	942	59	DISC	DISC	16.4	
PRL_6.FIN2	179.4	1.60	2.884	0.041	0.2336	0.0024	1375	11	1353	12	1411	26	1353.0	12.0	1.6	
PRL_7.FIN2	376	1.43	2.881	0.052	0.2392	0.0028	1375	13	1382	14	1364	31	1382.0	14.0	0.5	
PRL_8.FIN2	29.8	1.38	1.84	0.11	0.1834	0.005	1051	38	1085	27	960	120	1085.0	27.0	3.2	
PRL_9.FIN2	157.5	2.50	0.883	0.02	0.101	0.0014	643	10	620.2	8.3	708	56	620.2	8.3	3.5	
PRL_10.FIN2	216	1.24	2.887	0.041	0.238	0.0024	1376	11	1376	13	1376	27	1376.0	13.0	0.0	
PRL_11.FIN2	168	1.12	3.957	0.059	0.2931	0.0027	1623	12	1656	14	1581	25	1581.0	14.0	2.0	
PRL_12.FIN2	65.2	1.08	1.899	0.066	0.1771	0.0033	1073	23	1051	18	1115	71	1051.0	18.0	2.1	
PRL_13.FIN2	422	1.34	0.535	0.02	0.0679	0.0015	434	13	423.2	8.8	482	70	423.2	8.8	2.5	
PRL_14.FIN2	473	3.19	5.09	0.15	0.3119	0.0087	1832	25	1749	43	1932	44	1932.0	44.0	9.5	
PRL_15.FIN2	141.3	7.70	14.04	0.39	0.546	0.011	2745	27	2805	45	2708	27	2708.0	27.0	3.6	
PRL_16.FIN2	45.5	1.60	10.64	0.38	0.467	0.017	2489	32	2468	74	2532	44	2532.0	44.0	2.5	Rim
PRL_16.FIN2	167	3.08	15.77	0.3	0.5693	0.0097	2858	19	2907	41	2835	17	2835.0	17.0	2.5	Core
PRL_17.FIN2	76.2	0.62	1.734	0.041	0.173	0.0022	1017	15	1028	12	989	47	1028.0	12.0	1.1	
PRL_18.FIN2	233.4	0.99	4.448	0.051	0.311	0.0032	1719.8	9.5	1745	16	1693	22	1693.0	22.0	3.1	
PRL_19.FIN2	181.2	1.77	2.849	0.038	0.2354	0.0027	1367	10	1362	14	1380	27	1362.0	14.0	0.4	
PRL_20.FIN2	533	2.85	1.878	0.056	0.1764	0.0041	1072	20	1047	23	1123	58	1047.0	23.0	2.3	Rim

PRL_20.FIN2	285	2.91	2.968	0.065	0.2348	0.0033	1397	17	1359	17	1456	35	1359.0	17.0	2.7	Core
PRL_21.FIN2	540	2.26	1.68	0.043	0.1662	0.0042	999	16	990	23	1030	43	990.0	23.0	0.9	
PRL_22.FIN2	177	1.96	0.652	0.025	0.0753	0.0015	507	16	467.8	9.1	682	90	467.8	9.1	7.7	
PRL_23.FIN2	94.5	0.63	4.103	0.068	0.2919	0.0034	1653	13	1650	17	1656	29	1656.0	29.0	0.4	
PRL_24.FIN2	537	5.82	3.636	0.031	0.2752	0.0026	1556.6	6.8	1567	13	1548	18	1567.0	13.0	0.7	
PRL_25.FIN2	110.1	0.89	3.119	0.072	0.2427	0.003	1434	18	1400	16	1489	40	1400.0	16.0	2.4	
PRL_26.FIN2	138	1.08	4.314	0.074	0.3005	0.004	1693	14	1693	20	1694	29	1694.0	29.0	0.1	
PRL_27.FIN2	338	4.36	0.514	0.014	0.0681	0.0011	422	9.5	424.8	6.5	395	57	424.8	6.5	0.7	
PRL_28.FIN2	275	4.11	2.811	0.048	0.2337	0.0035	1357	13	1353	19	1363	28	1353.0	19.0	0.3	
PRL_29.FIN2	182	22.20	1.662	0.096	0.1658	0.0065	991	36	989	36	990	100	989.0	36.0	0.2	Rim
PRL_29.FIN2	91.7	2.01	3.167	0.069	0.2462	0.0033	1448	16	1418	17	1495	37	1418.0	17.0	2.1	Core
PRL_30.FIN2	916	4.28	6.03	0.19	0.2739	0.0085	1979	28	1560	43	2452	41	DISC	DISC	21.2	Rim
PRL_30.FIN2	58.1	0.42	13.14	0.24	0.5117	0.0085	2688	18	2661	36	2707	25	2707.0	25.0	1.7	Core
PRL_31.FIN2	321	4.63	3.398	0.042	0.2648	0.0026	1502.1	9.7	1514	13	1489	21	1514.0	13.0	0.8	
PRL_32.FIN2	553	9.55	1.944	0.039	0.1873	0.003	1095	14	1106	17	1074	37	1106.0	17.0	1.0	
PRL_33.FIN2	404	3.84	1.841	0.024	0.1802	0.0017	1061.1	9.1	1067.8	9.3	1045	27	1067.8	9.3	0.6	
PRL_34.FIN2	55.7	2.72	4.663	0.087	0.3193	0.004	1756	15	1785	20	1722	32	1722.0	32.0	3.7	
PRL_35.FIN2	217	1.44	3.501	0.048	0.269	0.0031	1525	11	1535	16	1518	25	1535.0	16.0	0.7	
PRL_36.FIN2	198	1.14	2.773	0.068	0.2281	0.004	1346	18	1324	21	1382	42	1324.0	21.0	1.6	
PRL_37.FIN2	204	0.67	2.62	0.049	0.2191	0.0038	1304	14	1276	20	1353	31	1276.0	20.0	2.1	
PRL_38.FIN2	114	0.66	0.588	0.022	0.0747	0.0012	467	15	464.5	7.1	466	85	464.5	7.1	0.5	
PRL_39.FIN2	653	1.26	2.762	0.059	0.221	0.0045	1344	16	1287	24	1439	34	1287.0	24.0	4.2	
PRL_40.FIN2	213.8	1.52	4.658	0.058	0.3107	0.0037	1759	10	1743	18	1780	22	1780.0	22.0	2.1	
PRL_41.FIN2	113	-2.70	1.874	0.046	0.1811	0.0025	1069	16	1073	13	1077	47	1073.0	13.0	0.4	
PRL_42.FIN2	427	2.11	0.932	0.029	0.1059	0.0027	667	15	648	16	732	59	648.0	16.0	2.8	
PRL_43.FIN2	123.6	0.65	0.852	0.022	0.1031	0.0015	623	12	632.5	8.5	581	55	632.5	8.5	1.5	
PRL_44.FIN2	177	0.57	2.92	0.05	0.2308	0.0029	1384	13	1338	15	1460	30	1338.0	15.0	3.3	
PRL_45.FIN2	446	38.40	1.941	0.024	0.1845	0.0021	1093.9	8.2	1091	11	1101	23	1091.0	11.0	0.3	

PRL_46.FIN2	46.6	0.71	13.8	0.18	0.5325	0.0066	2736	13	2750	28	2723	24	2723.0	24.0	1.0	
PRL_47.FIN2	154	2.14	1.877	0.06	0.1806	0.0037	1070	21	1070	20	1075	58	1070.0	20.0	0.0	
PRL_48.FIN2	129	0.68	0.517	0.018	0.0687	0.0011	421	12	428.4	6.8	375	76	428.4	6.8	1.8	
PRL_49.FIN2	35.4	0.76	2.733	0.091	0.2281	0.0046	1326	25	1323	24	1335	63	1323.0	24.0	0.2	
PRL_50.FIN2	116.6	0.51	5.466	0.072	0.3501	0.0046	1894	12	1934	22	1859	24	1859.0	24.0	4.0	
PRL_51.FIN2	419	4.87	3.551	0.045	0.267	0.0026	1537	10	1525	13	1562	19	1525.0	13.0	0.8	
PRL_52.FIN2	260	3.88	1.7	0.025	0.1697	0.0016	1006.8	9.4	1011.4	9.3	999	33	1011.4	9.3	0.5	
PRL_53.FIN2	42.6	1.61	2.181	0.06	0.1987	0.0033	1173	19	1167	18	1170	55	1167.0	18.0	0.5	
PRL_54.FIN2	87.1	1.45	16.15	0.2	0.5706	0.0063	2883	12	2908	26	2866	17	2866.0	17.0	1.5	
PRL_55.FIN2	235	2.09	0.638	0.016	0.0767	0.0011	499.1	9.6	476.1	6.4	594	54	476.1	6.4	4.6	
PRL_56.FIN2	269.2	0.82	0.511	0.023	0.0649	0.0017	418	15	405	10	460	110	405.0	10.0	3.1	
PRL_57.FIN2	489	1.39	3.482	0.045	0.2676	0.0029	1522.5	9.8	1528	15	1517	20	1528.0	15.0	0.4	
PRL_58.FIN2	275	0.94	1.871	0.046	0.1729	0.0041	1069	16	1028	23	1173	54	1028.0	23.0	3.8	
PRL_59.FIN2	120	2.15	5.01	0.1	0.3256	0.0056	1819	17	1816	27	1825	41	1825.0	41.0	0.5	
PRL_60.FIN2	286	7.55	1.805	0.031	0.176	0.002	1046	11	1045	11	1042	32	1045.0	11.0	0.1	
PRL_61.FIN2	209	1.63	3.253	0.052	0.2564	0.0032	1467	12	1471	17	1465	29	1471.0	17.0	0.3	
PRL_62.FIN2	138.3	2.12	2.745	0.051	0.2264	0.0026	1341	14	1315	14	1376	37	1315.0	14.0	1.9	
PRL_63.FIN2	378	1.17	1.814	0.029	0.1741	0.0019	1049	11	1034	10	1077	28	1034.0	10.0	1.4	
PRL_64.FIN2	383	2.74	1.791	0.027	0.1769	0.002	1042	10	1050	11	1023	30	1050.0	11.0	0.8	
PRL_65.FIN2	154.6	0.89	4.742	0.08	0.3054	0.0038	1774	14	1717	19	1838	32	1838.0	32.0	6.6	
PRL_66.FIN2	247	1.61	0.552	0.014	0.07192	0.00094	444.9	9.2	447.6	5.7	413	55	447.6	5.7	0.6	
PRL_67.FIN2	286	0.80	0.56	0.014	0.0714	0.001	449.8	9.3	444.2	6.3	454	57	444.2	6.3	1.2	
PRL_68.FIN2	290	1.91	7.19	0.15	0.2874	0.0058	2130	19	1626	29	2659	20	DISC	DISC	38.8	
PRL_69.FIN2	246	0.64	3.1	0.055	0.249	0.0036	1431	14	1433	18	1419	29	1433.0	18.0	0.1	
PRL_70.FIN2	82.7	1.09	1.851	0.042	0.1792	0.0024	1061	15	1062	13	1036	46	1062.0	13.0	0.1	
PRL_71.FIN2	160	2.28	4.167	0.064	0.2981	0.0034	1665	13	1681	17	1640	26	1640.0	26.0	2.5	
PRL_72.FIN2	114.5	1.02	13.47	0.16	0.5279	0.0064	2711	11	2730	27	2690	16	2690.0	16.0	1.5	
PRL_73.FIN2	323	3.16	0.721	0.037	0.0721	0.0025	550	22	448	15	980	130	DISC	DISC	18.5	Rim

PRL_73.FIN2	23.1	0.80	1.921	0.095	0.1831	0.0048	1075	33	1083	26	1030	110	1083.0	26.0	0.7	Core
PRL_74.FIN2	424	18.30	1.907	0.029	0.1818	0.002	1081	10	1076	11	1086	27	1076.0	11.0	0.5	
PRL_75.FIN2	134	1.50	2.909	0.05	0.2384	0.003	1381	13	1377	16	1386	29	1377.0	16.0	0.3	
PRL_76.FIN2	133.1	0.94	1.708	0.031	0.171	0.0021	1009	12	1017	12	975	37	1017.0	12.0	0.8	
PRL_77.FIN2	137	1.00	1.82	0.14	0.182	0.014	1071	66	1077	74	1050	150	1077.0	74.0	0.6	Rim
PRL_77.FIN2	92.2	0.58	4.115	0.085	0.2976	0.0045	1653	17	1678	22	1612	33	1612.0	33.0	4.1	Core
PRL_78.FIN2	90.9	1.03	0.501	0.021	0.0682	0.0013	411	15	424.8	8	321	88	424.8	8.0	3.4	
PRL_79.FIN2	67.9	1.09	2.1	0.053	0.1931	0.0029	1145	18	1137	16	1151	52	1137.0	16.0	0.7	
PRL_80.FIN2	296	1.22	4.619	0.066	0.3155	0.0037	1751	12	1767	18	1736	23	1736.0	23.0	1.8	
PRL_81.FIN2	81.8	1.16	3.178	0.059	0.2595	0.0035	1450	14	1486	18	1403	36	1486.0	18.0	2.5	
PRL_82.FIN2	185.6	1.51	2.187	0.036	0.2018	0.0025	1176	11	1185	14	1161	29	1185.0	14.0	0.8	
PRL_83.FIN2	216.3	2.59	1.951	0.039	0.1869	0.0024	1096	13	1104	13	1076	39	1104.0	13.0	0.7	
PRL_84.FIN2	648	1.38	1.74	0.027	0.1679	0.0022	1021.7	9.8	1000	12	1078	24	1000.0	12.0	2.1	
PRL_85.FIN2	198.1	2.32	0.519	0.014	0.0669	0.00084	423.2	9.3	417.4	5.1	454	59	417.4	5.1	1.4	
PRL_86.FIN2	114.6	0.69	10.92	0.22	0.4183	0.0091	2513	19	2251	41	2742	23	2742.0	23.0	17.9	
PRL_87.FIN2	294	0.55	0.483	0.011	0.06313	0.00077	399	7.6	394.6	4.6	428	51	394.6	4.6	1.1	
PRL_88.FIN2	151	2.41	3.363	0.053	0.2684	0.0034	1494	13	1532	17	1458	28	1532.0	17.0	2.5	
PRL_89.FIN2	79.7	0.98	14.53	0.18	0.5384	0.0071	2782	12	2774	30	2800	18	2800.0	18.0	0.9	
PRL_90.FIN2	208	2.44	4.72	0.11	0.31	0.0073	1764	19	1737	36	1820	19	1820.0	19.0	4.6	
PRL_91.FIN2	349.4	0.64	0.649	0.017	0.0826	0.0017	507	11	511.7	9.9	508	60	511.7	9.9	0.9	
PRL_92.FIN2	165	1.20	0.743	0.021	0.0919	0.0013	563	12	566.7	7.6	548	66	566.7	7.6	0.7	
PRL_93.FIN2	234.1	1.24	4.919	0.058	0.3204	0.0032	1804	10	1791	16	1826	22	1826.0	22.0	1.9	
PRL_94.FIN2	213	2.21	1.807	0.029	0.1778	0.0022	1046	10	1055	12	1030	30	1055.0	12.0	0.9	
PRL_95.FIN2	178.8	0.90	2.61	0.042	0.2199	0.0025	1301	12	1281	13	1345	30	1281.0	13.0	1.5	
PRL_96.FIN2	47.8	0.92	1.949	0.066	0.1889	0.0032	1091	23	1115	17	1043	65	1115.0	17.0	2.2	
PRL_97.FIN2	272	1.14	3.039	0.05	0.2417	0.0028	1415	12	1395	14	1447	26	1395.0	14.0	1.4	
PRL_98.FIN2	618	0.94	0.575	0.01	0.07375	0.00091	460.1	6.8	458.6	5.5	451	37	458.6	5.5	0.3	
PRL_99.FIN2	166.2	1.19	4.15	0.13	0.2927	0.0069	1661	26	1654	34	1650	50	1650.0	50.0	0.2	

PRL_100.FIN2	115.7	1.28	2.584	0.064	0.2227	0.0041	1293	18	1296	22	1286	40	1296.0	22.0	0.2	
PRL_101.FIN2	254.6	3.11	4.83	0.11	0.2944	0.0049	1786	20	1663	25	1916	39	1916.0	39.0	13.2	
PRL_102.FIN2	130.3	0.75	1.795	0.086	0.1751	0.006	1039	31	1039	33	1023	81	1039.0	33.0	0.0	
PRL_103.FIN2	184.8	1.85	1.882	0.037	0.1774	0.0025	1074	13	1052	13	1099	38	1052.0	13.0	2.0	
PRL_104.FIN2	156.8	1.13	0.905	0.025	0.1066	0.0018	653	13	653	11	613	56	653.0	11.0	0.0	
PRL_105.FIN2	147	0.96	0.559	0.018	0.0732	0.001	451	11	455	6.3	387	72	455.0	6.3	0.9	
PRL_106.FIN2	211.8	1.06	1.921	0.031	0.1835	0.002	1086	11	1086	11	1062	34	1086.0	11.0	0.0	
PRL_107.FIN2	189.3	0.83	1.785	0.035	0.1735	0.002	1038	13	1031	11	1024	35	1031.0	11.0	0.7	
PRL_108.FIN2	199	1.63	4.277	0.064	0.293	0.0039	1686	13	1655	20	1706	24	1706.0	24.0	3.0	
PRL_109.FIN2	31.6	1.08	0.491	0.031	0.0566	0.0015	397	21	354.5	9.4	570	130	354.5	9.4	10.7	
PRL_110.FIN2	195	0.57	4.146	0.056	0.2918	0.0029	1661	11	1650	15	1655	21	1655.0	21.0	0.3	
PRL_111.FIN2	347	3.31	3.103	0.051	0.2524	0.0041	1433	13	1450	21	1390	27	1450.0	21.0	1.2	
PRL_112.FIN2	205.2	0.82	3.905	0.069	0.2827	0.004	1613	14	1604	20	1600	24	1600.0	24.0	0.6	
PRL_114.FIN2	443	2.21	2.156	0.024	0.1998	0.0018	1165.9	7.7	1173.8	9.9	1139	21	1173.8	9.9	0.7	
PRL_115.FIN2	256.1	0.44	2.762	0.064	0.2117	0.0045	1344	17	1237	24	1504	44	1237.0	24.0	8.0	
PRL_116.FIN2	583	4.40	5.09	0.1	0.329	0.0061	1834	17	1833	30	1822	25	1822.0	25.0	0.6	Rim
PRL_116.FIN2	253.3	1.54	8.22	0.13	0.406	0.0052	2254	14	2196	24	2299	17	2299.0	17.0	4.5	Core
PRL_117.FIN2	220	1.00	3.423	0.093	0.2565	0.0047	1507	21	1471	24	1545	41	1471.0	24.0	2.4	
PRL_118.FIN2	135.1	0.76	13.46	0.15	0.5285	0.0058	2713	11	2733	24	2692	16	2692.0	16.0	1.5	
PRL_119.FIN2	172	2.02	5.148	0.075	0.3366	0.0047	1844	12	1872	22	1803	22	1803.0	22.0	3.8	
PRL_120.FIN2	335	1.90	3.467	0.039	0.2657	0.0027	1518.3	8.9	1518	14	1506	20	1518.0	14.0	0.0	
PRL_121.FIN2	88.6	1.68	4.33	0.11	0.2928	0.0052	1690	20	1653	26	1734	33	1734.0	33.0	4.7	
PRL_122.FIN2	434	1.25	0.599	0.012	0.0769	0.001	476.6	7.8	478.1	6	463	43	478.1	6.0	0.3	

PRL_123.FIN2	207.7	1.50	0.706	0.018	0.086	0.001	540	10	531.9	6	557	50	531.9	6.0	1.5	
PRL_124.FIN2	414	10.60	0.607	0.031	0.0748	0.0019	480	20	465	12	530	110	465.0	12.0	3.1	Rim
PRL_124.FIN2	18.6	0.71	1.85	0.1	0.1725	0.005	1052	37	1024	27	1070	110	1024.0	27.0	2.7	Core
PRL_125.FIN2	147.5	1.88	1.945	0.042	0.1774	0.0021	1093	14	1053	11	1170	41	1053.0	11.0	3.7	
PRL_126.FIN2	301	1.73	3.918	0.071	0.2806	0.0044	1614	15	1593	22	1640	25	1593.0	22.0	1.3	
PRL_127.FIN2	172.7	1.48	2.219	0.034	0.2036	0.0023	1185	11	1196	12	1165	30	1196.0	12.0	0.9	
PRL_128.FIN2	448	2.39	0.468	0.012	0.06257	0.00092	388.9	8.1	391.1	5.6	368	51	391.1	5.6	0.6	
PRL_129.FIN2	393.8	1.19	0.73	0.013	0.0868	0.0011	555.8	7.4	536.3	6.4	646	36	536.3	6.4	3.5	
PRL_130.FIN2	353.4	1.34	0.552	0.011	0.07168	0.00089	446.1	6.9	446.2	5.3	431	42	446.2	5.3	0.0	

Sample Name: LAN							207/235		206/238		207/206		Best age			
Grain #	[U] ppm	U/Th	207/235	2σ error	206/238	2σ error	Age (Ma)	2σ error	Age (Ma)	2σ error	Age (Ma)	2σ error	(Ma)	2σ error	% Disc*	Rim/ Core
LAN_1.FIN2	136	4.09	4.38	0.043	0.3079	0.0028	1707.3	8.1	1730	14	1676	19	1676.0	19.0	3.2	
LAN_3.FIN2	98.8	1.15	4.316	0.059	0.2927	0.0035	1694	11	1654	17	1726	23	1726.0	23.0	4.2	
LAN_4.FIN2	212	1.20	0.481	0.015	0.0619	0.0011	398	10	387.3	6.6	430	63	387.3	6.6	2.7	
LAN_5.FIN2	253.6	2.36	4.864	0.052	0.331	0.0032	1795.9	9.3	1843	15	1718	17	1718.0	17.0	7.3	
LAN_6.FIN2	552	0.94	2.022	0.026	0.1886	0.0022	1122	8.8	1115	12	1109	24	1115.0	12.0	0.6	
LAN_7.FIN2	62.2	1.10	13.11	0.15	0.5257	0.0054	2686	11	2722	23	2642	17	2642.0	17.0	3.0	
LAN_8.FIN2	133.8	1.42	0.615	0.015	0.0764	0.0011	485.6	9.6	474.7	6.4	516	58	474.7	6.4	2.2	
LAN_10.FIN2	211	1.13	3.104	0.037	0.2549	0.0022	1433.5	9.3	1464	11	1382	21	1464.0	11.0	2.1	
LAN_11.FIN2	228	2.85	13.28	0.11	0.5412	0.0042	2698.8	7.8	2788	18	2639	11	2639.0	11.0	5.6	
LAN_12.FIN2	197.1	1.44	3.234	0.033	0.2599	0.0024	1465.1	7.7	1489	12	1438	20	1489.0	12.0	1.6	
LAN_13.FIN2	199.4	1.94	3.298	0.048	0.2456	0.0023	1478	11	1415	12	1581	25	1415.0	12.0	4.3	
LAN_14.FIN2	603	0.54	0.797	0.028	0.0655	0.002	595	16	409	12	1401	62	DISC	DISC	31.3	

LAN_15.FIN2	116.9	1.60	1.819	0.029	0.1773	0.0021	1050	11	1052	11	1057	34	1052.0	11.0	0.2
LAN_16.FIN2	205.3	1.38	13.28	0.18	0.5168	0.0081	2698	13	2682	34	2722	23	2722.0	23.0	1.5
LAN_17.FIN2	103	0.74	0.667	0.032	0.0693	0.0016	517	19	431.8	9.6	890	110	DISC	DISC	16.5
LAN_18.FIN2	175.8	1.31	4.94	0.053	0.3314	0.0036	1807.7	8.9	1844	17	1773	20	1773.0	20.0	4.0
LAN_19.FIN2	238.4	2.02	2.908	0.037	0.2433	0.0023	1382.4	9.5	1403	12	1356	23	1403.0	12.0	1.5
LAN_20.FIN2	122.5	0.77	15.3	0.14	0.5538	0.0054	2832.6	9	2840	23	2832	14	2832.0	14.0	0.3
LAN_21.FIN2	171.9	2.82	5.149	0.063	0.3397	0.0044	1843	10	1884	21	1798	20	1798.0	20.0	4.8
LAN_22.FIN2	57.7	0.87	0.598	0.021	0.075	0.0013	474	14	466.2	7.7	486	80	466.2	7.7	1.6
LAN_23.FIN2	485	1.10	0.594	0.013	0.0768	0.0015	472.7	8.3	476.7	8.9	446	44	476.7	8.9	0.8
LAN_24.FIN2	116.3	1.69	2.236	0.039	0.2052	0.0025	1190	12	1203	13	1152	36	1203.0	13.0	1.1
LAN_26.FIN2	174	0.96	0.617	0.012	0.07825	0.00071	486.9	7.8	485.6	4.2	467	50	485.6	4.2	0.3
LAN_27.FIN2	108.1	2.14	1.82	0.032	0.1777	0.0018	1051	11	1054	9.9	1032	37	1054.0	9.9	0.3
LAN_28.FIN2	212	2.71	4.694	0.051	0.3166	0.0028	1764.7	9	1772	14	1752	15	1752.0	15.0	1.1
LAN_29.FIN2	449	11.86	0.5557	0.0076	0.07241	0.0006	448.3	4.9	450.6	3.6	430	32	450.6	3.6	0.5
LAN_30.FIN2	288	1.81	0.5163	0.0096	0.06747	0.00071	421.9	6.4	420.8	4.3	417	42	420.8	4.3	0.3
LAN_31.FIN2	374	1.15	4.551	0.064	0.2941	0.004	1739	12	1662	20	1838	28	1838.0	28.0	9.6
LAN_33.FIN2	150	0.71	0.561	0.024	0.0656	0.0014	451	16	409.6	8.2	642	88	409.6	8.2	9.2
LAN_34.FIN2	140	1.63	3.495	0.042	0.2712	0.0025	1524.4	9.6	1546	13	1494	23	1546.0	13.0	1.4
LAN_35.FIN2	59	0.97	2.994	0.064	0.2484	0.0032	1402	17	1430	17	1360	42	1430.0	17.0	2.0
LAN_37.FIN2	212.2	1.53	0.542	0.012	0.07121	0.00083	438.8	7.8	443.4	5	409	49	443.4	5.0	1.0
LAN_38.FIN2	662	1.43	0.894	0.018	0.1004	0.0018	648.1	9.7	617	11	766	51	617.0	11.0	4.8
LAN_39.FIN2	830.7	1.54	0.5379	0.0067	0.07066	0.00066	436.6	4.5	440.1	4	417	24	440.1	4.0	0.8
LAN_40.FIN2	26.6	1.08	1.892	0.061	0.1818	0.0028	1072	22	1076	15	1054	66	1076.0	15.0	0.4
LAN_41.FIN2	181.8	1.25	3.706	0.061	0.2729	0.0036	1571	13	1555	18	1594	30	1555.0	18.0	1.0
LAN_42.FIN2	157.7	2.80	2.334	0.042	0.2023	0.0023	1221	13	1188	12	1270	27	1188.0	12.0	2.7
LAN_43.FIN2	57	0.48	5.324	0.076	0.345	0.0041	1870	12	1910	20	1823	24	1823.0	24.0	4.8
LAN_44.FIN2	344	2.49	4.64	0.1	0.3109	0.0071	1753	19	1742	35	1763	18	1763.0	18.0	1.2
LAN_45.FIN2	65.5	1.60	1.74	0.039	0.1669	0.0024	1022	14	995	13	1047	44	995.0	13.0	2.6

LAN_46.FIN2	231.4	1.59	4.37	0.04	0.3021	0.0026	1705.7	7.6	1701	13	1695	18	1695.0	18.0	0.4	
LAN_47.FIN2	191.8	2.88	16.57	0.16	0.5884	0.0055	2908.9	8.9	2982	22	2849	12	2849.0	12.0	4.7	
LAN_48.FIN2	469.4	1.08	0.6104	0.0078	0.07833	0.00075	483.4	4.9	486.1	4.5	463	30	486.1	4.5	0.6	
LAN_49.FIN2	387	3.53	4.586	0.053	0.3056	0.0035	1745.2	9.6	1718	17	1772	15	1772.0	15.0	3.0	
LAN_50.FIN2	373	2.89	4.092	0.05	0.2774	0.0032	1652	10	1578	16	1747	19	1578.0	16.0	4.5	
LAN_51.FIN2	100	1.12	3.134	0.053	0.2552	0.0027	1438	13	1465	14	1405	33	1465.0	14.0	1.9	
LAN_52.FIN2	170	2.03	1.802	0.035	0.1774	0.0021	1044	13	1052	11	1039	40	1052.0	11.0	0.8	
LAN_53.FIN2	215.6	1.64	1.726	0.022	0.1723	0.0016	1018	8.3	1024.6	8.6	1011	25	1024.6	8.6	0.6	
LAN_54.FIN2	193	4.87	4.753	0.079	0.3032	0.005	1774	14	1706	25	1859	24	1859.0	24.0	8.2	
LAN_55.FIN2	174	0.80	3.275	0.049	0.2651	0.003	1474	12	1516	15	1424	28	1516.0	15.0	2.8	
LAN_56.FIN2	128.6	14.00	0.647	0.022	0.0786	0.0015	508	15	487.6	8.9	585	81	487.6	8.9	4.0	Rim
LAN_56.FIN2	257.6	2.35	1.598	0.044	0.1639	0.0034	967	17	978	19	939	41	978.0	19.0	1.1	Core
LAN_57.FIN2	207	-6.00	2.078	0.075	0.1882	0.0051	1140	24	1111	28	1186	95	1111.0	28.0	2.5	Rim
LAN_57.FIN2	149	2.02	2.923	0.041	0.2417	0.0025	1386	11	1395	13	1361	25	1395.0	13.0	0.6	Core
LAN_58.FIN2	85.7	1.71	0.643	0.018	0.0795	0.0011	502	11	493.1	6.6	513	61	493.1	6.6	1.8	
LAN_59.FIN2	120.5	1.12	2.852	0.04	0.2384	0.0031	1368	11	1378	16	1333	32	1378.0	16.0	0.7	
LAN_60.FIN2	207	3.29	5.239	0.049	0.3449	0.0036	1857.8	7.9	1910	17	1782	16	1782.0	16.0	7.2	
LAN_62.FIN2	126.7	0.50	0.536	0.014	0.0701	0.001	433.8	9.5	436.5	6.2	396	64	436.5	6.2	0.6	
LAN_63.FIN2	362	2.25	0.554	0.016	0.0694	0.0013	447	10	432.7	7.7	488	55	432.7	7.7	3.2	
LAN_64.FIN2	185	0.43	0.984	0.018	0.1131	0.0015	694.8	9.3	690.3	8.5	689	40	690.3	8.5	0.6	
LAN_65.FIN2	164	2.37	4.975	0.052	0.3337	0.0038	1813.9	8.8	1855	18	1757	19	1757.0	19.0	5.6	
LAN_66.FIN2	214	1.36	0.665	0.015	0.0839	0.0011	516.1	9.2	519.2	6.3	486	50	519.2	6.3	0.6	
LAN_67.FIN2	89.6	0.98	0.648	0.023	0.082	0.0014	505	14	508.1	8.5	467	80	508.1	8.5	0.6	
LAN_68.FIN2	167.7	2.82	5.702	0.095	0.3431	0.0049	1930	14	1901	23	1957	30	1957.0	30.0	2.9	
LAN_69.FIN2	140	1.11	4.185	0.06	0.301	0.004	1668	12	1695	20	1631	24	1631.0	24.0	3.9	
LAN_71.FIN2	301.9	1.62	4.852	0.047	0.3255	0.0032	1792.9	8.1	1816	16	1753	16	1753.0	16.0	3.6	
LAN_72.FIN2	548	3.77	2.612	0.065	0.2018	0.0052	1302	19	1184	28	1485	26	1184.0	28.0	9.1	
LAN_73.FIN2	146.3	2.49	2.375	0.034	0.2127	0.0024	1234.4	9.9	1243	13	1198	25	1243.0	13.0	0.7	

LAN_74.FIN2	183	2.10	1.84	0.03	0.1787	0.0019	1058	11	1059	10	1026	33	1059.0	10.0	0.1
LAN_75.FIN2	388	1.93	0.614	0.018	0.0755	0.0017	485	11	469	10	525	61	469.0	10.0	3.3
LAN_76.FIN2	120.8	1.60	2.968	0.043	0.2479	0.0028	1399	11	1427	14	1328	26	1427.0	14.0	2.0
LAN_77.FIN2	409	5.19	1.946	0.022	0.1873	0.0019	1096.2	7.5	1106	10	1052	21	1106.0	10.0	0.9
LAN_78.FIN2	117.2	2.26	1.828	0.028	0.1786	0.002	1054	10	1060	10	1019	33	1060.0	10.0	0.6
LAN_79.FIN2	658	9.44	1.866	0.043	0.1795	0.0038	1070	15	1064	21	1065	24	1064.0	21.0	0.6
LAN_80.FIN2	505	0.84	0.6305	0.0099	0.08022	0.00093	495.7	6.1	497.4	5.6	475	33	497.4	5.6	0.3
LAN_81.FIN2	542	3.93	0.7057	0.0099	0.08784	0.00095	541.7	5.9	542.7	5.6	536	29	542.7	5.6	0.2
LAN_82.FIN2	422.1	0.80	0.575	0.018	0.0734	0.0016	460	12	456.4	9.8	462	73	456.4	9.8	0.8
LAN_84.FIN2	231.7	0.98	2.952	0.037	0.2431	0.0024	1394	9.5	1403	13	1390	24	1403.0	13.0	0.6
LAN_85.FIN2	457	1.25	1.713	0.025	0.1722	0.0021	1012.1	9.2	1024	12	1000	22	1024.0	12.0	1.2
LAN_86.FIN2	294	4.38	3.92	0.061	0.2925	0.0037	1615	13	1653	19	1583	22	1583.0	19.0	2.4
LAN_87.FIN2	108	1.03	3.025	0.065	0.2496	0.004	1412	17	1436	21	1378	39	1436.0	21.0	1.7
LAN_88.FIN2	343	2.56	3.017	0.055	0.2449	0.0041	1409	14	1411	21	1421	20	1411.0	21.0	0.1
LAN_89.FIN2	203	2.63	2.147	0.043	0.2039	0.0032	1161	14	1195	17	1103	29	1195.0	17.0	2.9
LAN_91.FIN2	257	2.97	1.738	0.022	0.1752	0.0019	1021.6	8.3	1040	10	981	26	1040.0	10.0	1.8
LAN_92.FIN2	52.8	1.18	2.337	0.057	0.2189	0.0035	1220	18	1275	18	1112	49	1275.0	18.0	4.5
LAN_93.FIN2	118	1.82	13.96	0.15	0.5422	0.0064	2745	10	2790	27	2712	16	2712.0	16.0	2.9
LAN_94.FIN2	231	1.48	0.541	0.013	0.06906	0.00096	437.9	8.5	430.4	5.8	466	50	430.4	5.8	1.7
LAN_95.FIN2	146.6	0.68	0.688	0.025	0.0827	0.0018	529	15	512	11	591	81	512.0	11.0	3.2
LAN_96.FIN2	43.9	0.81	1.776	0.047	0.1793	0.0025	1038	17	1063	14	973	51	1063.0	14.0	2.4
LAN_97.FIN2	121	1.45	2.841	0.041	0.2386	0.0026	1367	12	1379	14	1345	29	1379.0	14.0	0.9
LAN_98.FIN2	151	1.55	4.494	0.048	0.3138	0.003	1728.4	8.8	1759	15	1685	20	1685.0	20.0	4.4
LAN_99.FIN2	39.5	1.32	5.27	0.12	0.3324	0.0043	1858	18	1849	21	1878	38	1878.0	38.0	1.5
LAN_101.FIN2	192	0.67	4.149	0.042	0.2961	0.0025	1664.2	8.7	1672	13	1653	20	1653.0	20.0	1.1
LAN_102.FIN2	324	1.17	13.29	0.2	0.5198	0.0075	2698	14	2696	32	2698	14	2698.0	14.0	0.1
LAN_103.FIN2	62.1	1.79	12.83	0.16	0.5281	0.0055	2665	12	2732	23	2613	19	2613.0	19.0	4.6

LAN_104.FIN2	107	0.69	0.931	0.022	0.109	0.0013	666	12	667	7.6	653	51	667.0	7.6	0.2
LAN_105.FIN2	249	1.65	1.79	0.03	0.1729	0.0023	1041	11	1028	13	1066	26	1028.0	13.0	1.2
LAN_106.FIN2	286	2.42	3.49	0.058	0.2167	0.0032	1524	13	1264	17	1905	25	DISC	DISC	17.1
LAN_107.FIN2	120	3.18	0.595	0.017	0.0764	0.0014	475	11	474.4	8.2	464	68	474.4	8.2	0.1
LAN_108.FIN2	162.4	3.38	2.959	0.042	0.2465	0.0028	1395	11	1420	15	1355	25	1420.0	15.0	1.8
LAN_109.FIN2	25.32	1.02	2.033	0.084	0.19	0.0043	1117	28	1120	23	1103	84	1120.0	23.0	0.3
LAN_110.FIN2	102	2.06	4.313	0.06	0.3107	0.0033	1694	11	1744	16	1641	25	1641.0	25.0	6.3
LAN_111.FIN2	25.3	0.31	0.866	0.038	0.1	0.0022	626	21	614	13	658	98	614.0	13.0	1.9
LAN_112.FIN2	201.3	1.23	3.988	0.049	0.2927	0.0039	1630	9.9	1654	19	1601	24	1601.0	24.0	3.3
LAN_113.FIN2	151.7	1.06	1.87	0.024	0.1822	0.0022	1070.1	8.9	1079	12	1064	28	1079.0	12.0	0.8
LAN_114.FIN2	139.7	2.61	2.879	0.069	0.2468	0.0044	1372	18	1421	23	1303	31	1421.0	23.0	3.6
LAN_115.FIN2	236.5	1.07	1.888	0.027	0.1843	0.002	1075.5	9.3	1090	11	1047	28	1090.0	11.0	1.3
LAN_116.FIN2	60	0.54	1.835	0.048	0.1826	0.0028	1053	17	1080	15	986	55	1080.0	15.0	2.6
LAN_117.FIN2	443	6.89	0.506	0.0087	0.06696	0.0007	415.1	5.9	417.8	4.2	392	37	417.8	4.2	0.7
LAN_118.FIN2	226.2	1.70	1.943	0.034	0.1852	0.0028	1094	12	1095	15	1093	35	1095.0	15.0	0.1
LAN_119.FIN2	56.3	2.31	4.132	0.072	0.2959	0.0045	1660	14	1669	22	1644	32	1644.0	32.0	1.5
LAN_120.FIN2	137.3	2.57	1.788	0.026	0.1793	0.0023	1040.8	9.7	1063	12	987	36	1063.0	12.0	2.1
LAN_121.FIN2	110.4	1.68	2.971	0.046	0.2478	0.0026	1398	12	1427	13	1349	29	1427.0	13.0	2.1
LAN_123.FIN2	258	1.31	0.514	0.019	0.066	0.0013	420	12	411.7	8.1	456	76	411.7	8.1	2.0
LAN_124.FIN2	157.4	1.51	3.176	0.07	0.2537	0.0047	1449	17	1457	24	1433	38	1457.0	24.0	0.6
LAN_125.FIN2	219.6	1.09	4.088	0.057	0.2967	0.0035	1650	11	1674	17	1622	22	1622.0	22.0	3.2
LAN_126.FIN2	363	1.61	2.218	0.028	0.2053	0.0022	1185.4	8.8	1204	12	1162	20	1204.0	12.0	1.6
LAN_128.FIN2	327.4	2.15	2.939	0.034	0.2433	0.0022	1390.6	8.7	1403	11	1386	18	1403.0	11.0	0.9

LAN_129.FIN2	134.9	0.54	0.546	0.013	0.07043	0.00088	440.9	8.2	438.7	5.3	440	50	438.7	5.3	0.5
LAN_130.FIN2	140.3	1.82	3.091	0.039	0.2587	0.0025	1428.9	9.6	1483	13	1361	24	1483.0	13.0	3.8

Sample Name: LAE							207/235		206/238		207/206		Best age			
Grain #	[U] ppm	U/Th	207/235	2σ error	206/238	2σ error	Age (Ma)	2σ error	Age (Ma)	2σ error	Age (Ma)	2σ error	(Ma)	2σ error	% Disc*	Rim/ Core
LAE_1.FIN2	204	1.54	2.906	0.048	0.2432	0.0027	1381	12	1403	14	1358	30	1403.0	14.0	1.6	
LAE_2.FIN2	199.7	0.67	13.46	0.12	0.5255	0.0053	2711.1	8.8	2721	22	2712	13	2712.0	13.0	0.3	
LAE_3.FIN2	290.9	7.84	0.614	0.012	0.0779	0.00082	484.9	7.3	483.5	4.9	491	46	483.5	4.9	0.3	
LAE_4.FIN2	83.2	1.05	1.738	0.05	0.1635	0.0024	1017	19	976	13	1113	57	976.0	13.0	4.0	
LAE_5.FIN2	118.6	0.81	0.607	0.016	0.0755	0.0011	480	10	469	6.9	518	61	469.0	6.9	2.3	
LAE_6.FIN2	103.8	1.69	2.119	0.044	0.1971	0.0029	1152	15	1159	15	1144	45	1159.0	15.0	0.6	
LAE_7.FIN2	76.9	5.05	1.601	0.056	0.1564	0.0029	965	22	936	16	1029	72	936.0	16.0	3.0	
LAE_8.FIN2	221.3	1.61	3.17	0.055	0.2538	0.0037	1448	13	1458	19	1450	27	1458.0	19.0	0.7	
LAE_9.FIN2	35.4	1.71	1.687	0.078	0.1686	0.0041	994	30	1004	22	958	99	1004.0	22.0	1.0	
LAE_10.FIN2	178	2.33	1.646	0.028	0.167	0.0018	986	11	995.4	9.8	966	36	995.4	9.8	1.0	
LAE_12.FIN2	62.2	0.71	2.857	0.071	0.2376	0.0041	1370	18	1373	21	1364	50	1373.0	21.0	0.2	
LAE_13.FIN2	23.35	1.55	2.7	0.11	0.223	0.0045	1312	30	1296	24	1330	79	1296.0	24.0	1.2	
LAE_14.FIN2	220.5	0.65	1.913	0.033	0.18	0.0021	1083	11	1067	12	1119	29	1067.0	12.0	1.5	
LAE_15.FIN2	239.7	1.12	2.21	0.035	0.2015	0.0023	1183	11	1183	12	1197	34	1183.0	12.0	0.0	
LAE_16.FIN2	170	0.99	2.259	0.044	0.2059	0.0025	1196	14	1208	14	1178	37	1208.0	14.0	1.0	
LAE_17.FIN2	249.1	1.57	10.85	0.12	0.4831	0.0052	2508	10	2540	23	2493	14	2493.0	14.0	1.9	
LAE_18.FIN2	189.8	1.54	0.613	0.014	0.07556	0.00093	485.5	8.6	469.5	5.6	574	49	469.5	5.6	3.3	
LAE_19.FIN2	151	1.50	14.94	0.17	0.5355	0.0067	2811	11	2763	28	2856	15	2856.0	15.0	3.3	
LAE_20.FIN2	186.8	0.58	0.563	0.017	0.071	0.0011	452	11	441.8	6.6	496	71	441.8	6.6	2.3	

LAE_21.FIN2	88.3	0.71	3.97	0.068	0.2877	0.0033	1624	14	1629	16	1625	31	1625.0	31.0	0.2
LAE_23.FIN2	242	0.89	1.255	0.023	0.1348	0.0014	824	10	814.9	8.2	856	37	814.9	8.2	1.1
LAE_24.FIN2	477	0.86	0.615	0.016	0.07	0.001	486	10	436.3	6.1	737	48	436.3	6.1	10.2
LAE_25.FIN2	144.4	1.87	0.931	0.047	0.0999	0.0025	666	24	614	15	820	110	614.0	15.0	7.8
LAE_26.FIN2	153.4	1.70	2.048	0.043	0.1902	0.0029	1129	14	1122	15	1142	40	1122.0	15.0	0.6
LAE_27.FIN2	189.4	1.46	2.013	0.044	0.1896	0.0028	1117	15	1119	15	1112	43	1119.0	15.0	0.2
LAE_28.FIN2	151	3.30	2.048	0.04	0.1922	0.0023	1131	13	1133	13	1121	36	1133.0	13.0	0.2
LAE_29.FIN2	134.4	0.96	3.46	0.057	0.2677	0.0031	1515	13	1528	16	1501	27	1528.0	16.0	0.9
LAE_31.FIN2	141	1.47	3.254	0.061	0.2484	0.0042	1468	14	1429	22	1529	34	1429.0	22.0	2.7
LAE_32.FIN2	119.6	1.20	2.572	0.046	0.2215	0.0028	1291	13	1291	15	1297	33	1291.0	15.0	0.0
LAE_33.FIN2	143	1.03	3.84	0.059	0.2884	0.0035	1600	13	1632	18	1557	26	1557.0	18.0	2.0
LAE_34.FIN2	49.3	3.96	4.47	0.098	0.3085	0.0049	1723	18	1732	24	1708	41	1708.0	41.0	1.4
LAE_35.FIN2	125.9	2.18	1.87	0.04	0.1796	0.003	1068	14	1064	16	1084	40	1064.0	16.0	0.4
LAE_36.FIN2	188	0.95	0.565	0.013	0.07189	0.00094	453.6	8.6	447.4	5.7	479	54	447.4	5.7	1.4
LAE_37.FIN2	275	0.48	0.552	0.013	0.0707	0.00083	445.1	8.5	440.3	5	452	51	440.3	5.0	1.1
LAE_38.FIN2	36.5	0.97	3.45	0.1	0.2666	0.0054	1510	24	1522	27	1495	55	1522.0	27.0	0.8
LAE_39.FIN2	182.9	1.16	0.648	0.038	0.0749	0.0016	505	23	465.4	9.4	670	110	465.4	9.4	7.8
LAE_40.FIN2	72.8	1.47	2.424	0.048	0.2176	0.0027	1246	14	1268	14	1217	41	1268.0	14.0	1.8
LAE_41.FIN2	104.5	1.75	3.346	0.063	0.2595	0.0035	1488	15	1486	18	1494	34	1486.0	18.0	0.1
LAE_42.FIN2	709	1.42	5.23	0.11	0.3295	0.0075	1854	18	1834	36	1887	18	1887.0	18.0	2.8
LAE_43.FIN2	84.1	0.87	0.598	0.029	0.0749	0.0016	472	18	465.3	9.6	480	100	465.3	9.6	1.4
LAE_44.FIN2	130	0.52	1.643	0.031	0.1652	0.0021	987	12	985	12	991	42	985.0	12.0	0.2
LAE_45.FIN2	242.8	2.00	2.083	0.024	0.1938	0.002	1143.2	8	1141	11	1154	28	1141.0	11.0	0.2
LAE_46.FIN2	97.8	1.50	0.539	0.026	0.0691	0.0015	438	18	430.8	9.3	470	120	430.8	9.3	1.6
LAE_47.FIN2	334	2.33	0.649	0.024	0.0748	0.002	508	15	465	12	686	71	465.0	12.0	8.5
LAE_48.FIN2	185.7	5.10	2.505	0.05	0.2166	0.0031	1271	15	1264	17	1288	40	1264.0	17.0	0.6
LAE_49.FIN2	241	1.26	3.217	0.045	0.2572	0.0036	1461	11	1474	18	1443	24	1474.0	18.0	0.9
LAE_50.FIN2	175.2	0.94	2.506	0.035	0.2208	0.0023	1272	10	1286	12	1258	30	1286.0	12.0	1.1

LAE_51.FIN2	85.7	1.29	0.672	0.025	0.0841	0.0018	517	15	520	11	496	78	520.0	11.0	0.6
LAE_52.FIN2	175.8	0.83	1.368	0.029	0.1408	0.0017	873	12	849	9.5	929	43	849.0	9.5	2.7
LAE_53.FIN2	103.6	1.80	1.717	0.036	0.1729	0.0022	1012	13	1028	12	971	45	1028.0	12.0	1.6
LAE_54.FIN2	110.3	1.24	0.488	0.018	0.0651	0.001	401	13	406.2	6.1	364	83	406.2	6.1	1.3
LAE_55.FIN2	107.4	1.25	2.013	0.05	0.1823	0.0028	1116	17	1079	15	1182	50	1079.0	15.0	3.3
LAE_56.FIN2	250.3	2.13	0.643	0.036	0.0674	0.0018	502	22	420	11	880	120	DISC	DISC	16.3
LAE_57.FIN2	265	2.13	3.029	0.048	0.2467	0.0031	1414	12	1420	16	1406	23	1420.0	16.0	0.4
LAE_58.FIN2	119.9	1.07	0.582	0.022	0.075	0.0013	463	14	465.9	7.7	450	85	465.9	7.7	0.6
LAE_59.FIN2	184.6	0.78	0.542	0.015	0.0688	0.00088	438.4	9.8	428.9	5.3	481	62	428.9	5.3	2.2
LAE_60.FIN2	47.19	2.28	0.691	0.043	0.0707	0.0018	530	27	440	11	900	140	DISC	DISC	17.0
LAE_61.FIN2	135.7	1.29	2.236	0.039	0.1993	0.0024	1191	12	1171	13	1225	32	1171.0	13.0	1.7
LAE_63.FIN2	176.7	1.38	4.036	0.067	0.2873	0.0045	1638	14	1626	22	1662	27	1662.0	27.0	2.2
LAE_64.FIN2	465	0.82	0.601	0.014	0.0708	0.0012	476.8	8.9	441	7.1	649	61	441.0	7.1	7.5
LAE_65.FIN2	209.2	1.79	2.889	0.037	0.2389	0.0025	1378.8	9.9	1380	13	1371	23	1380.0	13.0	0.1
LAE_66.FIN2	544.6	1.59	0.61	0.012	0.0715	0.001	483.2	7.6	445.1	6.3	671	45	445.1	6.3	7.9
LAE_68.FIN2	55.8	0.82	1.644	0.044	0.1664	0.0024	984	17	992	13	957	58	992.0	13.0	0.8
LAE_69.FIN2	107	2.61	2.035	0.043	0.1899	0.003	1125	15	1120	16	1136	46	1120.0	16.0	0.4
LAE_70.FIN2	267	1.46	4.238	0.085	0.2944	0.0044	1682	17	1663	22	1709	32	1709.0	32.0	2.7
LAE_71.FIN2	123.8	0.40	0.515	0.024	0.0644	0.0015	419	16	402.4	9	494	96	402.4	9.0	4.0
LAE_72.FIN2	109	0.80	0.666	0.034	0.0802	0.002	515	21	497	12	580	110	497.0	12.0	3.5
LAE_73.FIN2	100.8	1.75	2.866	0.055	0.2383	0.0026	1369	14	1377	13	1356	35	1377.0	13.0	0.6
LAE_74.FIN2	81.6	0.61	0.91	0.035	0.1035	0.002	657	20	635	12	715	85	635.0	12.0	3.3
LAE_75.FIN2	123	1.10	0.549	0.015	0.0701	0.001	443	10	436.5	6.2	469	63	436.5	6.2	1.5
LAE_76.FIN2	390	0.98	4.024	0.05	0.2885	0.0029	1638	10	1634	15	1641	22	1641.0	22.0	0.4
LAE_78.FIN2	39.8	1.35	2.207	0.078	0.2014	0.0043	1176	25	1182	23	1155	73	1182.0	23.0	0.5
LAE_80.FIN2	150.9	1.31	0.629	0.018	0.0736	0.001	496	11	457.9	6.1	658	61	457.9	6.1	7.7
LAE_81.FIN2	149	1.52	13.74	0.15	0.534	0.0051	2732	10	2757	21	2705	18	2705.0	18.0	1.9
LAE_82.FIN2	87.5	2.25	2.062	0.041	0.194	0.0026	1133	14	1142	14	1103	39	1142.0	14.0	0.8

LAE_83.FIN2	502	0.91	0.579	0.022	0.0726	0.0015	463	14	451.8	9.2	509	82	451.8	9.2	2.4	
LAE_84.FIN2	94.5	1.36	2.424	0.074	0.2136	0.004	1247	22	1247	21	1237	64	1247.0	21.0	0.0	
LAE_85.FIN2	275.3	3.58	2.161	0.044	0.1961	0.0027	1170	13	1154	15	1184	45	1154.0	15.0	1.4	
LAE_86.FIN2	172	1.60	0.522	0.016	0.0661	0.0011	427	11	412.5	6.6	476	69	412.5	6.6	3.4	
LAE_87.FIN2	157.1	0.48	4.146	0.053	0.2942	0.0031	1661	10	1662	15	1658	25	1658.0	25.0	0.2	
LAE_88.FIN2	341.3	1.20	5.858	0.091	0.3517	0.0054	1953	14	1942	26	1962	22	1962.0	22.0	1.0	
LAE_89.FIN2	177.7	0.77	2.905	0.058	0.2373	0.0032	1381	15	1372	17	1385	37	1372.0	17.0	0.7	
LAE_90.FIN2	533	2.32	0.602	0.011	0.0755	0.00083	478.6	7.5	469.2	5	512	43	469.2	5.0	2.0	
LAE_91.FIN2	40	1.98	2.23	0.13	0.2011	0.0066	1186	41	1180	36	1180	120	1180.0	36.0	0.5	
LAE_92.FIN2	125.9	0.82	0.853	0.022	0.1015	0.0015	624	12	622.9	8.9	614	63	622.9	8.9	0.2	
LAE_93.FIN2	115.2	3.06	14.13	0.18	0.5388	0.0074	2755	12	2776	31	2735	20	2735.0	20.0	1.5	
LAE_94.FIN2	168.1	1.23	0.775	0.031	0.0821	0.0014	582	18	508.5	8.5	848	81	508.5	8.5	12.6	
LAE_95.FIN2	297	0.70	0.625	0.015	0.0781	0.001	491.5	9.1	484.6	6.1	498	55	484.6	6.1	1.4	
LAE_96.FIN2	129.5	1.02	0.524	0.019	0.0636	0.0011	427	13	397.4	6.5	542	78	397.4	6.5	6.9	
LAE_97.FIN2	75	0.81	3.121	0.067	0.2494	0.0037	1435	17	1434	19	1424	39	1434.0	19.0	0.1	
LAE_98.FIN2	540	6.47	0.521	0.011	0.0667	0.0011	425.1	7.7	416.3	6.8	455	49	416.3	6.8	2.1	
LAE_99.FIN2	51.5	2.20	1.789	0.053	0.1741	0.0027	1035	19	1034	15	1025	57	1034.0	15.0	0.1	
LAE_100.FIN2	191	1.28	2.918	0.046	0.2362	0.0028	1384	12	1366	14	1399	29	1366.0	14.0	1.3	
LAE_101.FIN2	136.5	1.56	0.524	0.019	0.0666	0.0011	427	12	416.2	6.8	443	83	416.2	6.8	2.5	
LAE_102.FIN2	196.8	1.23	4.638	0.063	0.3137	0.0044	1755	11	1758	22	1741	26	1741.0	26.0	1.0	
LAE_103.FIN2	143	1.71	1.678	0.052	0.1675	0.0031	998	19	998	17	977	64	998.0	17.0	0.0	
LAE_104.FIN2	509	3.91	1.805	0.024	0.1742	0.0018	1046.1	8.6	1035	10	1055	27	1035.0	10.0	1.1	
LAE_105.FIN2	169.6	2.29	1.84	0.038	0.177	0.0027	1058	14	1050	15	1058	41	1050.0	15.0	0.8	
LAE_106.FIN2	60.4	1.48	2.089	0.062	0.1932	0.0034	1147	22	1138	19	1143	61	1138.0	19.0	0.8	
LAE_107.FIN2	47.4	0.54	13.47	0.39	0.5	0.013	2708	28	2611	54	2773	40	2773.0	40.0	5.8	Rim
LAE_107.FIN2	270	1.02	37.33	0.8	0.777	0.015	3700	22	3704	54	3688	25	3688.0	25.0	0.4	Core
LAE_108.FIN2	274.9	1.30	0.572	0.018	0.0691	0.0013	459	12	430.5	8.1	578	78	430.5	8.1	6.2	
LAE_109.FIN2	133.3	2.40	4.367	0.061	0.3006	0.0036	1704	12	1693	18	1705	27	1705.0	27.0	0.7	

LAE_110.FIN2	49.3	1.79	2.742	0.075	0.2325	0.0037	1335	20	1347	19	1307	45	1347.0	19.0	0.9
LAE_111.FIN2	124.4	0.55	1.892	0.036	0.1834	0.0029	1075	13	1085	16	1044	38	1085.0	16.0	0.9
LAE_112.FIN2	47.5	1.57	0.831	0.035	0.0949	0.0019	608	19	584	11	648	89	584.0	11.0	3.9
LAE_113.FIN2	174	1.29	0.57	0.015	0.0736	0.00095	456.1	9.5	457.7	5.7	415	58	457.7	5.7	0.4
LAE_114.FIN2	114	1.94	3.184	0.074	0.2485	0.0035	1449	18	1430	18	1479	43	1430.0	18.0	1.3
LAE_115.FIN2	345	1.28	2.056	0.029	0.1928	0.0018	1132.5	9.5	1136.4	9.6	1118	25	1136.4	9.6	0.3
LAE_116.FIN2	117.4	0.82	1.724	0.034	0.1676	0.0022	1014	13	998	12	1043	39	998.0	12.0	1.6
LAE_117.FIN2	117.2	0.87	10.65	0.13	0.4703	0.0057	2494	12	2483	25	2495	21	2495.0	21.0	0.5
LAE_118.FIN2	170.9	1.00	1.862	0.035	0.1802	0.0021	1065	13	1068	12	1057	38	1068.0	12.0	0.3
LAE_119.FIN2	349	2.04	1.131	0.038	0.1189	0.0028	767	18	724	16	882	62	724.0	16.0	5.6
LAE_120.FIN2	346	7.83	0.611	0.018	0.0761	0.0015	486	10	473	9	520	70	473.0	9.0	2.7
LAE_121.FIN2	50	1.24	0.493	0.022	0.0639	0.0012	403	15	399	7	409	95	399.0	7.0	1.0
LAE_122.FIN2	184	1.32	2.239	0.034	0.2029	0.0023	1191	11	1190	12	1193	25	1190.0	12.0	0.1
LAE_123.FIN2	19.32	0.77	11.61	0.24	0.4881	0.0083	2572	21	2559	36	2575	37	2575.0	37.0	0.6
LAE_124.FIN2	181	1.39	2.905	0.046	0.2379	0.0033	1382	12	1375	17	1392	28	1375.0	17.0	0.5
LAE_125.FIN2	27	2.10	2.049	0.088	0.1992	0.006	1118	29	1172	33	1012	84	1172.0	33.0	4.8
LAE_126.FIN2	271.6	3.60	2.082	0.035	0.1929	0.0024	1141	11	1137	13	1155	30	1137.0	13.0	0.4
LAE_127.FIN2	238	0.94	0.648	0.017	0.074	0.0013	506	11	460.1	7.9	705	54	460.1	7.9	9.1
LAE_128.FIN2	175.4	1.94	1.901	0.029	0.1861	0.0017	1081	10	1100	9.4	1040	30	1100.0	9.4	1.8
LAE_129.FIN2	351	1.31	0.613	0.023	0.0647	0.002	485	14	404	12	880	82	DISC	DISC	16.7
LAE_130.FIN2	79.6	0.53	5.789	0.079	0.3468	0.0042	1942	12	1918	20	1966	26	1966.0	26.0	2.4

Sample Name: LAW							207/235		206/238		207/206		Best age			
Grain #	[U] ppm	U/Th	207/235	2σ error	206/238	2σ error	Age (Ma)	2σ error	Age (Ma)	2σ error	Age (Ma)	2σ error	(Ma)	2σ error	% Disc*	Rim/ Core
LAW_1.FIN2	231	0.67	0.459	0.014	0.06012	0.00089	382.1	9.7	376.3	5.4	388	71	376.3	5.4	1.5	
LAW_2.FIN2	109.3	0.92	2.845	0.059	0.2346	0.0037	1364	15	1358	19	1375	39	1358.0	19.0	0.4	
LAW_3.FIN2	281	0.68	0.554	0.012	0.07259	0.00079	446.3	7.7	451.7	4.7	414	48	451.7	4.7	1.2	
LAW_4.FIN2	445	1.92	2.47	0.038	0.2168	0.003	1263	11	1264	16	1263	24	1264.0	16.0	0.1	
LAW_5.FIN2	371	0.98	0.86	0.016	0.1016	0.0014	629	9	623.8	8.2	655	42	623.8	8.2	0.8	
LAW_6.FIN2	224.4	1.58	1.692	0.037	0.1664	0.0027	1008	14	991	15	1040	41	991.0	15.0	1.7	
LAW_7.FIN2	141.8	1.02	7.047	0.095	0.3881	0.0054	2115	12	2112	25	2122	19	2122.0	19.0	0.5	
LAW_8.FIN2	86	1.36	3.297	0.067	0.2558	0.004	1476	16	1467	20	1496	39	1467.0	20.0	0.6	
LAW_9.FIN2	131.8	1.16	0.54	0.019	0.0695	0.0011	436	12	433	6.4	433	73	433.0	6.4	0.7	
LAW_10.FIN2	142.2	1.18	3.45	0.05	0.2657	0.0032	1514	11	1518	16	1505	27	1518.0	16.0	0.3	
LAW_11.FIN2	278	1.85	1.547	0.029	0.1613	0.0021	950	12	964	12	918	39	964.0	12.0	1.5	
LAW_12.FIN2	193	2.86	6.22	0.12	0.3496	0.0059	2006	16	1935	27	2086	21	2086.0	21.0	7.2	
LAW_13.FIN2	45.3	0.87	15.11	0.42	0.536	0.013	2817	26	2764	54	2861	32	2861.0	32.0	3.4	
LAW_14.FIN2	130.3	1.96	1.899	0.04	0.1842	0.0019	1080	14	1090	10	1070	42	1090.0	10.0	0.9	
LAW_15.FIN2	50	1.66	0.553	0.027	0.0702	0.0013	443	18	437.3	8	438	99	437.3	8.0	1.3	
LAW_16.FIN2	180	1.25	3.308	0.045	0.2589	0.0028	1481	10	1484	14	1486	25	1484.0	14.0	0.2	
LAW_17.FIN2	128.7	1.61	2.038	0.038	0.1899	0.0025	1125	13	1120	13	1131	42	1120.0	13.0	0.4	
LAW_18.FIN2	147.6	3.95	4.819	0.069	0.3266	0.0036	1786	12	1821	18	1746	23	1746.0	23.0	4.3	
LAW_19.FIN2	226	0.95	4.692	0.064	0.3189	0.0034	1765	11	1784	16	1746	21	1746.0	21.0	2.2	
LAW_20.FIN2	173	0.54	5.091	0.084	0.3412	0.0051	1833	14	1891	24	1777	29	1777.0	29.0	6.4	
LAW_21.FIN2	101.2	0.86	2.826	0.059	0.2334	0.004	1358	16	1351	21	1371	38	1351.0	21.0	0.5	
LAW_22.FIN2	301	-3.00	1.829	0.029	0.1816	0.0024	1054	10	1075	13	1017	33	1075.0	13.0	2.0	
LAW_23.FIN2	79.6	0.67	1.244	0.046	0.1314	0.0029	817	21	796	17	866	79	796.0	17.0	2.6	
LAW_24.FIN2	218	1.68	1.629	0.032	0.1667	0.0027	980	12	993	15	950	44	993.0	15.0	1.3	
LAW_25.FIN2	160	1.49	1.78	0.043	0.1772	0.0029	1034	16	1051	16	977	53	1051.0	16.0	1.6	

LAW_26.FIN2	287	0.97	2.859	0.054	0.2379	0.004	1369	14	1375	21	1361	32	1375.0	21.0	0.4
LAW_27.FIN2	157.9	2.12	4.23	0.064	0.2941	0.004	1677	13	1661	20	1695	29	1695.0	29.0	2.0
LAW_28.FIN2	114.5	0.86	1.068	0.026	0.1185	0.0017	737	12	721.8	9.6	769	52	721.8	9.6	2.1
LAW_29.FIN2	154	1.22	0.485	0.013	0.06559	0.00097	399.9	9	409.4	5.8	338	62	409.4	5.8	2.4
LAW_30.FIN2	736.2	2.43	0.592	0.015	0.0749	0.0015	471.7	9.6	465.4	9.1	497	60	465.4	9.1	1.3
LAW_31.FIN2	134.1	1.21	0.583	0.024	0.0713	0.002	464	15	444	12	549	96	444.0	12.0	4.3
LAW_32.FIN2	87	1.30	2.757	0.076	0.2274	0.003	1337	21	1320	16	1362	54	1320.0	16.0	1.3
LAW_33.FIN2	77.8	0.74	1.883	0.04	0.1797	0.0025	1071	14	1065	14	1075	45	1065.0	14.0	0.6
LAW_35.FIN2	122.2	0.76	0.506	0.03	0.0652	0.0019	414	20	407	11	420	110	407.0	11.0	1.7
LAW_37.FIN2	110.7	1.50	1.965	0.039	0.1866	0.0024	1100	13	1102	13	1084	39	1102.0	13.0	0.2
LAW_38.FIN2	171.9	0.97	4.215	0.056	0.3012	0.0036	1677	11	1697	18	1642	25	1642.0	25.0	3.3
LAW_39.FIN2	430	1.10	0.587	0.011	0.07503	0.00092	468.6	7.5	466.3	5.5	463	43	466.3	5.5	0.5
LAW_40.FIN2	233.3	1.19	1.825	0.038	0.1836	0.0035	1058	15	1086	19	992	46	1086.0	19.0	2.6
LAW_41.FIN2	86.6	0.88	0.808	0.027	0.0986	0.0015	597	15	605.9	9	540	76	605.9	9.0	1.5
LAW_42.FIN2	295	4.54	1.072	0.017	0.1201	0.0013	738.3	8.4	732.1	7.7	752	34	732.1	7.7	0.8
LAW_43.FIN2	178.5	2.21	4.194	0.082	0.2954	0.0045	1670	16	1667	22	1660	29	1660.0	29.0	0.4
LAW_44.FIN2	185	1.02	0.539	0.019	0.0698	0.0013	435	12	435	8.1	402	71	435.0	8.1	0.0
LAW_45.FIN2	34.2	1.08	1.572	0.054	0.1622	0.0033	956	23	970	19	899	78	970.0	19.0	1.5
LAW_46.FIN2	258	2.22	0.512	0.017	0.0671	0.0011	418	11	418.5	6.7	386	76	418.5	6.7	0.1
LAW_47.FIN2	62.5	0.88	0.428	0.023	0.0581	0.0012	361	17	363.7	7.1	310	110	363.7	7.1	0.7
LAW_48.FIN2	135.2	1.81	1.654	0.031	0.1668	0.0024	988	12	994	13	973	41	994.0	13.0	0.6
LAW_49.FIN2	129.2	1.09	4.033	0.069	0.2931	0.0037	1640	14	1656	18	1605	27	1605.0	27.0	3.2
LAW_50.FIN2	162.1	0.94	2.78	0.042	0.2287	0.0027	1348	11	1327	14	1367	30	1327.0	14.0	1.6
LAW_52.FIN2	18.9	0.51	1.631	0.09	0.1591	0.0044	963	36	950	25	940	120	950.0	25.0	1.3
LAW_53.FIN2	948	1.16	0.532	0.026	0.0691	0.0026	432	17	431	16	420	100	431.0	16.0	0.2
LAW_54.FIN2	255	2.43	3.023	0.048	0.2486	0.003	1412	12	1431	16	1375	29	1431.0	16.0	1.3
LAW_55.FIN2	196	1.74	1.632	0.031	0.1639	0.0021	980	12	978	11	967	36	978.0	11.0	0.2
LAW_56.FIN2	99.6	2.29	2.873	0.076	0.233	0.0042	1372	20	1350	22	1392	55	1350.0	22.0	1.6

LAW_57.FIN2	290.9	1.13	0.552	0.013	0.07133	0.00086	445.8	8.5	444.1	5.2	429	50	444.1	5.2	0.4	
LAW_58.FIN2	70.1	0.82	0.922	0.033	0.1076	0.0021	662	17	659	12	631	81	659.0	12.0	0.5	
LAW_59.FIN2	65.8	0.84	2.586	0.071	0.2224	0.0044	1289	20	1293	23	1270	51	1293.0	23.0	0.3	
LAW_60.FIN2	154	1.11	0.451	0.013	0.05997	0.00094	376.7	9	375.3	5.7	361	64	375.3	5.7	0.4	
LAW_62.FIN2	222	1.04	1.579	0.028	0.1578	0.0021	961	11	944	12	983	37	944.0	12.0	1.8	
LAW_63.FIN2	99	0.82	0.527	0.018	0.0705	0.0012	429	12	439.1	7.2	350	77	439.1	7.2	2.4	
LAW_64.FIN2	173.3	1.08	0.419	0.012	0.05508	0.00069	354	8.7	345.6	4.2	374	61	345.6	4.2	2.4	
LAW_65.FIN2	209	0.71	13.09	0.2	0.5131	0.0063	2682	15	2668	27	2685	19	2685.0	19.0	0.6	
LAW_66.FIN2	206.6	4.42	4.785	0.071	0.311	0.0038	1781	13	1745	19	1818	22	1818.0	22.0	4.0	
LAW_67.FIN2	419	1.44	0.547	0.013	0.0705	0.001	441.5	8.7	439.1	6	448	48	439.1	6.0	0.5	
LAW_68.FIN2	202.3	1.23	1.237	0.022	0.1343	0.0016	818	11	812.2	9.4	831	37	812.2	9.4	0.7	
LAW_69.FIN2	572	2.04	0.417	0.019	0.0551	0.0019	354	14	346	11	390	130	346.0	11.0	2.3	
LAW_70.FIN2	151	2.32	1.64	0.03	0.1628	0.0019	983	12	972	11	985	39	972.0	11.0	1.1	
LAW_71.FIN2	157	3.35	1.884	0.082	0.1772	0.0047	1072	29	1051	26	1124	73	1051.0	26.0	2.0	
LAW_72.FIN2	127.2	1.80	3.758	0.059	0.272	0.0035	1581	13	1550	18	1610	29	1550.0	18.0	2.0	
LAW_73.FIN2	618	1.10	0.558	0.016	0.0714	0.0016	449	10	444.2	9.6	460	56	444.2	9.6	1.1	
LAW_74.FIN2	192	2.01	2.281	0.045	0.2063	0.0037	1203	14	1208	20	1187	34	1208.0	20.0	0.4	
LAW_75.FIN2	256	2.28	3.528	0.049	0.2719	0.0028	1531	11	1550	14	1501	24	1550.0	14.0	1.2	
LAW_76.FIN2	286.3	1.02	0.621	0.016	0.07678	0.00091	490	10	476.8	5.5	530	57	476.8	5.5	2.7	
LAW_77.FIN2	159.9	0.26	3.422	0.078	0.2571	0.0055	1506	18	1474	28	1540	45	1474.0	28.0	2.1	
LAW_78.FIN2	69.9	1.08	0.853	0.031	0.1016	0.0016	623	17	623.8	9.5	587	77	623.8	9.5	0.1	
LAW_79.FIN2	309	1.68	0.839	0.033	0.1	0.003	616	18	614	18	626	81	614.0	18.0	0.3	Rim
LAW_79.FIN2	352.5	1.26	5.89	0.11	0.336	0.005	1960	15	1867	24	2057	25	2057.0	25.0	9.2	Core
LAW_80.FIN2	138	0.74	0.608	0.019	0.07396	0.00098	480	12	459.9	5.9	552	70	459.9	5.9	4.2	
LAW_81.FIN2	32.43	-2.00	1.588	0.058	0.1574	0.0031	957	23	942	17	961	85	942.0	17.0	1.6	
LAW_82.FIN2	49.9	0.92	1.859	0.054	0.1767	0.0027	1060	19	1050	15	1058	61	1050.0	15.0	0.9	
LAW_83.FIN2	86.2	1.47	0.492	0.023	0.0648	0.0013	404	16	404.5	8.2	377	97	404.5	8.2	0.1	
LAW_84.FIN2	345	0.55	0.539	0.026	0.0675	0.0016	436	16	420.9	9.7	500	84	420.9	9.7	3.5	

LAW_85.FIN2	83.7	1.48	1.756	0.049	0.171	0.0033	1025	18	1017	18	1036	54	1017.0	18.0	0.8	
LAW_86.FIN2	427	2.07	1.774	0.025	0.1728	0.0017	1034.5	9.3	1027.2	9.6	1048	24	1027.2	9.6	0.7	
LAW_87.FIN2	129.3	0.80	0.744	0.035	0.0886	0.0019	562	21	547	11	590	110	547.0	11.0	2.7	
LAW_88.FIN2	642	14.44	1.707	0.027	0.1704	0.0024	1010	10	1014	13	989	25	1014.0	13.0	0.4	
LAW_90.FIN2	71.7	1.24	3.415	0.067	0.2624	0.0031	1503	15	1503	16	1496	36	1503.0	16.0	0.0	
LAW_91.FIN2	33.8	0.65	1.933	0.072	0.1783	0.0032	1081	25	1057	17	1104	72	1057.0	17.0	2.2	
LAW_92.FIN2	99.6	2.02	2.153	0.04	0.1995	0.0024	1164	13	1174	13	1145	38	1174.0	13.0	0.9	
LAW_93.FIN2	484	1.46	0.516	0.013	0.0675	0.0012	421.7	8.9	420.8	7.4	420	59	420.8	7.4	0.2	
LAW_94.FIN2	1210	42.00	0.462	0.024	0.0578	0.0027	385	17	362	16	510	110	362.0	16.0	6.0	Rim
LAW_94.FIN2	95.8	1.42	1.709	0.042	0.1711	0.0026	1014	16	1018	14	1000	50	1018.0	14.0	0.4	Core
LAW_95.FIN2	268	4.60	1.9	0.13	0.175	0.011	1071	45	1037	60	1154	74	1037.0	60.0	3.2	
LAW_96.FIN2	177.7	1.29	4.968	0.088	0.3249	0.0045	1812	14	1812	22	1810	23	1810.0	23.0	0.1	
LAW_97.FIN2	132.6	0.93	13.6	0.16	0.5308	0.0059	2721	11	2743	25	2702	17	2702.0	17.0	1.5	
LAW_98.FIN2	204	3.32	2.222	0.042	0.1988	0.0027	1185	13	1168	15	1211	34	1168.0	15.0	1.4	
LAW_99.FIN2	139	0.79	1.843	0.035	0.1786	0.0021	1059	13	1059	12	1061	41	1059.0	12.0	0.0	
LAW_100.FIN2	128.6	1.46	2.135	0.036	0.1965	0.0025	1158	12	1156	13	1156	33	1156.0	13.0	0.2	
LAW_101.FIN2	76.4	1.00	12.18	0.21	0.5047	0.0084	2619	17	2632	36	2608	26	2608.0	26.0	0.9	
LAW_102.FIN2	158.8	1.93	2.211	0.038	0.2048	0.0023	1182	12	1201	12	1144	31	1201.0	12.0	1.6	
LAW_103.FIN2	291	0.49	0.462	0.011	0.06019	0.00069	385.3	7.7	376.7	4.2	414	52	376.7	4.2	2.2	
LAW_104.FIN2	144	1.78	2.228	0.044	0.2056	0.0025	1187	14	1205	14	1149	39	1205.0	14.0	1.5	
LAW_105.FIN2	178	1.49	4.408	0.072	0.3124	0.0045	1711	14	1751	22	1653	24	1653.0	24.0	5.9	
LAW_106.FIN2	90.8	0.74	12.79	0.17	0.5105	0.006	2661	13	2657	25	2663	18	2663.0	18.0	0.2	
LAW_107.FIN2	230.8	1.73	3.353	0.051	0.2552	0.0033	1492	12	1465	17	1528	27	1465.0	17.0	1.8	
LAW_108.FIN2	103.4	1.07	1.664	0.036	0.167	0.0024	993	13	995	13	993	42	995.0	13.0	0.2	
LAW_109.FIN2	118.8	2.38	12.97	0.2	0.5151	0.0086	2676	14	2677	37	2674	26	2674.0	26.0	0.1	

LAW_110.FIN2	125.1	1.40	0.824	0.021	0.0994	0.0016	608	11	610.6	9.2	580	56	610.6	9.2	0.4	
LAW_111.FIN2	279.1	0.88	0.864	0.017	0.1002	0.0013	630.7	9	615.5	7.4	673	41	615.5	7.4	2.4	
LAW_112.FIN2	98.8	1.50	1.676	0.036	0.1706	0.0019	997	14	1015	10	957	42	1015.0	10.0	1.8	
LAW_113.FIN2	306	1.37	2.107	0.037	0.1993	0.0025	1149	12	1171	14	1103	30	1171.0	14.0	1.9	
LAW_114.FIN2	260.1	0.61	0.614	0.016	0.07955	0.00097	484	10	493.3	5.8	428	53	493.3	5.8	1.9	
LAW_115.FIN2	434	0.97	0.616	0.011	0.0802	0.00088	487.5	6.9	497.2	5.2	433	39	497.2	5.2	2.0	
LAW_116.FIN2	554	1.26	0.574	0.014	0.0739	0.0011	459.7	9.3	459.7	6.7	451	56	459.7	6.7	0.0	
LAW_117.FIN2	444	2.03	0.571	0.016	0.0686	0.0017	460	11	428	10	614	67	428.0	10.0	7.0	
LAW_118.FIN2	142	1.02	0.573	0.017	0.0731	0.0011	458	11	454.7	6.6	466	67	454.7	6.6	0.7	
LAW_119.FIN2	227.6	1.75	3.235	0.055	0.2556	0.0037	1462	13	1466	19	1460	23	1466.0	19.0	0.3	
LAW_120.FIN2	352	1.01	0.965	0.016	0.1124	0.0012	685.6	8.3	686.6	7.2	682	31	686.6	7.2	0.1	
LAW_121.FIN2	78	1.29	1.526	0.044	0.1584	0.0023	940	19	947	13	913	62	947.0	13.0	0.7	
LAW_122.FIN2	123.2	1.24	0.513	0.016	0.0693	0.001	418	11	431.7	6	342	70	431.7	6.0	3.3	
LAW_123.FIN2	264	3.31	3.68	0.039	0.2798	0.0025	1565.6	8.4	1590	13	1536	18	1590.0	13.0	1.6	
LAW_124.FIN2	279	1.70	1.035	0.018	0.1184	0.0016	721.3	8.9	721.2	9	722	37	721.2	9.0	0.0	
LAW_125.FIN2	40.8	-6.10	1.787	0.059	0.1775	0.0028	1035	22	1052	16	999	66	1052.0	16.0	1.6	
LAW_126.FIN2	34.7	0.65	4.51	0.14	0.3013	0.0053	1721	26	1696	26	1752	53	1752.0	53.0	3.2	
LAW_127.FIN2	950	33.80	0.541	0.025	0.0648	0.0023	438	16	405	14	613	74	405.0	14.0	7.5	Rim
LAW_127.FIN2	215.6	1.81	3.138	0.069	0.2463	0.0041	1443	18	1419	21	1479	31	1419.0	21.0	1.7	Core
LAW_128.FIN2	229.3	1.07	0.605	0.015	0.077	0.0011	478.6	9.2	478.2	6.3	468	53	478.2	6.3	0.1	
LAW_129.FIN2	198.7	1.26	2.244	0.034	0.2038	0.0021	1193	11	1195	11	1197	27	1195.0	11.0	0.2	
LAW_130.FIN2	140.3	1.24	0.487	0.035	0.0645	0.0016	401	24	402.7	9.8	370	140	402.7	9.8	0.4	

Sample Name: OVB							207/235		206/238		207/206		Best age			
Grain #	[U] ppm	U/Th	207/235	2σ error	206/238	2σ error	Age (Ma)	2σ error	Age (Ma)	2σ error	Age (Ma)	2σ error	(Ma)	2σ error	% Disc*	Rim/ Core
OVB_1.FIN2	148.2	1.38	1.718	0.025	0.1722	0.0016	1013.8	9.2	1024.1	9	993	29	1024.1	9.0	1.0	
OVB_2.FIN2	398	0.79	0.5481	0.0079	0.07053	0.00064	443.2	5.2	439.3	3.8	471	33	439.3	3.8	0.9	
OVB_3.FIN2	113.2	1.00	3.063	0.045	0.2455	0.0025	1421	11	1415	13	1444	26	1415.0	13.0	0.4	
OVB_4.FIN2	130	2.58	2.47	0.051	0.2264	0.0042	1259	15	1314	22	1179	27	1314.0	22.0	4.4	
OVB_5.FIN2	138	1.62	4.56	0.053	0.3202	0.0028	1740.2	9.6	1790	14	1690	20	1690.0	20.0	5.9	
OVB_6.FIN2	513	0.72	0.5356	0.0082	0.06958	0.00064	435	5.4	433.6	3.9	446	36	433.6	3.9	0.3	
OVB_7.FIN2	686	1.84	2.204	0.018	0.2026	0.0016	1181.6	5.8	1188.8	8.4	1176	14	1188.8	8.4	0.6	
OVB_8.FIN2	172.5	2.38	5.761	0.062	0.3628	0.0037	1940.1	9	1995	18	1884	16	1884.0	16.0	5.9	
OVB_9.FIN2	365	1.50	1.638	0.015	0.1687	0.0013	984.1	5.8	1004.6	7	938	20	1004.6	7.0	2.1	
OVB_10.FIN2	105	2.27	0.529	0.022	0.0687	0.0014	431	15	428.4	8.4	427	91	428.4	8.4	0.6	
OVB_11.FIN2	365	2.43	4.928	0.043	0.3326	0.0027	1806	7.4	1850	13	1756	12	1756.0	12.0	5.4	
OVB_12.FIN2	1233	7.60	2.152	0.034	0.1921	0.0037	1165	11	1133	20	1218	21	1133.0	20.0	2.7	
OVB_13.FIN2	294.9	0.55	6.318	0.061	0.3698	0.0036	2020.7	8.4	2028	17	2010	14	2010.0	14.0	0.9	
OVB_14.FIN2	251.8	0.67	0.591	0.02	0.0698	0.0019	471	13	435	11	638	67	435.0	11.0	7.6	
OVB_15.FIN2	130.2	1.59	2.422	0.029	0.2198	0.002	1247.6	8.5	1280	10	1181	25	1280.0	10.0	2.6	
OVB_16.FIN2	260.4	1.34	0.5703	0.0097	0.07286	0.00071	457.5	6.3	453.3	4.2	468	37	453.3	4.2	0.9	
OVB_17.FIN2	408	7.32	0.617	0.015	0.0773	0.0011	487	9.6	479.9	6.5	521	54	479.9	6.5	1.5	
OVB_18.FIN2	112.9	1.92	0.569	0.014	0.07392	0.00099	456.1	9.1	459.6	6	443	56	459.6	6.0	0.8	
OVB_19.FIN2	178	1.46	1.621	0.023	0.1646	0.0019	977.9	8.6	982	10	981	28	982.0	10.0	0.4	
OVB_20.FIN2	251	1.77	2.068	0.027	0.1965	0.002	1138	9	1156	11	1113	23	1156.0	11.0	1.6	
OVB_22.FIN2	700	0.60	0.609	0.011	0.076	0.0011	482.5	6.9	472.3	6.7	537	36	472.3	6.7	2.1	
OVB_23.FIN2	141.6	0.79	0.576	0.013	0.075	0.00087	460.4	8.6	466.2	5.2	414	51	466.2	5.2	1.3	
OVB_24.FIN2	55.6	1.31	0.615	0.022	0.0783	0.0012	485	14	485.8	7.3	447	74	485.8	7.3	0.2	
OVB_25.FIN2	182	1.44	2.287	0.051	0.1997	0.0035	1207	16	1173	19	1203	39	1173.0	19.0	2.8	
OVB_26.FIN2	104.6	2.44	5.411	0.057	0.3502	0.0036	1885	9	1934	17	1812	19	1812.0	19.0	6.7	

OVB_27.FIN2	419	2.74	4.779	0.044	0.3196	0.0041	1780.4	7.7	1787	20	1756	17	1756.0	17.0	1.8	
OVB_28.FIN2	267	3.45	0.5354	0.0095	0.06947	0.00072	434.7	6.3	432.9	4.3	424	42	432.9	4.3	0.4	
OVB_29.FIN2	262.4	2.51	2.303	0.027	0.2042	0.0026	1212.9	8.7	1197	14	1232	25	1197.0	14.0	1.3	
OVB_30.FIN2	668	2.43	10.74	0.18	0.4253	0.0065	2498	15	2282	30	2679	14	2679.0	14.0	14.8	
OVB_31.FIN2	29.5	0.46	1.912	0.057	0.1837	0.0032	1085	20	1086	17	1085	59	1086.0	17.0	0.1	
OVB_32.FIN2	39.4	1.25	1.35	0.04	0.1405	0.002	862	17	847	11	881	63	847.0	11.0	1.7	
OVB_33.FIN2	196	1.86	1.887	0.022	0.1867	0.0018	1076.4	8	1104.6	9.8	1018	25	1104.6	9.8	2.6	
OVB_34.FIN2	385	2.44	2.288	0.028	0.2088	0.0022	1207.1	8.8	1222	12	1190	21	1222.0	12.0	1.2	
OVB_35.FIN2	316	5.18	3.276	0.034	0.2628	0.0025	1475	8.2	1504	13	1439	18	1504.0	13.0	2.0	
OVB_36.FIN2	305	1.31	6.18	0.11	0.3373	0.0057	2000	16	1873	27	2143	24	2143.0	24.0	12.6	
OVB_37.FIN2	568	11.00	4.238	0.056	0.2996	0.0052	1681	11	1689	26	1692	21	1692.0	21.0	0.2	
OVB_38.FIN2	335	1.48	0.607	0.01	0.0772	0.00086	480.8	6.4	479.3	5.2	485	36	479.3	5.2	0.3	
OVB_40.FIN2	186.3	1.96	3.115	0.047	0.2548	0.0029	1434	11	1463	15	1402	28	1463.0	15.0	2.0	
OVB_41.FIN2	81.2	1.39	3.526	0.051	0.2731	0.0033	1531	11	1556	17	1504	28	1556.0	17.0	1.6	
OVB_42.FIN2	378	29.30	1.836	0.06	0.1755	0.0059	1057	22	1042	32	1096	68	1042.0	32.0	1.4	Rim
OVB_42.FIN2	93.7	2.05	2.629	0.047	0.2278	0.0023	1306	13	1323	12	1278	34	1323.0	12.0	1.3	Core
OVB_43.FIN2	424.2	2.44	1.827	0.023	0.1762	0.0015	1054.2	8.1	1046.2	8.5	1072	24	1046.2	8.5	0.8	
OVB_44.FIN2	392	1.91	0.83	0.012	0.10009	0.00096	612.8	6.5	614.8	5.6	605	30	614.8	5.6	0.3	
OVB_46.FIN2	197	1.20	3.503	0.039	0.2673	0.0028	1526.5	8.9	1528	14	1519	19	1528.0	14.0	0.1	
OVB_47.FIN2	87.9	1.89	1.777	0.033	0.1709	0.0018	1034	12	1017	10	1057	37	1017.0	10.0	1.6	
OVB_48.FIN2	684	1.05	2.29	0.04	0.1452	0.0017	1207	12	873.5	9.7	1842	27	DISC	DISC	27.6	
OVB_49.FIN2	299.1	2.12	2.494	0.064	0.2003	0.0047	1268	19	1177	25	1423	41	1177.0	25.0	7.2	
OVB_50.FIN2	285.1	1.31	0.587	0.01	0.07461	0.00076	468.3	6.4	463.8	4.6	469	42	463.8	4.6	1.0	
OVB_51.FIN2	169.6	0.74	0.884	0.018	0.1038	0.0014	641.8	9.8	636.3	8.1	654	51	636.3	8.1	0.9	
OVB_52.FIN2	46.7	1.39	1.607	0.041	0.1627	0.0023	968	16	971	12	948	53	971.0	12.0	0.3	
OVB_53.FIN2	182	1.61	1.727	0.028	0.1697	0.0022	1017	10	1010	12	1033	33	1010.0	12.0	0.7	
OVB_54.FIN2	108.4	1.48	0.537	0.015	0.0706	0.0012	435	10	439.3	6.9	408	60	439.3	6.9	1.0	
OVB_56.FIN2	113.7	0.80	1.736	0.03	0.1729	0.0019	1020	11	1028	11	1022	36	1028.0	11.0	0.8	

OVB_57.FIN2	425	1.56	3.053	0.086	0.2308	0.0053	1419	21	1338	28	1565	53	1338.0	28.0	5.7
OVB_58.FIN2	414	1.45	0.71	0.01	0.08879	0.00093	545	6.3	548.3	5.5	547	31	548.3	5.5	0.6
OVB_59.FIN2	159	1.31	2.109	0.046	0.2002	0.0037	1150	15	1176	20	1124	37	1176.0	20.0	2.3
OVB_60.FIN2	387	1.63	3.562	0.037	0.276	0.0027	1540.2	8.1	1571	14	1515	18	1571.0	14.0	2.0
OVB_61.FIN2	130	1.24	2.921	0.048	0.244	0.0031	1386	12	1407	16	1361	26	1407.0	16.0	1.5
OVB_62.FIN2	291.2	2.67	0.4895	0.0088	0.06523	0.00061	403.9	6	407.3	3.7	386	42	407.3	3.7	0.8
OVB_63.FIN2	50.1	1.03	1.868	0.043	0.182	0.0026	1068	15	1077	14	1037	47	1077.0	14.0	0.8
OVB_64.FIN2	211	1.06	0.572	0.01	0.07307	0.00076	459.6	6.6	454.6	4.6	466	42	454.6	4.6	1.1
OVB_65.FIN2	210.1	0.70	0.681	0.018	0.0842	0.0012	527	11	520.9	7.1	530	54	520.9	7.1	1.2
OVB_66.FIN2	162.2	1.20	0.611	0.014	0.0787	0.0015	484.1	9	488.2	8.8	446	56	488.2	8.8	0.8
OVB_67.FIN2	350	1.22	0.516	0.011	0.06738	0.00075	421.9	7.2	420.3	4.5	408	43	420.3	4.5	0.4
OVB_68.FIN2	235	1.35	0.533	0.012	0.07066	0.00079	434.1	8	440.1	4.8	401	49	440.1	4.8	1.4
OVB_69.FIN2	359.4	1.33	2.98	0.055	0.2362	0.0046	1401	14	1367	24	1449	29	1367.0	24.0	2.4
OVB_70.FIN2	137.1	1.11	3.038	0.043	0.2508	0.0028	1416	11	1442	14	1364	26	1442.0	14.0	1.8
OVB_71.FIN2	379	0.66	0.533	0.02	0.0685	0.0015	433	13	426.9	8.8	447	69	426.9	8.8	1.4
OVB_72.FIN2	106	2.26	2.983	0.043	0.2476	0.0028	1403	11	1426	15	1360	26	1426.0	15.0	1.6
OVB_73.FIN2	66.8	1.28	2.941	0.053	0.2406	0.0025	1389	14	1389	13	1377	33	1389.0	13.0	0.0
OVB_74.FIN2	234.2	1.01	0.679	0.021	0.0814	0.0014	525	13	504.4	8.3	588	68	504.4	8.3	3.9
OVB_75.FIN2	88	1.89	0.918	0.024	0.1059	0.0014	660	12	648.7	8.3	675	55	648.7	8.3	1.7
OVB_76.FIN2	33.7	1.21	1.755	0.072	0.1717	0.0037	1020	26	1021	20	988	76	1021.0	20.0	0.1
OVB_77.FIN2	50.9	1.41	2.379	0.058	0.2101	0.0028	1234	18	1229	15	1224	46	1229.0	15.0	0.4
OVB_78.FIN2	777	6.26	2.02	0.026	0.1451	0.0018	1121.4	8.7	873.2	9.9	1624	26	DISC	DISC	22.1
OVB_79.FIN2	530	4.09	1.67	0.025	0.1612	0.0024	996.1	9.5	963	13	1063	27	963.0	13.0	3.3
OVB_80.FIN2	40.8	2.04	1.724	0.046	0.1714	0.0029	1015	17	1019	16	985	54	1019.0	16.0	0.4
OVB_82.FIN2	165	1.36	3.487	0.037	0.2706	0.0028	1522.9	8.4	1543	14	1496	24	1543.0	14.0	1.3
OVB_83.FIN2	578	1.48	0.978	0.017	0.0937	0.0011	691.8	8.7	577.1	6.5	1077	34	DISC	DISC	16.6
OVB_84.FIN2	202	1.11	3.059	0.078	0.2179	0.0037	1419	19	1270	20	1640	40	1270.0	20.0	10.5
OVB_85.FIN2	233	1.16	4.456	0.055	0.3108	0.0033	1721	10	1744	16	1690	21	1690.0	21.0	3.2

OVB_86.FIN2	60.3	1.66	1.907	0.037	0.1854	0.002	1082	13	1098	11	1041	37	1098.0	11.0	1.5	
OVB_87.FIN2	144	1.61	0.661	0.017	0.0827	0.0011	513	11	511.9	6.4	501	58	511.9	6.4	0.2	
OVB_88.FIN2	198	0.96	1.832	0.025	0.1775	0.0016	1055.3	9	1053.1	8.8	1065	29	1053.1	8.8	0.2	
OVB_89.FIN2	90.5	0.80	13.36	0.17	0.5176	0.0064	2703	12	2687	27	2710	15	2710.0	15.0	0.8	
OVB_90.FIN2	60.7	0.46	5.51	0.085	0.3621	0.0048	1900	13	1991	23	1801	24	1801.0	24.0	10.5	
OVB_91.FIN2	195	1.67	3.613	0.062	0.2775	0.0032	1549	14	1578	16	1506	24	1578.0	16.0	1.9	
OVB_92.FIN2	110.4	0.99	4.269	0.052	0.3013	0.003	1686	10	1697	15	1675	21	1675.0	21.0	1.3	
OVB_93.FIN2	316	1.23	0.887	0.038	0.0776	0.002	643	20	482	12	1247	68	DISC	DISC	25.0	
OVB_94.FIN2	176.7	1.10	4.535	0.058	0.3021	0.0049	1736	11	1701	24	1780	26	1780.0	26.0	4.4	
OVB_95.FIN2	32.1	1.33	1.774	0.049	0.1765	0.0028	1031	18	1047	15	998	59	1047.0	15.0	1.6	
OVB_96.FIN2	1003	9.80	0.664	0.031	0.0729	0.0043	517	19	454	26	816	33	454.0	26.0	12.2	Rim
OVB_96.FIN2	470	3.91	4.392	0.058	0.3008	0.0045	1710	11	1695	22	1728	21	1728.0	21.0	1.9	Core
OVB_97.FIN2	504	2.31	2.181	0.021	0.2023	0.0019	1174	6.8	1188	10	1146	17	1188.0	10.0	1.2	
OVB_98.FIN2	481	1.98	0.835	0.014	0.0986	0.0011	615.5	7.6	606	6.7	645	35	606.0	6.7	1.5	
OVB_99.FIN2	164	2.55	2.491	0.033	0.2197	0.0024	1267.9	9.6	1280	13	1242	21	1280.0	13.0	1.0	
OVB_100.FIN2	158.6	0.88	0.497	0.011	0.0647	0.00092	408.8	7.1	404.1	5.6	413	50	404.1	5.6	1.1	
OVB_101.FIN2	605	1.44	0.555	0.017	0.0659	0.0024	448	11	412	15	620	74	412.0	15.0	8.0	
OVB_102.FIN2	96.6	1.93	4.866	0.056	0.3317	0.0034	1794.7	9.6	1846	17	1711	22	1711.0	22.0	7.9	
OVB_103.FIN2	289	3.02	2.559	0.073	0.1951	0.0058	1287	21	1148	31	1506	41	1148.0	31.0	10.8	
OVB_104.FIN2	168.4	3.04	3.424	0.042	0.2648	0.0024	1508.4	9.5	1514	12	1479	23	1514.0	12.0	0.4	
OVB_105.FIN2	203.7	1.70	2.963	0.039	0.2455	0.0026	1397	10	1415	14	1349	25	1415.0	14.0	1.3	
OVB_106.FIN2	43.4	1.41	0.816	0.031	0.094	0.0015	603	18	578.7	9.1	654	88	578.7	9.1	4.0	
OVB_107.FIN2	176	2.79	1.804	0.027	0.1778	0.0018	1046.4	9.6	1054.5	9.7	1016	30	1054.5	9.7	0.8	
OVB_108.FIN2	289	2.49	3.461	0.036	0.2692	0.0022	1517.3	8.1	1537	11	1485	19	1537.0	11.0	1.3	
OVB_109.FIN2	163.4	1.58	0.689	0.031	0.0737	0.0018	531	19	458	11	831	94	458.0	11.0	13.7	
OVB_110.FIN2	183.6	0.78	4.974	0.057	0.3243	0.0033	1814.4	9.5	1810	16	1818	19	1818.0	19.0	0.4	
OVB_111.FIN2	20.82	1.68	2.86	0.095	0.2358	0.0041	1361	25	1364	21	1354	59	1364.0	21.0	0.2	
OVB_112.FIN2	409	6.28	4.192	0.047	0.2739	0.0041	1670.8	9.2	1559	21	1825	23	1559.0	21.0	6.7	

OVB_113.FIN2	93.2	0.96	0.559	0.017	0.07156	0.00091	448	11	445.5	5.5	453	67	445.5	5.5	0.6	
OVB_114.FIN2	71.5	1.72	9.92	0.16	0.4348	0.006	2423	15	2325	27	2516	19	2516.0	19.0	7.6	
OVB_115.FIN2	723	13.90	0.559	0.031	0.0686	0.002	450	20	428	12	562	95	428.0	12.0	4.9	Rim
OVB_115.FIN2	208.3	4.17	1.473	0.047	0.1507	0.0034	918	19	905	19	946	73	905.0	19.0	1.4	Core
OVB_116.FIN2	188	3.70	1.718	0.033	0.1701	0.0023	1014	12	1012	13	1016	33	1012.0	13.0	0.2	
OVB_117.FIN2	156.8	0.97	4.315	0.059	0.3071	0.0034	1694	11	1726	17	1658	19	1658.0	19.0	4.1	
OVB_118.FIN2	483	2.16	0.884	0.011	0.10643	0.00095	642.6	5.8	651.9	5.5	602	24	651.9	5.5	1.4	
OVB_119.FIN2	161	1.28	0.6	0.017	0.0677	0.001	477	11	422.4	6.2	710	64	422.4	6.2	11.4	
OVB_120.FIN2	147.8	2.46	1.594	0.023	0.1637	0.0015	967.6	9.2	978.1	8.4	931	26	978.1	8.4	1.1	
OVB_121.FIN2	61.4	2.35	2.019	0.039	0.1922	0.0022	1119	13	1133	12	1082	45	1133.0	12.0	1.3	
OVB_122.FIN2	516	2.02	2.358	0.028	0.2108	0.0023	1229.7	8.4	1232	12	1226	19	1232.0	12.0	0.2	
OVB_123.FIN2	177.8	1.93	13.83	0.14	0.5343	0.0053	2737	10	2758	22	2720	13	2720.0	13.0	1.4	
OVB_124.FIN2	279	1.18	1.786	0.026	0.1678	0.002	1039	9.5	1000	11	1114	30	1000.0	11.0	3.8	
OVB_125.FIN2	112.4	0.75	3.229	0.041	0.2535	0.0024	1462.3	9.9	1458	13	1468	24	1458.0	13.0	0.3	
OVB_126.FIN2	347	4.68	0.513	0.01	0.06699	0.00067	420.4	6.7	418	4.1	434	43	418.0	4.1	0.6	
OVB_127.FIN2	262	0.66	0.4881	0.0098	0.06441	0.00079	403.7	6.8	402.3	4.8	409	47	402.3	4.8	0.3	
OVB_128.FIN2	448.6	1.91	3.019	0.029	0.2463	0.0019	1411.4	7.4	1419.3	9.8	1409	17	1419.3	9.8	0.6	
OVB_129.FIN2	286.5	0.89	2.019	0.022	0.1912	0.0016	1121.8	7.5	1127.8	8.9	1113	20	1127.8	8.9	0.5	
OVB_130.FIN2	429	2.07	0.554	0.01	0.07292	0.00071	447	6.7	453.7	4.3	410	40	453.7	4.3	1.5	

Sample Name:							**207/235**		**206/238**		**207/206**		**Best age**			
Grain #	**[U] ppm**	**U/Th**	**207/235**	**2σ error**	**206/238**	**2σ error**	**Age (Ma)**	**2σ error**	**Age (Ma)**	**2σ error**	**Age (Ma)**	**2σ error**	**(Ma)**	**2σ error**	**% Disc***	**Rim/ Core**
RCN_1.FIN2	145	1.16	1.736	0.044	0.1693	0.0036	1018	16	1007	20	1035	34	1007.0	20.0	1.1	
RCN_2.FIN2	275	1.88	0.519	0.016	0.0648	0.0013	423	11	405.9	8.1	513	60	405.9	8.1	4.0	
RCN_3.FIN2	80.2	1.52	0.491	0.021	0.0645	0.0013	402	14	403	7.8	385	93	403.0	7.8	0.2	

RCN_4.FIN2	451	1.23	2.978	0.042	0.2354	0.0026	1400	11	1364	14	1446	22	1364.0	14.0	2.6
RCN_5.FIN2	36.2	1.41	1.77	0.059	0.1675	0.0031	1025	22	998	17	1052	74	998.0	17.0	2.6
RCN_6.FIN2	18.7	1.80	1.65	0.11	0.1604	0.0044	973	45	958	24	950	140	958.0	24.0	1.5
RCN_7.FIN2	170.3	1.16	1.872	0.035	0.1808	0.0032	1070	13	1070	18	1055	39	1070.0	18.0	0.0
RCN_8.FIN2	84.8	0.59	1.719	0.042	0.1709	0.0028	1011	16	1016	16	979	53	1016.0	16.0	0.5
RCN_9.FIN2	141.7	2.01	0.547	0.017	0.0678	0.0012	441	11	423	7.2	509	74	423.0	7.2	4.1
RCN_10.FIN2	291	0.84	2.685	0.047	0.2248	0.0039	1321	13	1306	20	1348	30	1306.0	20.0	1.1
RCN_11.FIN2	84.2	1.85	3.931	0.073	0.2857	0.0041	1616	15	1619	21	1608	34	1608.0	34.0	0.7
RCN_12.FIN2	238.3	1.17	0.582	0.014	0.07355	0.00097	464.4	8.9	457.4	5.8	480	53	457.4	5.8	1.5
RCN_13.FIN2	122.7	1.45	2.224	0.043	0.1959	0.0026	1185	13	1153	14	1230	39	1153.0	14.0	2.7
RCN_14.FIN2	175.9	1.64	2.171	0.036	0.1973	0.0024	1169	12	1160	13	1179	32	1160.0	13.0	0.8
RCN_15.FIN2	83.1	0.78	1.977	0.051	0.1891	0.0027	1102	18	1116	15	1063	49	1116.0	15.0	1.3
RCN_16.FIN2	108	1.83	4.291	0.064	0.2994	0.0037	1690	13	1687	19	1684	25	1684.0	25.0	0.2
RCN_17.FIN2	506	2.69	13.97	0.14	0.5199	0.0052	2745.9	9.8	2697	22	2777	12	2777.0	12.0	2.9
RCN_18.FIN2	221	0.71	1.74	0.032	0.1704	0.0022	1021	12	1014	12	1027	34	1014.0	12.0	0.7
RCN_19.FIN2	244.6	1.32	0.608	0.015	0.0758	0.0011	480.3	9.7	470.6	6.6	505	53	470.6	6.6	2.0
RCN_20.FIN2	429	1.58	4.742	0.06	0.3165	0.0036	1773	11	1771	18	1769	17	1769.0	17.0	0.1
RCN_21.FIN2	473	1.67	4.551	0.066	0.3056	0.0044	1740	12	1718	22	1752	18	1752.0	18.0	1.9
RCN_22.FIN2	127	0.81	1.893	0.052	0.1822	0.0035	1074	18	1078	19	1043	53	1078.0	19.0	0.4
RCN_23.FIN2	424	2.33	1.956	0.041	0.1771	0.0033	1098	14	1050	18	1179	26	1050.0	18.0	4.4
RCN_24.FIN2	103.2	1.57	1.682	0.045	0.1648	0.0029	998	18	982	16	1010	42	982.0	16.0	1.6
RCN_25.FIN2	241	1.90	1.747	0.029	0.1719	0.0023	1024	11	1022	13	1018	32	1022.0	13.0	0.2
RCN_26.FIN2	79.9	1.71	3.206	0.071	0.2577	0.0037	1453	17	1477	19	1407	42	1477.0	19.0	1.7
RCN_27.FIN2	1203	3.65	1.792	0.088	0.1681	0.0091	1040	32	1001	50	1128	59	1001.0	50.0	3.8
RCN_28.FIN2	212.6	2.08	2.088	0.035	0.1934	0.0024	1142	12	1139	13	1138	32	1139.0	13.0	0.3
RCN_29.FIN2	90.6	0.90	3.712	0.09	0.2808	0.006	1569	19	1597	29	1524	43	1597.0	29.0	1.8
RCN_30.FIN2	385	2.02	4.557	0.064	0.305	0.0043	1739	12	1715	21	1764	23	1764.0	23.0	2.8
RCN_31.FIN2	128	1.00	15	0.2	0.5392	0.006	2814	12	2778	25	2831	18	2831.0	18.0	1.9

RCN_32.FIN2	53.8	1.39	0.519	0.027	0.0687	0.0015	420	19	428	8.8	350	100	428.0	8.8	1.9	
RCN_33.FIN2	121.4	1.55	11.67	0.16	0.4782	0.007	2577	13	2517	30	2621	19	2621.0	19.0	4.0	
RCN_34.FIN2	428	2.55	0.609	0.013	0.0788	0.0011	482.9	8	488.6	6.6	437	43	488.6	6.6	1.2	
RCN_35.FIN2	244.4	0.70	0.601	0.016	0.077	0.0011	476	10	477.8	6.4	447	58	477.8	6.4	0.4	
RCN_36.FIN2	292	1.65	1.889	0.037	0.1812	0.0033	1074	13	1072	18	1072	35	1072.0	18.0	0.2	
RCN_37.FIN2	210	0.80	0.591	0.017	0.0755	0.0011	470	10	470.2	7	441	58	470.2	7.0	0.0	
RCN_38.FIN2	96.3	1.16	0.589	0.027	0.0751	0.0013	470	16	466.7	8	444	95	466.7	8.0	0.7	
RCN_39.FIN2	210	1.65	2.799	0.06	0.2338	0.004	1354	16	1353	21	1348	36	1353.0	21.0	0.1	
RCN_40.FIN2	499	1.55	2.927	0.049	0.2393	0.0035	1386	13	1382	18	1391	21	1382.0	18.0	0.3	
RCN_41.FIN2	28.6	0.81	1.841	0.073	0.1749	0.0037	1051	25	1041	21	1037	83	1041.0	21.0	1.0	
RCN_42.FIN2	214	3.26	5.44	0.11	0.3326	0.006	1888	18	1852	30	1932	34	1932.0	34.0	4.1	
RCN_43.FIN2	161.2	1.33	3.406	0.059	0.2557	0.0039	1502	14	1466	20	1549	29	1466.0	20.0	2.4	
RCN_44.FIN2	158.4	0.95	0.526	0.019	0.06501	0.00098	428	12	405.9	5.9	512	75	405.9	5.9	5.2	
RCN_45.FIN2	96.2	1.09	0.585	0.021	0.0743	0.0013	464	13	461.7	7.7	451	78	461.7	7.7	0.5	
RCN_46.FIN2	75.3	0.69	1.863	0.053	0.1788	0.0031	1067	20	1059	17	1063	62	1059.0	17.0	0.7	
RCN_47.FIN2	224	2.02	2.014	0.042	0.1885	0.0033	1119	14	1112	18	1135	32	1112.0	18.0	0.6	
RCN_48.FIN2	209	0.64	2.83	0.061	0.2326	0.0032	1362	16	1347	17	1368	34	1347.0	17.0	1.1	
RCN_49.FIN2	279	1.24	2.535	0.051	0.2022	0.0033	1280	15	1190	19	1429	38	1190.0	19.0	7.0	
RCN_50.FIN2	439	1.76	1.714	0.027	0.1696	0.0024	1012	10	1010	13	1011	31	1010.0	13.0	0.2	
RCN_52.FIN2	290	28.00	1.94	0.12	0.1854	0.0093	1090	42	1095	51	1082	95	1095.0	51.0	0.5	Rim
RCN_52.FIN2	142.6	1.87	3.112	0.062	0.2471	0.0037	1434	15	1423	19	1441	34	1423.0	19.0	0.8	Core
RCN_53.FIN2	51.8	1.34	1.649	0.055	0.1586	0.0028	981	21	948	15	1030	68	948.0	15.0	3.4	
RCN_54.FIN2	127.3	3.98	1.755	0.036	0.1749	0.0026	1028	14	1038	14	1007	41	1038.0	14.0	1.0	
RCN_55.FIN2	77.3	0.86	0.558	0.024	0.072	0.0017	445	16	448	10	418	92	448.0	10.0	0.7	
RCN_56.FIN2	169.7	1.22	2.125	0.035	0.1917	0.0024	1154	11	1130	13	1202	35	1130.0	13.0	2.1	
RCN_57.FIN2	511	1.44	0.557	0.018	0.0678	0.0018	449	12	423	11	572	63	423.0	11.0	5.8	
RCN_58.FIN2	83.9	0.85	12.95	0.25	0.5088	0.0083	2671	18	2648	35	2686	22	2686.0	22.0	1.4	
RCN_59.FIN2	205.1	0.70	0.507	0.014	0.0651	0.0011	416.2	8.9	407.4	6.7	434	56	407.4	6.7	2.1	

RCN_60.FIN2	175.4	1.31	1.007	0.026	0.1167	0.0018	705	13	711	10	677	58	711.0	10.0	0.9
RCN_61.FIN2	31.4	0.34	12.31	0.39	0.474	0.013	2620	31	2495	55	2731	44	2731.0	44.0	8.6
RCN_62.FIN2	107.3	1.57	0.623	0.023	0.0807	0.0013	488	14	499.8	7.9	403	76	499.8	7.9	2.4
RCN_63.FIN2	63.1	1.19	1.864	0.057	0.1807	0.0041	1065	20	1069	22	1035	60	1069.0	22.0	0.4
RCN_64.FIN2	272.4	1.39	2.023	0.035	0.1892	0.0029	1122	12	1116	15	1128	30	1116.0	15.0	0.5
RCN_65.FIN2	247	3.73	1.811	0.036	0.1784	0.0031	1046	13	1057	17	1035	34	1057.0	17.0	1.1
RCN_66.FIN2	187	1.48	2.089	0.039	0.1928	0.0025	1144	13	1136	14	1155	33	1136.0	14.0	0.7
RCN_67.FIN2	263	2.07	1.758	0.034	0.153	0.0031	1029	13	917	17	1283	40	917.0	17.0	10.9
RCN_69.FIN2	619	7.10	1.69	0.025	0.1683	0.0019	1004.2	9.5	1002	10	1001	24	1002.0	10.0	0.2
RCN_70.FIN2	114	1.13	4.048	0.065	0.2877	0.0039	1642	13	1629	19	1651	27	1651.0	27.0	1.3
RCN_71.FIN2	386	1.63	2.949	0.043	0.2426	0.003	1392	11	1401	15	1377	23	1401.0	15.0	0.6
RCN_72.FIN2	68	2.71	1.873	0.064	0.1767	0.0033	1071	22	1048	18	1094	69	1048.0	18.0	2.1
RCN_73.FIN2	174.6	0.80	0.667	0.033	0.0789	0.0028	525	20	489	16	630	100	489.0	16.0	6.9
RCN_74.FIN2	343	0.66	0.563	0.016	0.0732	0.0013	452	11	455	7.7	422	61	455.0	7.7	0.7
RCN_75.FIN2	210	1.58	5.226	0.073	0.3348	0.0045	1856	12	1860	22	1844	23	1844.0	23.0	0.9
RCN_76.FIN2	207	1.71	1.841	0.047	0.1783	0.0033	1057	17	1057	18	1052	54	1057.0	18.0	0.0
RCN_77.FIN2	58.6	0.80	2.86	0.1	0.2395	0.0058	1373	27	1382	30	1334	67	1382.0	30.0	0.7
RCN_78.FIN2	43.3	0.47	5.75	0.18	0.3549	0.009	1931	27	1953	43	1893	55	1893.0	55.0	3.2
RCN_79.FIN2	207.4	1.72	15.51	0.2	0.5555	0.0073	2844	13	2845	30	2837	15	2837.0	15.0	0.3
RCN_80.FIN2	130	2.19	1.925	0.044	0.1865	0.003	1087	16	1101	17	1045	40	1101.0	17.0	1.3
RCN_81.FIN2	88.9	1.72	1.888	0.045	0.1774	0.0028	1072	16	1052	15	1110	46	1052.0	15.0	1.9
RCN_82.FIN2	529	2.42	1.577	0.032	0.1529	0.0028	959	12	916	16	1046	37	916.0	16.0	4.5
RCN_83.FIN2	59	0.62	3.503	0.083	0.2697	0.0039	1524	18	1538	20	1497	39	1538.0	20.0	0.9
RCN_84.FIN2	55.8	1.53	1.766	0.062	0.1728	0.0032	1027	23	1027	17	1010	64	1027.0	17.0	0.0
RCN_85.FIN2	136	0.88	0.447	0.019	0.0603	0.0013	373	14	377.6	7.7	348	90	377.6	7.7	1.2
RCN_86.FIN2	53.5	1.26	1.672	0.05	0.1673	0.0025	994	19	997	14	974	63	997.0	14.0	0.3
RCN_87.FIN2	164.1	2.83	1.652	0.036	0.1675	0.0023	989	14	998	13	964	41	998.0	13.0	0.9
RCN_88.FIN2	253.3	0.37	0.469	0.011	0.06281	0.00082	389.3	7.7	392.6	5	358	51	392.6	5.0	0.8

RCN_89.FIN2	14.31	1.79	1.621	0.083	0.1692	0.0056	966	34	1005	31	840	110	1005.0	31.0	4.0
RCN_90.FIN2	133	-13.10	2.164	0.068	0.1993	0.0036	1165	22	1171	20	1160	46	1171.0	20.0	0.5
RCN_91.FIN2	191	0.72	0.497	0.016	0.0655	0.0012	409	11	408.7	7.4	407	70	408.7	7.4	0.1
RCN_92.FIN2	33.7	1.20	3.96	0.2	0.271	0.011	1612	43	1542	55	1705	75	1542.0	55.0	4.3
RCN_93.FIN2	185.3	0.76	0.491	0.015	0.0649	0.001	403.9	9.9	405.3	6.1	376	63	405.3	6.1	0.3
RCN_94.FIN2	53.1	0.72	1.543	0.058	0.1575	0.0048	944	24	941	26	954	78	941.0	26.0	0.3
RCN_95.FIN2	132	1.21	4.223	0.06	0.297	0.003	1676	12	1676	15	1677	24	1677.0	24.0	0.1
RCN_96.FIN2	211	1.29	0.536	0.014	0.0708	0.001	434.3	9.4	440.9	6.2	383	59	440.9	6.2	1.5
RCN_97.FIN2	552	2.49	2.216	0.045	0.1901	0.0042	1186	15	1121	23	1315	31	1121.0	23.0	5.5
RCN_98.FIN2	168	1.33	0.569	0.016	0.0733	0.001	455	10	455.8	6.2	440	61	455.8	6.2	0.2
RCN_99.FIN2	61.6	1.82	2.133	0.07	0.1963	0.0043	1153	23	1154	23	1138	58	1154.0	23.0	0.1
RCN_100.FIN2	245	1.16	13.89	0.17	0.5382	0.0066	2740	12	2774	28	2713	15	2713.0	15.0	2.2
RCN_101.FIN2	58	1.02	1.763	0.05	0.175	0.0036	1028	18	1041	19	1005	64	1041.0	19.0	1.3
RCN_102.FIN2	65.1	0.85	4.126	0.085	0.2977	0.0061	1656	18	1677	30	1631	40	1631.0	40.0	2.8
RCN_103.FIN2	218	2.97	3.575	0.058	0.271	0.0037	1542	13	1545	19	1537	28	1545.0	19.0	0.2
RCN_104.FIN2	74.8	1.52	1.768	0.047	0.1743	0.0027	1028	17	1035	15	1006	53	1035.0	15.0	0.7
RCN_105.FIN2	58.4	0.99	1.904	0.051	0.1846	0.0029	1077	18	1092	16	1040	53	1092.0	16.0	1.4
RCN_106.FIN2	279	1.70	0.565	0.017	0.0731	0.002	452	11	454	12	452	58	454.0	12.0	0.4
RCN_107.FIN2	216	1.11	3.068	0.068	0.248	0.0049	1422	17	1430	26	1409	29	1430.0	26.0	0.6
RCN_108.FIN2	255	2.30	4.799	0.063	0.3225	0.0044	1782	11	1801	21	1765	20	1765.0	20.0	2.0
RCN_109.FIN2	174	1.47	0.531	0.017	0.0687	0.0014	430	11	428.3	8.4	437	68	428.3	8.4	0.4
RCN_110.FIN2	388	0.87	0.494	0.018	0.0638	0.0016	406	12	398.7	9.7	434	78	398.7	9.7	1.8
RCN_111.FIN2	56.1	1.69	1.827	0.066	0.1792	0.0035	1045	23	1062	19	1000	70	1062.0	19.0	1.6
RCN_112.FIN2	102.4	1.48	1.892	0.041	0.1817	0.0027	1076	15	1078	15	1077	44	1078.0	15.0	0.2
RCN_113.FIN2	176.3	1.49	2.987	0.068	0.2471	0.0055	1399	17	1421	28	1377	42	1421.0	28.0	1.6

RCN_114.FIN2	163.4	0.69	2.889	0.057	0.243	0.004	1377	15	1403	20	1340	31	1403.0	20.0	1.9
RCN_115.FIN2	166	0.77	2.63	0.056	0.2147	0.0045	1305	16	1255	25	1405	37	1255.0	25.0	3.8
RCN_116.FIN2	278	1.61	3.296	0.052	0.2626	0.0038	1479	13	1505	19	1441	30	1505.0	19.0	1.8
RCN_117.FIN2	531	16.09	1.805	0.026	0.1789	0.0026	1045.5	9.3	1061	14	1015	29	1061.0	14.0	1.5
RCN_118.FIN2	125.9	2.47	1.324	0.036	0.1377	0.0025	854	16	831	14	909	49	831.0	14.0	2.7
RCN_119.FIN2	200	2.04	3.966	0.058	0.2875	0.0038	1626	12	1628	19	1632	24	1632.0	24.0	0.2
RCN_120.FIN2	91.8	1.39	2.168	0.047	0.1997	0.0032	1166	15	1173	17	1147	41	1173.0	17.0	0.6
RCN_121.FIN2	165.5	0.90	0.61	0.018	0.0784	0.0011	482	11	486.6	6.7	446	57	486.6	6.7	1.0
RCN_122.FIN2	107	1.13	0.64	0.024	0.0794	0.0016	498	15	492.5	9.5	508	78	492.5	9.5	1.1
RCN_123.FIN2	188	1.18	4.057	0.068	0.2914	0.0046	1644	14	1647	23	1642	26	1642.0	26.0	0.3
RCN_124.FIN2	431	1.92	4.885	0.062	0.3294	0.0046	1798	11	1837	22	1753	19	1753.0	19.0	4.8
RCN_125.FIN2	56.6	1.16	1.898	0.074	0.1762	0.0048	1072	25	1044	26	1098	68	1044.0	26.0	2.6
RCN_126.FIN2	249	2.30	2.523	0.039	0.2223	0.003	1278	11	1293	16	1261	30	1293.0	16.0	1.2
RCN_127.FIN2	297	0.36	0.694	0.019	0.0862	0.002	536	11	533	12	533	66	533.0	12.0	0.6
RCN_128.FIN2	277	1.75	4.224	0.092	0.3002	0.0056	1675	17	1690	28	1659	30	1659.0	30.0	1.9
RCN_129.FIN2	628	3.82	2.153	0.028	0.1969	0.0022	1165.5	9	1158	12	1180	21	1158.0	12.0	0.6
RCN_130.FIN2	180	0.81	4.076	0.055	0.2962	0.0037	1647	11	1671	18	1619	23	1619.0	23.0	3.2

Sample Name: RCS							207/235		206/238		207/206		Best age			
Grain #	[U] ppm	U/Th	207/235	2σ error	206/238	2σ error	Age (Ma)	2σ error	Age (Ma)	2σ error	Age (Ma)	2σ error	(Ma)	2σ error	% Disc*	Rim/ Core
RCS_1.FIN2	139.4	1.18	1.877	0.031	0.1845	0.0022	1071	11	1091	12	1030	28	1091.0	12.0	1.9	
RCS_2.FIN2	132.5	1.32	1.677	0.02	0.1711	0.0016	998.9	7.7	1017.9	8.9	956	28	1017.9	8.9	1.9	
RCS_3.FIN2	86.7	1.50	0.755	0.019	0.0913	0.00099	569	11	563.1	5.9	576	52	563.1	5.9	1.0	
RCS_4.FIN2	270	1.06	6.132	0.067	0.3647	0.0045	1993.3	9.5	2003	21	1983	15	1983.0	15.0	1.0	
RCS_5.FIN2	126.7	2.70	2.927	0.049	0.2428	0.0034	1387	13	1401	18	1373	27	1401.0	18.0	1.0	
RCS_6.FIN2	625	22.10	1.213	0.044	0.1315	0.0038	806	20	796	22	830	43	796.0	22.0	1.2	Rim
RCS_6.FIN2	54.1	0.85	1.873	0.044	0.1818	0.0027	1069	16	1076	15	1058	43	1076.0	15.0	0.7	Core
RCS_7.FIN2	221	1.66	0.544	0.01	0.0709	0.00088	440.8	7	441.5	5.3	422	39	441.5	5.3	0.2	
RCS_8.FIN2	118	1.67	1.878	0.033	0.1833	0.0025	1071	12	1084	14	1043	33	1084.0	14.0	1.2	
RCS_10.FIN2	149	1.66	1.973	0.045	0.1875	0.0033	1102	16	1107	18	1101	28	1107.0	18.0	0.5	
RCS_11.FIN2	359.1	1.10	1.538	0.015	0.1583	0.0013	945.2	5.9	947	7.4	942	18	947.0	7.4	0.2	
RCS_12.FIN2	209	1.96	3.445	0.039	0.2659	0.0029	1513.4	8.8	1519	15	1510	17	1519.0	15.0	0.4	
RCS_13.FIN2	203	0.92	3.47	0.047	0.2626	0.0034	1519	11	1503	17	1543	21	1503.0	17.0	1.1	
RCS_14.FIN2	69.3	2.43	1.63	0.03	0.1658	0.0018	982	11	989	10	954	38	989.0	10.0	0.7	
RCS_15.FIN2	93.3	0.91	1.913	0.027	0.1865	0.0021	1085.2	9.2	1102	11	1047	29	1102.0	11.0	1.5	
RCS_16.FIN2	391	2.06	2.784	0.041	0.2261	0.0036	1350	11	1313	19	1413	21	1313.0	19.0	2.7	
RCS_17.FIN2	201	1.29	4.162	0.043	0.2978	0.0033	1665.2	8.6	1680	16	1653	17	1653.0	17.0	1.6	
RCS_18.FIN2	44.8	1.23	1.771	0.039	0.1759	0.0023	1035	14	1044	13	1007	44	1044.0	13.0	0.9	
RCS_19.FIN2	117.5	1.96	3.382	0.047	0.2633	0.0036	1500	11	1506	18	1496	24	1506.0	18.0	0.4	
RCS_20.FIN2	108	1.94	0.593	0.04	0.0751	0.0022	477	22	467	13	510	110	467.0	13.0	2.1	
RCS_21.FIN2	46.8	1.50	1.75	0.054	0.1741	0.0032	1024	20	1034	17	999	64	1034.0	17.0	1.0	
RCS_22.FIN2	384	1.18	5.505	0.075	0.3362	0.0043	1900	12	1868	21	1938	16	1938.0	16.0	3.6	
RCS_23.FIN2	150.3	1.73	0.526	0.017	0.0694	0.0011	428	11	432.3	6.4	394	71	432.3	6.4	1.0	
RCS_24.FIN2	67.1	0.67	1.8	0.031	0.1787	0.0025	1043	11	1059	14	1021	37	1059.0	14.0	1.5	
RCS_25.FIN2	735	10.89	1.793	0.019	0.1727	0.0019	1042.1	7	1027	11	1078	17	1027.0	11.0	1.4	

RCS_26.FIN2	290	5.48	1.79	0.027	0.1752	0.0028	1040	9.8	1040	15	1048	22	1040.0	15.0	0.0	
RCS_27.FIN2	290	2.49	1.675	0.024	0.169	0.0021	997.6	9.2	1006	11	975	21	1006.0	11.0	0.8	
RCS_28.FIN2	322	2.38	1.765	0.022	0.1753	0.0021	1032.4	8.5	1041	12	1019	21	1041.0	12.0	0.8	
RCS_29.FIN2	334.1	1.38	3.202	0.043	0.251	0.0029	1456	10	1443	15	1478	19	1443.0	15.0	0.9	
RCS_30.FIN2	964	3.64	1.9	0.022	0.1823	0.0024	1080.4	7.5	1079	13	1094	21	1079.0	13.0	0.1	
RCS_31.FIN2	338	0.84	0.527	0.011	0.0685	0.00085	430	7.4	427	5.1	443	41	427.0	5.1	0.7	
RCS_32.FIN2	183	0.53	0.471	0.011	0.06253	0.00081	391	7.3	390.9	4.9	390	47	390.9	4.9	0.0	
RCS_33.FIN2	39.4	2.05	1.53	0.035	0.1591	0.0023	941	14	951	13	909	45	951.0	13.0	1.1	
RCS_34.FIN2	245	1.75	2.467	0.036	0.2169	0.0029	1262	11	1265	15	1261	20	1265.0	15.0	0.2	
RCS_35.FIN2	149	1.08	4.212	0.052	0.3011	0.0037	1675	10	1696	18	1653	19	1653.0	19.0	2.6	
RCS_36.FIN2	43.4	1.21	14.77	0.23	0.5355	0.0069	2802	14	2762	29	2835	19	2835.0	19.0	2.6	
RCS_37.FIN2	186.9	1.67	2.029	0.023	0.1894	0.0019	1125	8	1118	10	1141	20	1118.0	10.0	0.6	
RCS_38.FIN2	130.7	2.64	2.696	0.052	0.2292	0.0035	1324	14	1329	18	1324	28	1329.0	18.0	0.4	
RCS_39.FIN2	252	2.35	5.238	0.072	0.3405	0.0048	1857	12	1888	23	1825	17	1825.0	17.0	3.5	
RCS_40.FIN2	435	1.62	3.29	0.048	0.2564	0.0037	1477	11	1470	19	1493	19	1470.0	19.0	0.5	
RCS_41.FIN2	90.4	0.58	7.14	0.1	0.3951	0.0052	2127	13	2145	24	2111	19	2111.0	19.0	1.6	
RCS_42.FIN2	84.6	1.34	0.902	0.02	0.1082	0.0015	651	11	662.2	8.5	599	49	662.2	8.5	1.7	
RCS_43.FIN2	185	6.03	3.27	0.12	0.2259	0.0084	1469	30	1311	44	1701	37	1311.0	44.0	10.8	Rim
RCS_43.FIN2	101.8	0.57	11.05	0.19	0.448	0.0075	2525	16	2385	34	2615	25	2615.0	25.0	8.8	Core
RCS_45.FIN2	173.6	0.96	3.479	0.062	0.2612	0.0041	1520	14	1495	21	1555	22	1495.0	21.0	1.6	
RCS_46.FIN2	340.2	1.56	0.5275	0.0087	0.06792	0.00068	429.5	5.8	423.5	4.1	455	34	423.5	4.1	1.4	
RCS_47.FIN2	159	2.32	2.227	0.037	0.2045	0.0026	1187	12	1199	14	1168	28	1199.0	14.0	1.0	
RCS_48.FIN2	96.7	0.98	14.48	0.17	0.5435	0.0059	2780	11	2797	25	2770	16	2770.0	16.0	1.0	
RCS_49.FIN2	211.8	2.14	3.04	0.046	0.2467	0.0031	1417	12	1421	16	1411	25	1421.0	16.0	0.3	
RCS_50.FIN2	111.5	0.76	3.878	0.051	0.2823	0.0033	1607	11	1602	16	1617	21	1617.0	21.0	0.9	
RC5_53.FIN2	232.6	1.43	3.441	0.054	0.2626	0.0035	1512	12	1502	18	1524	24	1502.0	18.0	0.7	
RC5_54.FIN2	591	1.28	0.4155	0.0099	0.047	0.0011	352.6	7.1	295.9	6.5	734	62	DISC	DISC	16.1	
RC5_55.FIN2	240	0.90	0.493	0.01	0.064	0.00062	406.5	6.9	399.9	3.8	427	47	399.9	3.8	1.6	

RC5_56.FIN2	130.4	1.44	0.518	0.013	0.068	0.00095	424.2	9	424	5.7	409	58	424.0	5.7	0.0
RC5_57.FIN2	246	2.15	2.704	0.032	0.2294	0.0025	1328.5	8.7	1331	13	1322	23	1331.0	13.0	0.2
RC5_58.FIN2	225	1.96	1.861	0.024	0.1792	0.0018	1066.9	8.9	1062.5	9.7	1066	25	1062.5	9.7	0.4
RC5_59.FIN2	64.7	0.91	4.199	0.062	0.2984	0.0028	1671	12	1684	14	1649	25	1649.0	25.0	2.1
RC5_60.FIN2	1084	2.20	2.872	0.08	0.2354	0.0061	1373	21	1362	32	1388	32	1362.0	32.0	0.8
RC5_61.FIN2	126.5	1.69	3.084	0.069	0.2383	0.0043	1426	17	1377	23	1496	34	1377.0	23.0	3.4
RC5_62.FIN2	112.7	2.46	2.259	0.032	0.2072	0.0019	1198	10	1214.7	9.8	1162	29	1214.7	9.8	1.4
RC5_63.FIN2	101.4	0.55	0.569	0.015	0.07323	0.00093	455.9	9.7	455.5	5.6	434	59	455.5	5.6	0.1
RC5_64.FIN2	301	0.65	0.596	0.011	0.07591	0.00091	473.7	7.1	471.6	5.4	472	42	471.6	5.4	0.4
RC5_65.FIN2	471	2.33	2.097	0.026	0.1864	0.0021	1146.4	8.3	1102	11	1233	19	1102.0	11.0	3.9
RC5_66.FIN2	282	1.56	2.7	0.031	0.2201	0.0024	1327.7	8.4	1282	13	1398	22	1282.0	13.0	3.4
RC5_67.FIN2	289	4.47	1.791	0.019	0.1772	0.0018	1042.4	7	1051.4	9.6	1024	22	1051.4	9.6	0.9
RC5_68.FIN2	251.2	1.00	5.294	0.048	0.3341	0.0025	1866.8	7.8	1858	12	1875	16	1875.0	16.0	0.9
RC5_69.FIN2	75.6	2.36	4.017	0.047	0.2867	0.0026	1635.9	9.5	1625	13	1648	22	1648.0	22.0	1.4
RC5_70.FIN2	131.1	2.40	4.616	0.045	0.3143	0.0028	1750.9	8.1	1761	14	1737	18	1737.0	18.0	1.4
RC5_71.FIN2	32.12	0.77	1.84	0.058	0.181	0.0029	1055	21	1072	16	1012	63	1072.0	16.0	1.6
RC5_72.FIN2	125	0.89	2.199	0.03	0.2027	0.0018	1179	9.6	1189.7	9.5	1153	28	1189.7	9.5	0.9
RC5_73.FIN2	175.8	2.03	0.557	0.011	0.07044	0.00085	448.4	7.2	438.7	5.1	487	45	438.7	5.1	2.2
RC5_74.FIN2	158	1.34	1.959	0.031	0.1876	0.0023	1101	11	1108	12	1084	29	1108.0	12.0	0.6
RC5_75.FIN2	48.1	1.54	1.228	0.03	0.1347	0.0019	810	14	814	11	781	61	814.0	11.0	0.5
RC5_76.FIN2	273	1.19	0.5821	0.0087	0.07569	0.00069	465.3	5.6	470.3	4.1	434	37	470.3	4.1	1.1
RC5_77.FIN2	190	1.32	3.668	0.046	0.2689	0.0028	1564	10	1535	14	1603	18	1535.0	14.0	1.9
RC5_78.FIN2	149.7	2.27	4.71	0.05	0.3145	0.0028	1767.6	9	1762	14	1777	17	1777.0	17.0	0.8
RC5_79.FIN2	199.9	3.02	4.935	0.044	0.3236	0.0029	1807.2	7.5	1807	14	1808	16	1808.0	16.0	0.1
RC5_80.FIN2	186.8	1.48	2.649	0.035	0.2255	0.0023	1312.7	9.8	1311	12	1315	21	1311.0	12.0	0.1
RC5_81.FIN2	60.9	1.91	2.975	0.048	0.2455	0.0025	1398	12	1417	12	1371	31	1417.0	12.0	1.4
RC5_82.FIN2	310	1.20	0.58	0.01	0.07422	0.00083	463.6	6.6	462.1	4.9	467	37	462.1	4.9	0.3
RC5_83.FIN2	305	2.34	3.489	0.041	0.2673	0.0024	1523.1	9.4	1526	12	1517	17	1526.0	12.0	0.2

RC5_84.FIN2	13.77	1.11	1.926	0.073	0.187	0.0037	1081	26	1104	20	1006	78	1104.0	20.0	2.1
RC5_85.FIN2	343	1.45	0.5428	0.0082	0.07071	0.00062	441.2	5.7	440.4	3.7	446	36	440.4	3.7	0.2
RC5_86.FIN2	263.9	1.88	3.372	0.057	0.2271	0.0036	1496	13	1318	19	1760	24	1318.0	19.0	11.9
RC5_87.FIN2	197.1	1.32	4.381	0.058	0.3079	0.0035	1707	11	1730	17	1679	18	1679.0	18.0	3.0
RC5_88.FIN2	56.8	1.88	15.35	0.23	0.559	0.0074	2834	14	2860	31	2812	21	2812.0	21.0	1.7
RC5_89.FIN2	195.5	1.88	2.32	0.036	0.2061	0.0033	1218	11	1208	18	1252	36	1208.0	18.0	0.8
RC5_90.FIN2	111.1	1.03	1.965	0.027	0.1895	0.0019	1101.9	9.3	1119	10	1068	27	1119.0	10.0	1.6
RC5_91.FIN2	88.8	0.91	3.4	0.061	0.2497	0.0029	1502	14	1437	15	1589	30	1437.0	15.0	4.3
RC5_92.FIN2	169.5	1.96	4.165	0.05	0.2892	0.0029	1665	10	1637	15	1709	18	1709.0	18.0	4.2
RC5_93.FIN2	211.5	2.86	3.618	0.031	0.2743	0.0024	1554.3	7.2	1562	12	1544	16	1562.0	12.0	0.5
RC5_94.FIN2	23.8	0.34	0.513	0.032	0.0718	0.0015	413	21	446.9	9.1	230	120	446.9	9.1	8.2
RC5_95.FIN2	46	2.04	4.716	0.071	0.3199	0.0036	1767	13	1788	18	1743	27	1743.0	27.0	2.6
RC5_96.FIN2	38.3	0.85	3.703	0.071	0.2822	0.0032	1568	15	1604	16	1524	38	1524.0	16.0	2.3
RC5_97.FIN2	304.3	1.52	0.5762	0.0098	0.07375	0.00071	461.3	6.3	458.7	4.3	470	39	458.7	4.3	0.6
RC5_98.FIN2	147	1.18	0.595	0.014	0.07659	0.0007	472.6	8.8	475.7	4.2	435	50	475.7	4.2	0.7
RC5_99.FIN2	286	0.50	1.72	0.016	0.168	0.0015	1015.4	5.8	1001.1	8	1047	21	1001.1	8.0	1.4
RC5_100.FIN2	136	0.69	0.635	0.015	0.0781	0.001	498	9.6	484.8	6	549	59	484.8	6.0	2.7
RC5_101.FIN2	473.6	8.57	1.793	0.02	0.1744	0.0017	1042	7.1	1036.2	9.2	1052	19	1036.2	9.2	0.6
RC5_102.FIN2	269	1.74	1.829	0.02	0.1767	0.0015	1054.9	7.3	1048.5	8.3	1063	20	1048.5	8.3	0.6
RC5_103.FIN2	298	4.91	1.761	0.016	0.1748	0.0016	1030.6	5.8	1038.4	8.9	1012	23	1038.4	8.9	0.8
RC5_104.FIN2	271.7	0.48	0.5211	0.0088	0.06815	0.0007	425.2	5.9	424.9	4.2	417	37	424.9	4.2	0.1
RC5_105.FIN2	131.3	2.94	2.178	0.028	0.2015	0.0017	1172.7	8.8	1183.3	9.3	1150	25	1183.3	9.3	0.9
RC5_106.FIN2	537	2.57	0.5078	0.0078	0.06705	0.00062	416.4	5.3	418.3	3.8	400	30	418.3	3.8	0.5
RC5_107.FIN2	409	2.27	0.698	0.018	0.0818	0.0015	536	11	506.9	9.1	653	49	506.9	9.1	5.4
RC5_108.FIN2	52.3	1.00	1.819	0.04	0.1786	0.0022	1050	15	1059	12	1020	47	1059.0	12.0	0.9
RC5_109.FIN2	230.4	1.63	0.5243	0.0094	0.06859	0.00066	428.1	6.1	427.6	4	419	39	427.6	4.0	0.1
RC5_110.FIN2	69.1	1.32	16.85	0.18	0.554	0.0067	2924	11	2843	28	2977	15	2977.0	15.0	4.5
RC5_111.FIN2	50	1.22	2.63	0.043	0.2278	0.0027	1306	12	1322	14	1285	35	1322.0	14.0	1.2

RC5_112.FIN2	209	2.64	1.786	0.021	0.1759	0.0016	1039.4	7.7	1044.4	8.8	1027	24	1044.4	8.8	0.5	
RC5_113.FIN2	214.3	2.19	2.273	0.024	0.205	0.0016	1203.1	7.4	1201.8	8.8	1201	20	1201.8	8.8	0.1	
RC5_114.FIN2	62.1	0.97	1.54	0.03	0.1595	0.0021	945	12	954	11	911	45	954.0	11.0	1.0	
RC5_115.FIN2	325	2.18	1.702	0.023	0.1688	0.0018	1008.3	8.6	1005.6	9.8	1009	27	1005.6	9.8	0.3	
RC5_116.FIN2	135.8	0.89	0.54	0.011	0.07048	0.00078	437.4	7.5	439	4.7	415	47	439.0	4.7	0.4	
RC5_117.FIN2	38.2	0.80	2.734	0.056	0.2299	0.0029	1333	15	1334	15	1329	38	1334.0	15.0	0.1	
RC5_118.FIN2	267.7	1.99	2.961	0.026	0.2405	0.0023	1396.9	6.8	1389	12	1410	19	1389.0	12.0	0.6	
RC5_119.FIN2	206.1	1.21	1.941	0.026	0.1823	0.0017	1093.7	9.1	1079.2	9.4	1122	25	1079.2	9.4	1.3	
RC5_120.FIN2	250.8	1.88	2.792	0.061	0.2234	0.0048	1351	16	1299	25	1431	24	1299.0	25.0	3.8	
RC5_121.FIN2	202.2	1.17	0.5128	0.008	0.0671	0.00072	419.8	5.4	418.6	4.3	423	40	418.6	4.3	0.3	
RC5_122.FIN2	286.8	2.04	2.098	0.031	0.194	0.0024	1147	10	1145	13	1148	28	1145.0	13.0	0.2	
RC5_123.FIN2	203	1.61	3.579	0.037	0.2723	0.0024	1543.6	8.2	1553	12	1531	17	1553.0	12.0	0.6	
RC5_124.FIN2	472	3.28	1.405	0.015	0.1464	0.0014	890.1	6.6	880.8	8	912	21	880.8	8.0	1.0	
RC5_125.FIN2	469	1.82	3.729	0.086	0.2552	0.0064	1574	19	1464	33	1729	24	1464.0	33.0	7.0	
RC5_126.FIN2	121.7	0.82	1.814	0.024	0.1792	0.0016	1050.1	9	1062.2	8.9	1022	29	1062.2	8.9	1.2	
RC5_127.FIN2	134	2.87	1.951	0.025	0.1855	0.0017	1098.6	8.8	1096.4	9.3	1101	28	1096.4	9.3	0.2	
RC5_128.FIN2	1100	23.00	1.846	0.019	0.1752	0.0018	1061.5	6.9	1040.5	9.8	1107	20	1040.5	9.8	2.0	
RC5_129.FIN2	191.8	1.75	1.953	0.024	0.1865	0.0016	1098.1	8.1	1102.2	8.8	1091	24	1102.2	8.8	0.4	
RC5_130.FIN2	195.1	1.28	0.5026	0.0098	0.06624	0.00069	412.6	6.6	413.4	4.2	398	46	413.4	4.2	0.2	
RC5_131.FIN2	466	5.37	0.572	0.032	0.0719	0.0027	458	21	448	16	511	91	448.0	16.0	2.2	Rim
RC5_131.FIN2	262	1.74	2.84	0.047	0.2328	0.0038	1365	13	1348	20	1391	26	1348.0	20.0	1.2	Core
RC5_132.FIN2	95.2	1.05	0.589	0.014	0.07733	0.00094	468.4	9	480.1	5.6	407	54	480.1	5.6	2.5	

REFERENCES

Allred, I. J., and Blum, M. D., 2021, Early Pennsylvanian sediment routing to the Ouachita Basin (southeastern United States) and barriers to transcontinental sediment transport sourced from the Appalachian orogen based on detrital zircon U-Pb and Hf analysis: Geosphere, v. 18, p. 350-369.

Alsalem, O. B., Fan, M., Zamora, J., Xie, X., and Griffin, W. R., 2017, Paleozoic sediment dispersal before and during the collision between Laurentia and Gondwana in the Fort Worth Basin, USA: Geosphere, v. 14, p. 325-342.

Amato, J. M., Boullion, A. O., Serna, A. M., Sanders, A. E., Farmer, G. L., Gehrels, G. E., and Wooden, J. L., 2008, Evolution of the Mazatzal province and the timing of the Mazatzal orogeny: Insights from U-Pb geochronology and geochemistry of igneous and metasedimentary rocks in southern New Mexico: GSA Bulletin, v. 120, p. 328-346.

Becker, T. P., Thomas, W. A., Samson, S. D., and Gehrels, G. E., 2005, Detrital zircon evidence of Laurentian crustal dominance in the Lower Pennsylvanian deposits of the Alleghanian clastic wedge in eastern North America: Sedimentary Geology, v. 182, p. 59-86.

Bennett, V. C., and Depaolo, D. J., 1987, Proterozoic crustal history of the western United States as determined by neodymium isotopic mapping: GSA Bulletin, v. 99, p. 674-685.

Blakey, R. C., 2013, Key Time Slices of North America: Colorado Plateau Geosystems Inc.

Chapman, A. D., and Laskowski, A. K., 2019, Detrital zircon U-Pb data reveal a Mississippian sediment dispersal network originating in the Appalachian Orogen, traversing North America along its southern shelf, and reaching as far as the Southwest United States: Lithosphere, v. 11, p. 581-587.

Craddock, J. P., Konstantinou, A., Vervoort, J. D., Wirth, K. R., Davidson, C., Finley-Blasi, L., Juda, N. A., and Walker, E., 2013, Detrital zircon provenance of the Mesoproterozoic Midcontinent Rift, Lake Superior Region, U.S.A: The Journal of Geology, v. 121, p. 57-73.

Drake, A. A., Jr., Sinha, A. K., Laird, J., and Guy, R. E., 1989, The Taconic orogen, *in* Hatcher, R. D., Jr., Thomas, W. A., and Viele, G. W., eds., The Appalachian-Ouachita Orogen in the United States, Volume F-2, Geological Society of America, p. 101-177.

Eriksson, K. A., Campbell, I. H., Palin, J. M., Allen, Charlotte M., and Bock, B., 2004, Evidence for multiple recycling in Neoproterozoic through Pennsylvanian sedimentary rocks of the Central Appalachian Basin: The Journal of Geology, v. 112, p. 261-276.

Gehrels, G., Valencia, V., Pullen, A., and Olszewski, T. D., 2006, Detrital zircon geochronology by laser-ablation multicollector ICPMS at the Arizona Laserchron Center: The Paleontological Society Papers, v. 12, p. 67-76.

Gehrels, G. E., Blakey, R., Karlstrom, K. E., Timmons, J. M., Dickinson, B., and Pecha, M., 2011, Detrital zircon U-Pb geochronology of Paleozoic strata in the Grand Canyon, Arizona: Lithosphere, v. 3, p. 183-200.

Granath, J. W., 1989, Structural evolution of the Ardmore Basin, Oklahoma: Progressive deformation in the foreland of the Ouachita collision: Tectonics, v. 8, p. 1015-1036.
Ham, W. E., Denison, R. E., and Merritt, C. A., 1964, Basement rocks and structural evolution of southern Oklahoma: Bulletin - Oklahoma Geological Survey, p. 302.
Hanson, R. E., Puckett, R. E., Jr., Keller, G. R., Brueseke, M. E., Bulen, C. L., Mertzman, S. A., Finegan, S. A., and McCleery, D. A., 2013, Intraplate magmatism related to opening of the southern Iapetus Ocean; Cambrian Wichita igneous province in the Southern Oklahoma rift zone: Lithos, v. 174, p. 57-70.
Hart, N. R., Stockli, D. F., and Hayman, N. W., 2016, Provenance evolution during progressive rifting and hyperextension using bedrock and detrital zircon U-Pb geochronology, Mauléon Basin, western Pyrenees: Geosphere, v. 12, p. 1166-1186.
Hemish, L. A., and Andrews, R. D., 2001, Stratigraphy and depositional environments of the sandstones of the Springer Formation and the Primrose Member of the Golf Course Formation in the Ardmore Basin, Oklahoma: Guidebook - Oklahoma Geological Survey, v. 32, p. 1-37.
Hoffman, P. F., 1989, Precambrian geology and tectonic history of North America, *in* Bally, A. W., and Palmer, A. R., eds., The geology of North America - an overview, Geological Society of America, p. 447-512.
Hollingworth, R. S., Leary, R. J., and Heizler, M. T., 2021, Detrital U-Pb zircon and ^{40}Ar/^{39}Ar muscovite geochronology from Middle Pennsylvanian strata in the Anadarko Basin, Texas Panhandle, USA: Palaeogeography, Palaeoclimatology, Palaeoecology, v. 579, p. 1-12.
Jackson, S. E., Pearson, N. J., Griffin, W. L., and Belousova, E. A., 2004, The application of laser ablation-inductively coupled plasma-mass spectrometry to in situ U–Pb zircon geochronology: Chemical Geology, v. 211, p. 47-69.
Johnson, K. S., Amsden, T. W., Denison, R. E., Dutton, S. P., Goldstein, A. G., Bailey Rascoe, J., Sutherland, P. K., and Thompson, D. M., 1989, Geology of the Southern Midcontinent: Oklahoma Geological Survey 1989, Special Publication 89-2, p. 1-53.
Kissock, J. K., Finzel, E. S., Malone, D. H., and Craddock, J. P., 2017, Lower–Middle Pennsylvanian strata in the North American midcontinent record the interplay between erosional unroofing of the Appalachians and eustatic sea-level rise: Geosphere, v. 14, p. 141-161.
Konstantinou, A., Wirth, K. R., Vervoort, J. D., Malone, D. H., Davidson, C., and Craddock, J. P., 2014, Provenance of quartz arenites of the Early Paleozoic midcontinent region, USA: The Journal of Geology, v. 122, p. 201-216.
Krogh, T. E., Strong, D. F., O'Brien, S. J., and Papezik, V. S., 1988, Precise U-Pb zircon dates from the Avalon Terrane in Newfoundland: Canadian Journal of Earth Sciences, Revue Canadienne des Sciences de la Terre, v. 25, p. 442-453.
Lang, R. C., 1966, The Pennsylvanian Rocks of the Lake Murray Area: Ardmore Geological Society, p. 13-18.
Lawton, T. F., Blakey, R. C., Stockli, D. F., and Liu, L., 2021, Late Paleozoic (Late Mississippian-Middle Permian) sediment provenance and dispersal in western equatorial Pangea: Palaeogeography, Palaeoclimatology, Palaeoecology, v. 572, p. 1-35.
Leary, R. J., Umhoefer, P., Smith, M. E., Smith, T. M., Saylor, J. E., Riggs, N., Burr, G., Lodes, E., Foley, D., Licht, A., Mueller, M. A., and Baird, C., 2020, Provenance of

Pennsylvanian–Permian sedimentary rocks associated with the Ancestral Rocky Mountains orogeny in southwestern Laurentia: Implications for continental-scale Laurentian sediment transport systems: Lithosphere, v. 12, p. 88-121.
Liu, L., Stockli, D. F., Lawton, T. F., Xu, J., Stockli, L. D., Fan, M., and Nadon, G. C., 2022, Reconstructing source-to-sink systems from detrital zircon core and rim ages: Geology, v. 50, p. 691-696.
Lovell, T. R., and Bowen, B. B., 2013, Fluctuations in Sedimentary Provenance of the Upper Cambrian Mount Simon Sandstone, Illinois Basin, United States: The Journal of Geology, v. 121, p. 129-154.
Maley, M. P., 1986, Depositional history of the upper Morrowan (Pennsylvanian) strata of the Ardmore Basin, Oklahoma [MS thesis]: University of Oklahoma, 206 p.
McBride, M. H., 1986, A petrologic and diagenetic study of outcroppping and subsurface Springer and lower Morrowan Sandstones, Ardmore and Anadarko Basins, Oklahoma [MS thesis]: The University of Tulsa 160 p.
McGuire, P. R., 2017, U-Pb detrital zircon signature of the Ouachita orogenic belt [MS thesis]: Texas Christian University, 78 p.
Medaris, L. G., Singer, B. S., Jicha, B. R., Malone, D. H., Schwartz, J. J., Stewart, E. K., Van Lankvelt, A., Williams, M. L., and Reiners, P. W., 2021, Early Mesoproterozoic evolution of midcontinental Laurentia: Defining the geon 14 Baraboo orogeny: Geoscience Frontiers, v. 12, p. 1-17.
Meek, F. B., Elmore, R. D., Sutherland, P. K., and Hayward, O. T., 1988, Lithostratigraphy and depositional environments of the Springer and lower Golf Course Formations, Ardmore Basin, Oklahoma, Geological Society of America Centennial Field Guide - South-Central Section, Geological Society of America, p. 189-194.
Meek, F. B. I., 1983, The lithostratigraphy and depositional environments of the Springer and lower Golf Course Formations (Mississippian-Pennsylvanian) in the Ardmore Basin, Oklahoma [MS thesis]: University of Oklahoma, 212 p.
Miall, A. D., 2019, The southern Midcontinent, Permian Basin, and Ouachitas, *in* Miall, A. D., ed., The sedimentary basins of the United States and Canada (second edition), Elsevier, p. 369-399.
Miall, A. D., and Blakey, R. C., 2019, The Phanerozoic tectonic and sedimentary evolution of North America, *in* Miall, A. D., ed., The sedimentary basins of the United States and Canada (second edition), Elsevier, p. 1-38.
Mickus, K. L., and Keller, G. R., 1992, Lithospheric structure of the south-central United States: Geology, v. 20, p. 335-338.
Morris, R. C., 1989, Stratigraphy and sedimentary history of post-Arkansas Novaculite Carboniferous rocks of the Ouachita Mountains, *in* Hatcher, R. D., Jr., Thomas, W. A., and Viele, G. W., eds., The Appalachian-Ouachita Orogen in the United States, Volume F-2, Geological Society of America, p. 591-602.
Mueller, P. A., Heatherington, A. L., Foster, D. A., Thomas, W. A., Wooden, J. L., Zaw, K., Santosh, M., and Graham, I. T., 2014, The Suwannee Suture; significance for Gondwana-Laurentia terrane transfer and formation of Pangaea: Gondwana Research, v. 26, p. 365-373.
Mueller, P. A., Heatherington, A. L., Wooden, J. L., Shuster, R. D., Nutman, A. P., and Williams, I. S., 1994, Precambrian zircons from the Florida basement: A Gondwanan connection: Geology, v. 22, p. 119-122.

Park, H., Barbeau, D. L., Jr., Rickenbaker, A., Bachmann-Krug, D., and Gehrels, G. E., 2010, Application of foreland basin detrital-zircon geochronology to the reconstruction of the Southern and Central Appalachian Orogen: Journal of Geology, v. 118, p. 23-44.

Pastor-Galan, D., Gutierrez Alonso, G., Murphy, J. B., Fernandez Suarez, J., Hofmann, M., Linnemann, U., Faryad, S. W., Dobrzhinetskaya, L., Hoinkes, G., and Zhang, J., 2013, Provenance analysis of the Paleozoic sequences of the northern Gondwana margin in NW Iberia; passive margin to Variscan collision and orocline development: Gondwana Research, v. 23, p. 1089-1103.

Paton, C., Hellstrom, J., Paul, B., Woodhead, J., and Hergt, J., 2011, Iolite: Freeware for the Visualisation and Processing of Mass Spectrometric Data: Journal of Analytical Atomic Spectrometry, v. 26, p. 2508-2518.

Perry, W. J., Jr., 1989, Tectonic evolution of the Anadarko Basin region, Oklahoma: U. S. Geological Survey Bulletin, p. A1-A19.

Petrus, J. A., and Kamber, B. S., 2012, VizualAge: A Novel Approach to Laser Ablation ICP-MS U-Pb Geochronology Data Reduction: Geostandards and Geoanalytical Research, v. 36, p. 247-270.

Pickell, M. J., 2012, Detrital zircon geochronology of Middle Ordovician siliciclastic sediment of the southern Laurentian shelf [MS thesis]: Texas A&M University, 120 p.

Rascoe, B., Jr., and Adler, F. J., 1983, Permo-Carboniferous Hydrocarbon Accumulations, Mid-Continent, U.S.A: AAPG Bulletin, v. 67, no. 6, p. 979-1001.

Sharman, G. R., Sharman, J. P., and Sylvester, Z., 2018, detritalPy: A Python-based toolset for visualizing and analysing detrital geo-thermochronologic data: The Depositional Record, v. 4, p. 202-215.

Sharrah, K. L., 2006, Comparative study of the sedimentology and provenance of the Atoka Formation in the frontal Ouachita thrust belt, Oklahoma [PhD dissertation]: University of Tulsa, 252 p.

Shaw, J., Gutiérrez-Alonso, G., Johnston, S. T., and Galán, D. P., 2014, Provenance variability along the Early Ordovician north Gondwana margin: Paleogeographic and tectonic implications of U-Pb detrital zircon ages from the Armorican Quartzite of the Iberian Variscan belt: GSA Bulletin, v. 126, p. 702-719.

Sloss, L. L., 1963, Sequences in the Cratonic Interior of North America: GSA Bulletin, v. 74, no. 2, p. 93-114.

Stanley, T. M., and Chang, J. M., 2012, Preliminary Geologic map of the Ardmore 30' x 60' Quadrangle and the Oklahoma part of the Gainesville 30' x 60' Quadrangle, Carter, Jefferson, Love, Murray, and Stephens Counties, Oklahoma: Oklahoma Geological Survey.

Stockli, D. F., and Stockli, L. D., 2013, Unlocking provenance secrets from single detrital zircons by U-Pb and trace-element depth-profile laser-ablation-split-stream ICP-MS analysis and (U-Th)/He double dating: Abstracts with Programs - Geological Society of America, v. 45, p. 744.

Straka, J. J., 1972, Conodont Evidence of Age of Goddard and Springer Formations, Ardmore Basin, Oklahoma: American Association of Petroleum Geologists, Bulletin v. 56, p. 1087-1099.

Thomas, W. A., 1977, Evolution of Appalachian-Ouachita salients and recesses from reentrants and promontories in the continental margin: American Journal of Science, v. 277, p. 1233-1278.
Thomas, W. A., 2006, Tectonic inheritance at a continental margin: GSA Today, v. 16, p. 4-11.
Thomas, W. A., and Astini, R. A., 1999, Simple-shear conjugate rift margins of the Argentine Precordillera and the Ouachita embayment of Laurentia: GSA Bulletin, v. 111, p. 1069-1079.
Thomas, W. A., Becker, T. P., Samson, S. D., and Hamilton, M. A., 2004, Detrital zircon evidence of a recycled orogenic foreland provenance for Alleghanian clastic-wedge sandstones: The Journal of Geology, v. 112, p. 23-37.
Thomas, W. A., Gehrels, G. E., Greb, S. F., Nadon, G. C., Satkoski, A. M., and Romero, M. C., 2017, Detrital zircons and sediment dispersal in the Appalachian foreland: Geosphere, v. 13, p. 2206-2230.
Thomas, W. A., Gehrels, G. E., and Romero, M. C., 2016, Detrital zircons from crystalline rocks along the Southern Oklahoma fault system, Wichita and Arbuckle Mountains, USA: Geosphere, v. 12, p. 1224-1234.
Thomas, W. A., Gehrels, G. E., Sundell, K. E., Greb, S. F., Finzel, E. S., Clark, R. J., Malone, D. H., Hampton, B. A., and Romero, M. C., 2020a, Detrital zircons and sediment dispersal in the eastern Midcontinent of North America: Geosphere (Boulder, CO), v. 16, p. 817-843.
Thomas, W. A., Gehrels, G. E., Sundell, K. E., and Romero, M. C., 2020b, Detrital-zircon analyses, provenance, and late Paleozoic sediment dispersal in the context of tectonic evolution of the Ouachita Orogen: Geosphere (Boulder, CO), v. 17, p. 1214-1247.
Thomas, W. A., Tollo, R. P., Bartholomew, M. J., Hibbard, J. P., and Karabinos, P. M., 2010, Interactions between the Southern Appalachian-Ouachita orogenic belt and basement faults in the orogenic footwall and foreland: Memoir - Geological Society of America, v. 206, p. 897-916.
Tomlinson, C. W., and McBee, W., 1959, Pennsylvanian Sediments and orogenies of Ardmore district, Oklahoma: Petroleum Geology of Southern Oklahoma: American Association of Petroleum Geologists, v. 2, p. 3-52.
Van Schmus, W. R., Bickford, M. E., Turek, A., van der Pluijm, B. A., and Catacosinos, P. A., 1996, Proterozoic geology of the east-central Midcontinent basement, Basement and basins of eastern North America, Volume 308, Geological Society of America, p. 7-32.
Vermeesch, P., 2004, How many grains are needed for a provenance study?: Earth and Planetary Science Letters, v. 224, p. 441-451.
Vermeesch, P., Resentini, A., Garzanti, E., Caracciolo, L., von Eynatten, H., and Jan Weltje, G., 2016, An R package for statistical provenance analysis: Sedimentary Geology, v. 336, p. 14-25.
Viele, G. W., and Thomas, W. A., 1989, Tectonic synthesis of the Ouachita orogenic belt, *in* Hatcher, R. D., Jr., Thomas, W. A., and Viele, G. W., eds., The Appalachian-Ouachita Orogen in the United States, Geological Society of America, p. 695-728.
Waite, L., Fan, M., Collins, D., Gehrels, G., and Stern, R. J., 2020, Detrital zircon provenance evidence for an Early Permian longitudinal river flowing into the Midland Basin of West Texas: International Geology Review, v. 62, p. 1224-1244.

Wall, C. J., Hanson, R. E., Schmitz, M., Price, J. D., Donovan, R. N., Boro, J. R., Eschberger, A. M., and Toews, C. E., 2020, Integrating zircon trace-element geochemistry and high-precision U-Pb zircon geochronology to resolve the timing and petrogenesis of the late Ediacaran-Cambrian Wichita igneous province, Southern Oklahoma Aulacogen, USA: Geology, v. 49, p. 268-272.

Wang, W., and Bidgoli, T. S., 2019, Detrital Zircon Geochronologic Constraints on Patterns and Drivers of Continental-Scale Sediment Dispersal in the Late Mississippian: Geochemistry, Geophysics, Geosystems, v. 20, p. 5522-5543.

Wang, W., Bidgoli, T. S., and Sturmer, D. M., 2022, Exploring the influence of Late Mississippian to Middle Pennsylvanian tectonics on sediment transport through detrital zircon geochronology, southwestern Kansas and northwestern Arkansas: Palaeogeography, Palaeoclimatology, Palaeoecology, v. 586, p. 1-16.

Whitmeyer, S. J., and Karlstrom, K. E., 2007, Tectonic model for the Proterozoic growth of North America: Geosphere, v. 3, p. 220-259.

Wortman, G. L., Samson, S. D., and Hibbard, J. P., 2000, Precise U-Pb zircon constraints on the earliest magmatic history of the Carolina Terrane: Journal of Geology, v. 108, p. 321-338.

Xie, X., Anthony, J. M., and Busbey, A. B., 2019, Provenance of Permian Delaware Mountain Group, central and southern Delaware Basin, and implications of sediment dispersal pathway near the southwestern terminus of Pangea: International Geology Review, v. 61, p. 361-380.

Xie, X., Cains, W., and Manger, W. L., 2016, U/Pb detrital zircon evidence of transcontinental sediment dispersal; provenance of Late Mississippian Wedington sandstone member, NW Arkansas: International Geology Review, v. 58, p. 1951-1966.

Xie, X., and Manger, W. L., 2022, Early Carboniferous (Mississippian) intertwining sediment dispersal network across the Laurentian cratonic interior: Sedimentary Geology, v. 428, p. 1-15.

VITA

Personal:

Fabián Hilario Peña

Born October 18, 1995 in Eagle Pass, TX

Raised in Eagle Pass, TX

Son of Efrén and Rosa Marina Peña

Education

High School Diploma, May 2014

Eagle Pass High School | Eagle Pass, TX

Bachelor of Science in Geology, August 2018

The University of Texas at San Antonio | San Antonio, TX

Master of Science in Geology, May 2023

Texas Christian University | Fort Worth, TX

Experience

Graduate Teaching Assistant, August 2020-May 2022

TCU Department of Geological Sciences | Fort Worth, TX

Geology and Reservoir Engineering Intern, June 2021-August 2021

Goodnight Midstream | Dallas, TX

Field Professional - Measurement While Drilling, December 2018-October 2019

Halliburton | Odessa, TX

ABSTRACT

DETRITAL ZIRCON GEOCHRONOLOGY OF UPPER MISSISSIPPIAN TO LOWER PENNSYLVANIAN STRATA OF THE ARDMORE BASIN, OKLAHOMA

By: Fabián Hilario Peña, M.S. 2023

Department of Geological Sciences

Texas Christian University

Thesis Advisor: Dr. Xiangyang Xie, Professor of Geology

Detrital zircon geochronology was used on nine Upper Mississippian to Lower Pennsylvanian sandstones of the Ardmore Basin in south-central Oklahoma and provided 1135 ages which revealed a clear transition in sediment provenance during the development of the Appalachian-Ouachita orogen. The Upper Mississippian (Chesterian) sandstones yielded a predominant middle to late Mesoproterozoic (Grenville) population, secondary middle Paleozoic (Appalachian), early Mesoproterozoic (Granite-Rhyolite), and late Paleoproterozoic (Yavapai-Mazatzal) populations, and minor Neoproterozoic to Cambrian (peri-Gondwanan) and Paleoproterozoic and older (> ~1825 Ma) age groups. Chesterian samples were likely derived from the Appalachian orogen and recycled sediment from the northern midcontinent, with an introduction of influence from the Ouachita orogen. Provenance shifted in the Early Pennsylvanian (Morrowan) where the northern part of the

basin experienced significant increases in early Mesoproterozoic (Granite-Rhyolite) and late Paleoproterozoic (Yavapai-Mazatzal) midcontinent age groups, which were being supplied by the nascent Ancestral Rocky Mountains along with Appalachian sediment. The southern part of the basin continued predominantly receiving Appalachian sediment along with minor amounts of detritus from the northern midcontinent and Ouachita orogen. Recycling of sediment from the local Criner Hills uplift is recorded in the youngest (Atokan) sample in this study.